# A systematic approach to airborne sensor orientation and calibration: method and models

Marta Blázquez González

May 2012

PhD Dissertation

| | |
|---|---|
| Title: | A systematic approach to airborne sensor orientation and calibration: method and models |
| Candidate: | Marta Blázquez González |
| Advisor: | Dr. Ismael Colomina |
| Centre: | Institute of Geomatics |
| PhD. Program: | Aerospace Science and Technology<br>Universitat Politècnica de Catalunya<br>Castelldefels, Spain |

**Per a tu i per a la nostra princesa.**
**Sense vosaltres, res no tindria sentit.**

**Resum**

Avui dia, s'estima que el mercat de la geomàtica mou pels volts de 30 bilions d'euros. Al darrera del creixement d'aquest mercat hi trobem noves tecnologies, projectes i aplicacions, com per exemple, "Global Positioning System"(GPS), Galileo, "Global Monitoring for Environment and Security"(GMES), Google Earth, etc. Actualment, la demanda i el consum de geoinformació està incrementant i, a més a més, aquesta ha de ser precisa, exacta, actualitzada i assequible. Amb l'objectiu d'acomplir aquests requisits tècnics i, en general, la demanda del mercat, la indústria i l'àmbit acadèmic estan introduint un darrera l'altre sistemes d'imatgeria, plataformes aèries i plataformes satel·litals. Però alhora, aquests sistemes d'adquisició introdueixen nous problemes com el calibratge i l'orientació de sensors, la navegació de les plataformes (de manera precisa i exacta segons el seu rendiment), la combinació de diferents tipus de sensors, la integració de dades auxiliars que provenen de diverses fonts, aspectes temporals com la gravació "contínua"en el temps dels sensors, la feble geometria d'alguns d'ells, etc. Alguns d'aquests problemes es poden resoldre amb els mètodes i estratègies actuals, sovint afegint pegats, però la majoria no es poden resoldre amb els mètodes vigents o no es poden resoldre amb els mètodes vigents amb fiabilitat i robustesa. Aquesta tesi presenta les abstraccions i generalitzacions necessàries que permeten desenvolupar la propera generació d'ajustos de xarxes i mètodes d'estimació amb l'objectiu de resoldre aquests problemes. A més, basada en aquestes idees, s'ha desenvolupat la principal eina d'aquesta recerca: la plataforma de software "Generic Extensible Network Approach"(GENA).

L'objectiu d'aquesta recerca és establir les bases metòdiques d'un concepte sistemàtic per l'orientació i el calibratge de sensors aeris i provar la seva validesa amb nous models i aplicacions. Així, en primer lloc, prenent distància sobre el que s'ha fet tradicionalment i tenint en compte tot el que ens ofereix la tecnologia INS/GNSS, aquesta tesi genera un mètode per l'explotació dels sistemes INS/GNSS en l'orientació i el calibratge de sensors aeris. I, en segon lloc, s'han proposat i testejat amb dades reals alguns models que conformen aquest concepte, com per exemple, l'ús de temps, posició i actitud donats pel sistema INS/GNSS en mode relatiu (eliminant la necessitat dels paràmetres d'absorció d'errors INS/GNSS o la matriu d'orientació relativa IMU-sensor), l'ús de temps, posició, velocitat i actitud pel calibratge de temps (utilitzant així la solució completa que donen els sistemes INS/GNSS per lligar les dimensions espacial i temporal) o reduir el nombre de mesures de l'orientació integrada de sensors tradicional, duent a terme la proposta "fast aerotriangulation", Fast AT. Aquesta recerca està presentada a la tesi com un compendi d'articles.

Així doncs, els resultats de la tesi no són només el document de la tesi en si mateix i les publicacions, hi ha també un software comercial i models i aplicacions que validen el mètode proposat i representen un nou panorama per l'orientació i el calibratge de sensors aeris.

**Paraules clau:** abstracció, modelatge, orientació, calibratge, aerotriangulació, xarxa, ajust, fotogrametria, INS/GNSS, software.

**Resumen**

En la actualidad, el mercado de la geomática está valorado en unos 30 billones de euros. Tras el crecimiento de dicho mercado, se hallan nuevas tecnologías, proyectos y aplicaciones, como por ejemplo, "Global Positioning System"(GPS), Galileo, "Global Monitoring for Environment and Security"(GMES), Google Earth, etc. Hoy en día, la demanda y el consumo de geoinformación está incrementándose y, además, dicha información debe ser precisa, exacta, actualizada y asequible. Intentando cumplir estos requisitos técnicos y, en general, la demanda del mercado, la industria y el ámbito académico están introduciendo uno tras otro sistemas de imagen, plataformas aéreas y plataformas satelitales. Pero a su vez, estos sistemas de adquisición introducen nuevos problemas como la calibración y la orientación de sensores, la navegación de las plataformas (debe ser precisa y exacta teniendo en cuenta su rendimiento particular), la combinación de diferentes tipos de sensor, la integración de datos auxiliares que proceden de diversas fuentes, aspectos temporales como la grabación "continua" en el tiempo de los sensores, la débil geometría de algunos de ellos, etc. Algunos de estos problemas pueden resolverse con los métodos y estrategias actuales, generalmente aplicando parches, pero la mayoría no se pueden resolver con los métodos vigentes o no se pueden resolver con los métodos vigentes con fiabilidad y robustez. Esta tesis presenta las abstracciones y generalizaciones necesarias que permiten desarrollar la próxima generación de ajustes de redes y métodos de estimación con el objetivo de resolver estos problemas. Es más, basada en estas ideas, se ha desarrollado la herramienta principal de esta investigación: la plataforma de software "Generic Extensible Network Approach"(GENA).

El objetivo de esta investigación es establecer las bases metódicas de un concepto sistemático para la orientación y la calibración de sensores aéreos, y probar su validez con nuevos modelos y aplicaciones. Así pues, en primer lugar, distanciándonos de lo que tradicionalmente se ha realizado y considerando lo que la tecnología INS/GNSS nos ofrece, esta tesis crea un método para la explotación de los sistemas INS/GNSS en la orientación y la calibración de sensores aéreos. Y, en segundo lugar, se proponen y testean con datos reales algunos modelos que constituyen este concepto, como por ejemplo, el uso de tiempo, posición y actitud dados por el sistema INS/GNSS en modo relativo (eliminando la necesidad de los parámetros de absorción de errores INS/GNSS o la matriz de orientación relativa IMU-sensor), el uso de tiempo, posición, velocidad y actitud para la calibración temporal (utilizando así la solución completa que dan los sistemas INS/GNSS para enlazar las dimensiones espacial y temporal) o reducir el número de medidas de la orientación integrada de sensores tradicional, llevando a cabo la propuesta "fast aerotriangulation", Fast AT. Esta investigación está presentada en la tesis como un compendio de artículos.

Resumiendo, los resultados de la tesis no son sólo el documento de la tesis en sí mismo y las publicaciones, existe también un software comercial y modelos y aplicaciones que validan el método propuesto y presentan un nuevo panorama para la orientación y la calibración de sensores aéreos.

**Palabras clave:** abstracción, modelado, orientación, calibración, aerotriangulación, red, ajuste, fotogrametría, INS/GNSS, software.

**Abstract**

The geomatic market has an estimated value of some 30 trillion euros. Behind this growing market, there are new technologies, projects and applications like Global Positioning System (GPS), Galileo, Global Monitoring for Environment and Security (GMES), Google Earth, etc. Modern society is increasingly demanding and consuming geoinformation that must be precise, accurate, up-to-date and affordable. In an attempt to meet these technical requirements and general market demand, industry and academia are introducing one imaging system, airborne platform and satellite platform after another. These acquisitions are introducing new problems such as calibration and orientation of the sensors, navigation of the platforms (with an accurate and precise processing of their individual performances), combination of different types of sensors, integration of auxiliary data provided from various sources, temporal issues of the "continuously" recording sensors, weak geometry of some sensors, etc. Some of the previous problems can be solved with current methods and strategies, oftentimes with a dose of patchwork. However, the vast majority of these problems cannot be solved with the current methods, or at least not with a like degree of robustness and reliability. This thesis presents the abstractions and generalizations needed to facilitate the development of the next generation of network adjustment and estimation methods that will make it possible to solve these problems. Moreover, the main tool of this research is a commercial software platform, "Generic Extensible Network Approach" (GENA), based on the proposed network approach.

The goal of this research is to establish a methodical basis of a systematic approach to airborne sensor orientation and calibration and to prove its validity with newly-developed models and applications. On one hand, viewing the traditional DiSO and ISO from a distance and considering the possibilities that the INS/GNSS technology offers, this thesis generates a method to exploit the INS/GNSS systems for airborne sensor orientation and calibration. On the other hand, several models that constitute this method are proposed and tested with independent actual data sets; for example, the use of INS/GNSS-derived time, position and attitude in relative mode (avoiding the need for GNSS linear shift parameters, that absorb the INS/GNSS errors, or the relative orientation IMU-to-sensor, boresight, matrix), the use of INS/GNSS-derived time, position, velocity and attitude for time calibration (exploiting the full solution of the INS/GNSS systems to link the space and time dimensions) or the measurement reduction of the traditional integrated sensor orientation to perform the proposed "fast aerotriangulation", or Fast AT. This research is presented in the thesis as compiled papers.

Therefore, the results of this thesis are not only the thesis document itself and a number of publications, but also a commercial software platform and models and applications that validate the proposed method and present a new panorama for airborne sensor orientation and calibration.

**Keywords:** abstraction, modeling, orientation, calibration, aerotriangulation, network, adjustment, photogrammetry, INS/GNSS, software.

# Acknowledgments

This thesis has involved a number of different people and companies that I would like to thank. Many thanks to the suppliers of the actual data sets used and GeoNumerics for its support of my research. I am also deeply grateful for the technical discussions and encouragement of Dr. Peter Frieß.

Però vull donar les gràcies de manera especial, no com un tràmit que han de fer tots els doctorands, al meu director de tesi, Dr. Ismael Colomina. Aquesta tesi no hagués estat possible, literalment, sense la teva empenta, el teu suport i, perquè no dir-ho, totes les teves hores (en aquest punt també vull donar les gràcies a la Carmina i als nens). He après moltes coses treballant al teu costat, professionals i personals, però sobretot has estat un model de rigor, professionalitat i treball ben fet. Gràcies.

Com la feina mai és d'una sola persona, vull donar les gràcies als meus companys de l'Institut de Geomàtica, als qui han estat i als qui encara hi són. Als companys de TA amb qui vaig començar la meva aventura en el món de la recerca. Gràcies Michele per l'oportunitat. Als meus companys de TI i de FORMA pel seu suport, especialment al Dr. José Antonio Navarro. Pep, gràcies per les nostres discussions tècniques i el teu treball. Als meu companys de GIN, moltes gràcies per les reunions constructives, per la paciència i pel vostre suport, especialment l'Eva Hernàndez. Eva, les nostres converses i els teus consells, m'han ajudat a crèixer. Vull també agrair al Patrick Bones la seva inestimable ajuda amb l'anglès. Per les teves correccions (fins al final, t'he passat les coses en l'últim minut ...), les teves explicacions i, sobretot, els teus ànims. Gràcies.

I com no, vull agrair a aquells que són més que companys, als meus amics: la Marta, l'Oriol i l'Eduard. Gràcies per estar sempre al meu costat. Pels vostres consells, per les confidències, pels riures, pels plors. Sou els millors. Us estimo.

Però sé que tots em perdonareu si faig una menció especial a la Lali. Ara que em calen, no tinc paraules per dir tot el que voldria dir i agraïr tot el que has fet. Això ha estat possible gràcies a tu: als teus ànims, als teus consells, a les discussions tècniques, a les teves correccions, al teu temps amb mi i amb els qui jo més m'estimo. You are my person. T'estimo.

Malgrat que no ho puguin llegir, vull recordar a dues persones molt especials que han marcat l'evolució d'aquesta tesi: l'àvia i la Montserrat. A les dues les vaig conèixer tard per elles mateixes, no per ser la mare de ... A les dues les he estimat. La primera sé que estaria molt orgullosa del que he aconseguit. Te quiero abuela. La segona estaria molt feliç per mi (no fa gaire encara llegia els teus correus ...). Allà on estigueu, gràcies per tenir cura de nosaltres.

Y como los últimos serán los primeros, quiero dar las gracias a mi familia. A mi hermano y a Elena. Sois fantásticos. Gracias por todo, ahora me tomaré

ese descanso. A mis padres. No estaría escribiendo estas líneas si no fuera por vosotros. Soy quien soy gracias a vuestro esfuerzo, apoyo y amor. Gracias por las oportunidades, por los sacrificios, por estar ahí, sobretodo cuando yo no podía. Os quiero.

Al meu marit, Marc, i a la meva filla, Laia, que són el millor de la meva vida. L'esforç no ha estat meu, ha estat vostre. Realment us dec les gràcies i molt més. Pel temps robat, pel suport, per la paciència, per l'amor. B29. Sempre.

Princesa tu, d'alguna manera, ets el fruit més important d'aquesta tesi. Ets la que més ha patit i la que menys ho ha entès. Espero que, en el futur, quan llegeixis aquestes paraules estiguis orgullosa de la teva mare i elles et transmetin tot l'amor que sovint no t'he pogut demostrar. T'estimo, patufa.

# Contents

# Chapter 1

# Introduction

The geomatic market has an estimated value of some 30 trillion euros. Behind this growing market, there are new technologies, projects and applications like Global Positioning System (GPS), Galileo, Global Monitoring for Environment and Security (GMES), Google Earth, etc.

Modern society is increasingly demanding and consuming geoinformation that must be precise, accurate, up-to-date and affordable. In an attempt to meet these technical requirements and general market demand, industry and academia are introducing one imaging system, airborne platform and satellite platform after another.

These acquisitions are introducing new problems such as calibration and orientation of the sensors, navigation of the platforms (with an accurate and precise processing of their individual performances), combination of different types of sensors, integration of auxiliary data provided from various sources, temporal issues of the "continuously" recording sensors, weak geometry of some sensors, etc.

Some of the previous problems can be solved with current methods and strategies, oftentimes with a dose of patchwork. However, the vast majority of these problems cannot be solved with the current methods, or at least not with a like degree of robustness and reliability.

The proposed network approach can solve part of these problems, but not all of them.

This thesis presents the abstractions and generalizations needed to facilitate the development of the next generation of network adjustment and estimation methods ([Colomina et al., 2012], reprinted in appendix 1).

The "Generic Extensible Network Approach" (GENA) platform software, which I largely developed for GeoNumerics (Barcelona, Spain), is not only the main tool of this research, it is also the materialization of the proposed network approach.

Beyond the conceptual and practical contributions of the software in the work conducted, the goal of this research is twofold: to establish the methodical basis of a systematic approach to airborne sensor orientation and calibration, and to prove its validity with newly-developed models and applications.

## 1.1 Method

The least-squares estimation technique is nothing new. The German mathematician, geodesist, astronomer and physicist Carl Friedrich Gauß (1777 - 1855) developed a proof of least-squares adjustment in 1809.

In 1810 he used this technique to adjust the first geodetic network of the state of Hannover.

The first network adjustments performed with digital computers date back to the nineteen-fifties where continent-wide geodetic networks were globally adjusted, mainly in the US and Western Europe.

[Ackermann et al., 1970], [Brown, 1971] and [Schmid, 1974] established the fundamentals of sensor orientation and calibration concepts in the late nineteen-sixties and early nineteen-seventies. But they did not only introduce these ideas, they also translated these ideas into software that went into the production lines of almost every photogrammetric production organization worldwide.

The self-calibrating bundle adjustment (SCBA) approach matured, and robust estimators ([Krarup et al., 1980] and [Klein and Förstner, 1984]) were introduced in the nineteen-eighties. Soon, bundle adjustment was exported to remote sensing ([Kratky, 1989]) and the GPS was imported to bundle adjustment ([Lucas, 1987] and [Frieß, 1991]).

By 1991, digital aerial triangulation was in the pipeline ([Tsingas, 1991]). The use of INS/GPS technology for Direct Sensor Orientation (DiSO) of frame cameras had already been proposed in 1993 ([Schwarz et al., 1993]). In parallel, INS/GNSS time-position-velocity-attitude determination became the basis for the DiSO of airborne digital line cameras, hyperspectral cameras, airborne laser scanning (ALS) and airborne Interferometric SAR (InSAR). Between 1995 and 2000, INS/GNSS technology penetrated the large-format metric aerial camera segment and became standard photogrammetric equipment ([Scherzinger, 1997]). The theoretically higher mechanical stability of digital cameras created high expectations for DiSO. However, practical experience ([Alamús et al., 2007] and [Cramer, 2007]) has demonstrated that even the high-end large-format digital cameras require SCBA. The same applies to medium-format digital cameras which, in the meantime, have created a market of their own. The last development wave is ALS block adjustment for orientation and calibration ([Frieß, 2006], [Kager, 2004], [Skaloud and Lichti, 2006] and [Angelats et al., 2012]).

In the realm of navigation, since 2004, the least-squares techniques have been explored to solve dynamic geomatic problems such as the modeling of trajectories for airborne and spaceborne imaging linear arrays, the calibration of inertial instruments (angular rate sensors and accelerometers) with "cross-over" types of observation equations and the estimation of geodetic networks for monitoring and prediction purposes ([Colomina and Blázquez, 2004] and [Colomina and Blázquez, 2005]). A parallel research effort is being conducted by A. Térmens ([Térmens and Colomina, 2004]) for inertial strapdown kinematic airborne gravimetry.

Furthermore, in the field of radiative transfer modeling and radiometric calibration, the radiometric block adjustment approach ([Honkavaara, 2008], [Martínez and Arbiol, 2008] and [Chandelier and Martinoty, 2009]) is progressing.

This evolution demonstrates that airborne sensor orientation and calibration is a fundamental capacity of current mapping systems and a fundamental research topic. Neither digital remote sensing acquisition systems nor direct orientation have made network adjustment method obsolete. On the contrary, the continuous flow of new sensors, platforms and applications points to the relevance of a general systematic approach.

This thesis proposes a method which can be understood as a general framework and systematic approach to airborne sensor orientation and calibration, in which the well-established Direct Sensor Orientation (DiSO) and Integrated Sensor Orientation (ISO) procedures are particular cases. The proposed method is the result of taking into account all the possibilities that the INS/GNSS technology offers for the airborne sensor orientation and calibration problem. If viewed from a distance, the three axes depicted in Figure 1.1 illustrate the method:

- the "aerial control" axis represents how the INS/GNSS-derived data is used to orient and to calibrate the airborne sensor;
- the "procedure" axis represents the measurements used to orient and to calibrate the airborne sensor, in addition to the INS/GNSS-derived data; and,
- the "time" axis represents whether the time dimension of the airborne sensor orientation and calibration problem is, or is not taken into account when the INS/GNSS systems are involved.

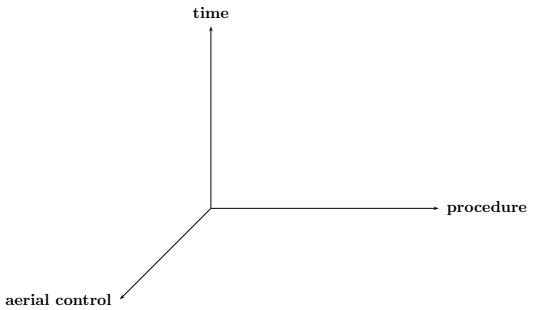


Figure 1.1: Method for a systematic approach.

## 1.2 Models

Since the thesis is not only a theoretical research project, the development of new models and applications for the systematic approach to airborne sensor orientation and calibration is at least as important as the theory behind the technology. The compiled papers that make up this thesis are the materialization of this theoretical and applied goal.

The next chapters reprint the papers with the models and applications that are built on the proposed method. They are the natural result of thinking in generic and abstract terms to identify applications such as:

- traditional geomatic applications that can be solved in the sense of robustness and reliability, such as the critical use of the boresight matrix in the ISO procedure;
- undeveloped geomatic applications such as the calibration of the temporal dimension in multi-sensor systems; and
- geomatic applications that need low-cost procedures without losing reliability.

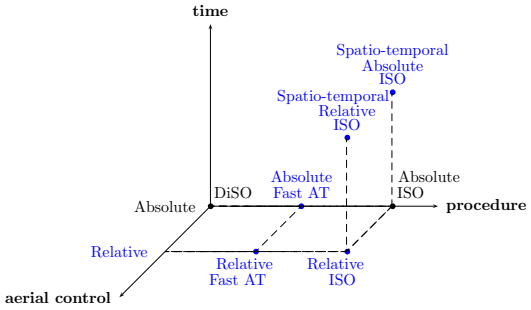


Figure 1.2: Systematic approach: method and models.

Figure 1.2 depicts the proposed models for a systematic approach to airborne sensor orientation and calibration in the dimensions of:

- "aerial control": traditional INS/GNSS absolute aerial control versus new proposed INS/GNSS relative aerial control (Chapters 2 and 3);
- "procedure": traditional DiSO and ISO procedures versus new "fast aerotriangulation", Fast AT (Chapter 5); and
- "time": traditional spatial aerial control versus new proposed spatio-temporal aerial control (Chapters 2 and 4).

Therefore, Figure 1.2 includes the traditional DiSO and ISO procedures, which are based on the use of INS/GNSS-derived data in absolute mode, and extends the traditional panorama with new airborne sensor orientation and calibration models. It shows how the new panorama provides more possibilities like Fast AT, time calibration using available INS/GNSS-derived velocity or the use of the INS/GNSS-derived data in relative mode.

# Chapter 2

# Spatio-temporal calibration

This chapter is the first paper of a paper series that demonstrating the potential of the proposed method with two new models for airborne sensor orientation and calibration: relative aerial control and temporal calibration.

The relative aerial control is a new and rigorous approach to use INS/GNSS-derived position and attitude in relative mode. It is based on transferring the relative orientation of an INS/GNSS system between two epochs to the relative orientation of a rigidly attached sensor between the same two epochs. The relative aerial control eliminates the INS/GNSS linear shift parameters (to absorb INS/GNSS errors) and IMU-to-sensor relative orientation (boresight) matrix. The temporal calibration model is a new model that uses the INS/GNSS-derived linear and angular velocities to handle the sensor-system synchronization problem at the SW level. The INS/GNSS velocities allow the calibration of a constant time shift parameter and decorrelate time errors from space errors. Figure 2.1 shows how the full exploitation of INS/GNSS-derived control data takes us from the traditional 3D spatial to the 4D spatio-temporal orientation and calibration of multi-sensor systems. In this paper, the spatial absolute and relative and the spatio-temporal absolute aerial control models are validated with one actual data set and one simulated-perturbed data set, respectively.

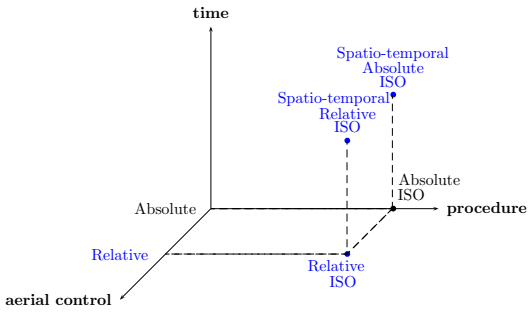


Figure 2.1: Relative and spatio-temporal aerial control models.

Although I am the only author of this paper, Dr. Ismael Colomina promoted and supervised the research.

*Blázquez, M., 2008. A new approach to spatio-temporal calibration of multi-sensor systems. International Archives of the Photogrammetry, Remote Sensing and Spatial Information Sciences 37(B1), pp. 481–486.*

This article is a peer-reviewed conference article and won the ISPRS Best Young Author Award.

# A NEW APPROACH TO SPATIO-TEMPORAL CALIBRATION OF MULTI-SENSOR SYSTEMS

M. Blázquez

Institute of Geomatics
Generalitat de Catalunya & Universitat Politècnica de Catalunya
Parc Mediterrani de la Tecnologia
Av. del Canal Olímpic s/n, Castelldefels, Spain
marta.blazquez@ideg.es

**KEY WORDS:** photogrammetry, calibration, spatio-temporal, modeling, orientation, sensor, INS/GPS

**ABSTRACT:**

The purpose of this paper is to propose new, rigorous, more robust and reliable models and methods for the calibration and orientation of multi-sensor systems with INS/GPS data. On the one hand, the classical spatial sensor orientation and calibration problem is reformulated as a relative control problem by transferring the relative orientation of an Inertial Measurement Unit (IMU) between two epochs to the relative orientation of a rigidly attached sensor between the same two epochs. This approach eliminates the need for the IMU-to-sensor relative orientation [boresight] calibration parameter. On the other hand, a rigorous 4D —spatio-temporal— model, based on the full exploitation of the INS/GPS-derived control data, is introduced. The paper discusses the key ideas behind both proposed approaches, presents the corresponding mathematical models, identifies some of their advantages, and demonstrates their potential through real data.

## 1 INTRODUCTION

Nowadays, the use of INS/GPS time, position and attitude (tPA) derived information as aerial control to support sensor orientation and calibration is a well-established procedure (Lucas, 1987, Schwarz et al., 1993). For some sensor designs, the use of tPA aerial control is a must. For others, it is just an option; be it for the purpose of better geometric accuracy, for more flexible mission design or just to match competitors' equipment. Whatever the reason is, INS/GPS instrumentation has become a "de facto" standard companion to the mapping sensors. This situation, in turn, has consolidated two well-defined calibration and orientation procedures: Direct Sensor Orientation (DSO) and the so-called Integrated Sensor Orientation (ISO). In DSO, sensor position and attitude literally depend on INS/GPS-derived tPA control information. ISO does not depend from it, it just benefits from it.

DSO is the procedure that directly provides the orientation parameters of the sensor (Schwarz et al., 1993). ISO is the procedure that combines measurements on the mapping sensors' data with whatever other available control data in order to compute the sensor orientation parameters in a block adjustment (Ackermann and Schade, 1993, Frieß, 1991). In practice, most times, the ISO procedure is nothing else than a traditional aerial triangulation adjustment with tPA aerial control and a few ground control points. With this combination, the ISO procedure inherits the advantages of traditional block adjustment, reduces ground control and relaxes mission geometric constraints.

ISO is both an orientation and calibration procedure; i.e., the calibration and orientation parameters are estimated simultaneously in the block adjustment. On the other side —although this depends on the project and on the precision and accuracy requirements— DSO requires a previous ISO step to calibrate the sensors and the sensor-system (Colomina, 1999).

The paper proposes new 3D models for the traditional ISO procedure. The proposed models, more robust and reliable, are based on the fact that the relative attitude of the sensor between two epochs coincides with the relative orientation of the IMU between the same two epochs (assuming that the sensor and IMU are rigidly attached). This rationale brings us to the equations which model the orientation of the sensor in terms of the tPA aerial control without the need of the boresight calibration matrix (Blázquez and Colomina, 2008). Actual data are used to show the first results and demonstrate the potential of this approach.

The classical ISO models, algorithms, methods and procedures just tackle the spatial calibration aspects. However, experience tells that incorrect or just inaccurate time synchronization between sensors is a big troublemaker. While spatial calibration is dealt both at the HW and SW levels, temporal calibration —time synchronization— is left to the HW. This results in reasonable robust and resilient systems as for geometry and weak systems as for time. In other words, current models for sensor and sensor-system calibration are 3D —restricted to geometry— while the problem is a genuine 4D, spatio-temporal one (Blázquez and Colomina, 2008).

The paper also proposes models and methods to solve the above 4D problem. In this sense, the contribution of the paper is twofold: firstly, genuine spatio-temporal orientation and calibration models are derived and, secondly, appropriate observational control data (for example, INS/GPS velocity) are identified for the precise estimation of the 4D model parameters.

In a multi-sensor system there are two types of time errors: individual sensor internal errors and system synchro-

nization ones. In the case of individual sensor errors, the calibration method must be based on particular mathematical models of the sensor. In the other case, even if all the sensor oscillators are "perfect," inaccurate time synchronization between the various system sensors can spoil the system performance and the sensor-system inconsistencies must be modeled. It is often the case, that individual sensor time drifts are dominated by external GPS receiver-generated precise [ambiguous] time pulses and that, for various technical and commercial reasons, inter-sensor constant temporal shifts occur. The paper focuses on the modeling of the sensor-system time synchronization problem.

For the estimation of the temporal calibration parameters, the use of the full INS/GPS-derived control data is proposed. In fact, INS/GPS delivers not only time, position and attitude (tPA) but also velocity (tPVA). These velocities can be used for calibrating the time errors and for decorrelating them from the space errors. This general principle is valid for any multi-sensor system and, in the paper, is formulated for the frame camera sensors.

The paper concludes by reporting on preliminary results of actual data tests performed for concept validation purposes. The results indicate that the new models make sense, behave as expected and deliver good results.

## 2 AERIAL CONTROL MODELS

### 2.1 Classical Aerial Control Models Extensions

The classical ISO procedure optimally estimates multi-sensor system parameters (unknowns) in the sense of least-squares relating observations (measurements) with these parameters through models. These models can be sensor models or aerial control models. The first ones are composed by the equations that model the own sensor behavior (sensor observations and its own orientation and calibration parameters). One example of sensor model is the collinearity equations. The second ones are composed by the equations which model the relation between the sensor, the GPS antenna receiver, and the IMU. The improvement of the classical aerial control mathematical functional models is the focus of this research.

The classical aerial control model relates tPA aerial control with the sensor orientation parameters, sensor-to-GPS antenna receiver parameters and sensor-to-IMU parameters for each epoch. In this paper, this model is referred to as spatial absolute aerial control model. Based on the following two obvious facts the classical aerial control models can be extended:

*1. The sensor calibration and orientation problem is not a 3D spatial problem, it is a 4D spatio-temporal one. Moreover, the INS/GPS-derived data contain not only positions and attitudes, they also contain velocities.*

*2. If a sensor and an IMU are rigidly attached, the sensor relative attitude between any two epochs is the same as the IMU relative attitude between the same two epochs.*

The extended model which takes into account the temporal dimension of the sensor orientation and calibration problem is referred to as spatio-temporal absolute aerial control model. This proposed model relates tPVA aerial control with the sensor orientation parameters, sensor-to-GPS antenna receiver parameters, sensor-to-IMU parameters, and multi-sensor time synchronization parameter for each epoch.

The extended model which takes into account the orientation and calibration problem for two epochs is referred to as spatial relative aerial control model. This proposed model relates tPA aerial control with the sensor orientation parameters, sensor-to-GPS antenna receiver parameters and sensor-to-IMU parameters for two epochs.

For the sake of completeness, the extended model which takes into account the temporal dimension of sensor orientation and calibration problem for two epochs is referred to as spatio-temporal relative aerial control model. This proposed model relates tPVA aerial control with the sensor orientation parameters, sensor-to-GPS antenna receiver parameters, sensor-to-IMU parameters, and multi-sensor time synchronization parameter for two epochs.

### 2.2 Naming and notation conventions

In the presented mathematical functional models, the involved reference frames and coordinate systems are listed in table 1.

| | |
|---|---|
| $\mathrm{l}$ | Cartesian local terrestrial frame (east-north-up) |
| $\mathrm{b}$ | IMU instrumental frame (forward-left-up) |
| $\mathrm{c}$ | camera instrumental frame |
| $\mathrm{l}'$ | Cartesian local terrestrial frame (north-east-down) |
| $\mathrm{b}'$ | IMU instrumental frame (forward-right-down) |
| $\mathrm{i}$ | inertial reference frame |

Table 1: Reference frames and coordinate systems.

If a variable $x$ involves just one reference frame $a$, it is written $x^a$. If a variable involves two reference frames, the subscript symbol defines the "from" or "origin" ($f$) reference frame and the superscript symbol defines the "to" or "destination" ($t$) one like in $x_f^t$.

The observations and their residuals are denoted by lowercase symbols, $\mathrm{a}$; the parameters are denoted by uppercase symbols, $\mathrm{A}$; and the constant values (instrumental constant, observational auxiliary values, and constant rotation matrices) are denoted by the italic typestyle, $a$. The vector accent above a variable, $\vec{\mathrm{a}}$, indicates that this variable is a 3-dimensional vector. For the sake of simplicity, $\vec{X}^f = (x, y, z)^f$ is used instead of the rigorous mathematical formulation $\vec{X}^f = [(x, y, z)^f]^T$. The observational residuals are denoted by the symbol $\mathrm{v}$ with the observation symbol as a subscript, for example, $\mathrm{v_a}$ denotes the residual of the observation $\mathrm{a}$.

The eccentricity vector $\vec{\mathrm{A}}^{\mathrm{c}}=(\mathrm{a_x}, \mathrm{a_y}, \mathrm{a_z})^{\mathrm{c}}$ from the camera projection centre to the GPS receiver antenna parameter; the $\vec{N}^c = (0, 0, n)^c$ constant vector, where $n$ is the camera nodal distance; and the $R_{l'}^l$ rotation constant matrix are involved in all the mathematical functional models.

### 2.3 Absolute Aerial Control Models

Absolute aerial control functional models (spatial absolute aerial control models (2.3.1) and spatio-temporal absolute aerial control models (2.3.2)) involve the following observations and their residuals: the GPS- or INS/GPS-derived position, $\vec{\mathrm{x}}^{\mathrm{l}} = (\mathrm{x}, \mathrm{y}, \mathrm{z})^{\mathrm{l}}$ and the traditional [heading, pitch, roll] Euler angles, $\chi = (\psi, \vartheta, \gamma)$, that parameterize the $\mathrm{R}^{\mathrm{l}'}_{\mathrm{b}'}$ rotation matrix. In both absolute aerial control models, the involved parameters are: the camera projection centre, $\vec{\mathrm{X}}^{\mathrm{l}} = (\mathrm{X}, \mathrm{Y}, \mathrm{Z})^{\mathrm{l}}$; the traditional Euler angles, $\Gamma = (\omega, \varphi, \kappa)$, that parameterize the $\mathrm{R}^{\mathrm{l}}_{\mathrm{c}}$ rotation matrix; the GPS positioning errors, $\vec{\mathrm{S}}^{\mathrm{l}} = (\mathrm{s_x}, \mathrm{s_y}, \mathrm{s_z})^{\mathrm{l}}$; and the $\mathrm{R}^{\mathrm{b}}_{\mathrm{c}}(\Upsilon)$ IMU-to-camera relative orientation [boresight] calibration parameter[1]. $R^{b'}_{b}$ is a constant rotation matrix.

**2.3.1 Spatial Absolute Aerial Control:** The functional models for the spatial absolute aerial control are

$$\vec{\mathrm{x}}^{\mathrm{l}} + \vec{\mathrm{v}}^{\mathrm{l}}_{\mathrm{x}} = \vec{\mathrm{X}}^{\mathrm{l}} + \mathrm{R}^{\mathrm{l}}_{\mathrm{c}}(\Gamma) \cdot (\vec{\mathrm{A}}^{\mathrm{c}} + \vec{N}^{c}) + \vec{\mathrm{S}}^{\mathrm{l}}, \quad (1)$$

$$\mathrm{R}^{\mathrm{l}}_{\mathrm{c}}(\Gamma) = R^{l}_{l'} \cdot \mathrm{R}^{\mathrm{l}'}_{\mathrm{b}'}(\chi + \vec{\mathrm{v}}_{\chi}) \cdot R^{b'}_{b} \cdot \mathrm{R}^{\mathrm{b}}_{\mathrm{c}}(\Upsilon) \quad (2)$$

for position and attitude respectively. Note, that in the above equation 2 for attitude control, in contrast to other formulations, the original INS/GPS-derived $\psi, \vartheta, \gamma$ IMU attitude angles can be directly used with no intermediate reparameterization steps.

**2.3.2 Spatio-temporal Absolute Aerial Control:** The functional models for the spatio-temporal absolute aerial control are:

$$\vec{\mathrm{x}}^{\mathrm{l}} + \vec{\mathrm{v}}^{\mathrm{l}}_{\mathrm{x}} = \vec{\mathrm{X}}^{\mathrm{l}} + \mathrm{R}^{\mathrm{l}}_{\mathrm{c}}(\Gamma) \cdot (\vec{\mathrm{A}}^{\mathrm{c}} + \vec{N}^{c}) + \vec{\mathrm{S}}^{\mathrm{l}} - \left(\vec{\mathbf{v}}^{\mathrm{l}} + \vec{\mathrm{v}}^{\mathrm{l}}_{\mathbf{v}}\right) \cdot \Delta\mathrm{t}, \quad (3)$$

$$\mathrm{R}^{\mathrm{l}}_{\mathrm{c}}(\Gamma) = R^{l}_{l'} \cdot [\mathrm{R}^{\mathrm{l}'}_{\mathrm{b}'}(\chi + \vec{\mathrm{v}}_{\chi}) + \dot{\mathrm{R}}^{\mathrm{l}'}_{\mathrm{b}'}(\chi + \vec{\mathrm{v}}_{\chi}) \cdot \Delta\mathrm{t}] \cdot R^{b'}_{b} \cdot \mathrm{R}^{\mathrm{b}}_{\mathrm{c}}(\Upsilon). \quad (4)$$

In equation 3, the observables are the usual GPS or INS/GPS positions $\vec{\mathrm{x}}^{\mathrm{l}}$ and the INS/GPS linear velocities $\vec{\mathbf{v}}$[2].

In equation 4, note the time derivative rotation matrix $\dot{\mathrm{R}}^{\mathrm{l}'}_{\mathrm{b}'}$ that can be computed after the relationship

$$\dot{\mathrm{R}}^{\mathrm{l}'}_{\mathrm{b}'}(\chi + \vec{\mathrm{v}}_{\chi}) = \mathrm{R}^{\mathrm{l}'}_{\mathrm{b}'}(\chi + \vec{\mathrm{v}}_{\chi}) \cdot (\Omega^{b'}_{ib'} - \Omega^{b'}_{il'}),$$

where $\Omega^{b'}_{ib'}$ and $\Omega^{b'}_{il'}$ are observational auxiliary matrices. $\Omega^{b'}_{ib'} = \Omega^{b'}_{ib'}(\omega_{\mathrm{x}}, \omega_{\mathrm{y}}, \omega_{\mathrm{z}})$ is an angular velocity matrix where $(\omega_x, \omega_y, \omega_z)$ are the calibrated IMU angular velocities. $\Omega^{b'}_{il'} = \Omega^{b'}_{il'}(\lambda, \phi, \dot{\lambda}, \dot{\phi}, \omega_e)$ is an angular velocity matrix which depends on the known sensor position and on the Earth angular rate[3]. $\Delta t$ is the multi-sensor time synchronization parameter which is used in both absolute control models (here) and in the spatio-temporal relative control models (section 2.4.2).

[1] The boresight matrix can be parameterized in different ways. No parameterization is specified because it is not relevant to this research.

[2] Note that the symbol $\mathbf{v}$ which denotes velocity is different from the symbol v which denotes residuals.

[3] The $\Omega^{b'}_{ib'}$ matrix and the $\Omega^{b'}_{il'}$ matrix are well-known and can be found in any inertial navigation book as for example (Jekeli, 2001).

### 2.4 Relative Aerial Control Models

Relative aerial control functional models (spatial relative aerial control models (2.4.1) and spatio-temporal relative aerial control models (2.4.2)) involve the following observations and their residuals: the GPS- or INS/GPS-derived positions at epoch $\mathrm{t}_2$, $\vec{\mathrm{x}}^{\mathrm{l}}_2 = (\mathrm{x}_2, \mathrm{y}_2, \mathrm{z}_2)^{\mathrm{l}}$ and the Euler angles that parameterize the $\mathrm{R}^{\mathrm{l}'}_{\mathrm{b}'}$ rotation matrix at epoch $\mathrm{t}_2$, $\chi_2 = (\psi_2, \vartheta_2, \gamma_2)$. The involved parameters are: the camera projection centre at epoch $\mathrm{t}_1$, $\vec{\mathrm{X}}^{\mathrm{l}}_1 = (\mathrm{X}_1, \mathrm{Y}_1, \mathrm{Z}_1)^{\mathrm{l}}$; the Euler angles that parameterize the $\mathrm{R}^{\mathrm{l}}_{\mathrm{c}}$ rotation matrix at epoch $\mathrm{t}_1$, $\Gamma_1 = (\omega_1, \varphi_1, \kappa_1)$; the camera projection centre at epoch $\mathrm{t}_2$, $\vec{\mathrm{X}}^{\mathrm{l}}_2 = (\mathrm{X}_2, \mathrm{Y}_2, \mathrm{Z}_2)^{\mathrm{l}}$; and the Euler angles that parameterize the $\mathrm{R}^{\mathrm{l}}_{\mathrm{c}}$ rotation matrix at epoch $\mathrm{t}_2$, $\Gamma_2 = (\omega_2, \varphi_2, \kappa_2)$. The models of this section involve the following observational auxiliary values: the GPS- or INS-/GPS-derived positions at epoch $\mathrm{t}_1$, $\vec{x}^{l}_{1} = (x_1, y_1, z_1)^{l}$ and the Euler angles that parameterize the $R^{l'}_{b'}$ rotation matrix at epoch $\mathrm{t}_1$, $\chi_1 = (\psi_1, \vartheta_1, \gamma_1)$.

In the relative aerial control models, tPA (or tPVA in the case of spatio-temporal models) aerial control are introduced as observational auxiliary data (constant information) at epoch $\mathrm{t}_1$ for numerical related issues.

**2.4.1 Spatial Relative Aerial Control:** The functional models for the spatial relative aerial control are:

$$\vec{x}^{l}_{1} - \left(\vec{\mathrm{x}}^{\mathrm{l}}_2 + \vec{\mathrm{v}}^{\mathrm{l}}_{\mathrm{x}_2}\right) = \vec{\mathrm{X}}^{\mathrm{l}}_1 - \vec{\mathrm{X}}^{\mathrm{l}}_2 + \left[\mathrm{R}^{\mathrm{l}}_{\mathrm{c}}(\Gamma_1) - \mathrm{R}^{\mathrm{l}}_{\mathrm{c}}(\Gamma_2)\right] \cdot (\vec{\mathrm{A}}^{\mathrm{c}} + \vec{N}^{c}), \quad (5)$$

$$\mathrm{R}^{\mathrm{l}}_{\mathrm{c}}(\Gamma_1) \cdot \mathrm{R}^{\mathrm{c}}_{\mathrm{l}}(\Gamma_2) = R^{l}_{l'} \cdot R^{l'}_{b'}(\chi_1) \cdot \mathrm{R}^{\mathrm{b}'}_{\mathrm{l}'}(\chi_2 + \vec{\mathrm{v}}_{\chi_2}) \cdot R^{l'}_{l}. \quad (6)$$

Equations 5 and 6 are obtained from equations 1 and 2 respectively by straightforward algebraic operations. Note, that in equation 5 the positioning calibration parameter $\vec{\mathrm{S}}^{\mathrm{l}}$ has vanished and that in equation 6 the IMU-to-sensor boresight rotation matrix $\mathrm{R}^{\mathrm{b}}_{\mathrm{c}}(\Upsilon)$ has vanished as well.

**2.4.2 Spatio-temporal Relative Aerial Control:** The functional models for the spatio-temporal relative aerial control are:

$$\vec{x}^{l}_{1} - \left(\vec{\mathrm{x}}^{\mathrm{l}}_2 + \vec{\mathrm{v}}^{\mathrm{l}}_{\mathrm{x}_2}\right) = \vec{\mathrm{X}}^{\mathrm{l}}_1 - \vec{\mathrm{X}}^{\mathrm{l}}_2 + \left[\mathrm{R}^{\mathrm{l}}_{\mathrm{c}}(\Gamma_1) - \mathrm{R}^{\mathrm{l}}_{\mathrm{c}}(\Gamma_2)\right] \cdot (\vec{\mathrm{A}}^{\mathrm{c}} + \vec{N}^{c}) - \left[\vec{v}^{l}_{1} - \left(\vec{\mathbf{v}}^{\mathrm{l}}_2 + \vec{\mathrm{v}}^{\mathrm{l}}_{\mathbf{v}_2}\right)\right] \cdot \Delta\mathrm{t} \quad (7)$$

$$\mathrm{R}^{\mathrm{l}}_{\mathrm{c}}(\Gamma_1) \cdot \mathrm{R}^{\mathrm{c}}_{\mathrm{l}}(\Gamma_2) = R^{l}_{l'} \cdot [R^{l'}_{b'}(\chi_1) + \dot{R}^{l'}_{b'}(\chi_1) \cdot \Delta\mathrm{t}] \cdot [\mathrm{R}^{\mathrm{l}'}_{\mathrm{b}'}(\chi_2 + \vec{\mathrm{v}}_{\chi_2}) + \dot{\mathrm{R}}^{\mathrm{l}'}_{\mathrm{b}'}(\chi_2 + \vec{\mathrm{v}}_{\chi_2}) \cdot \Delta\mathrm{t}]^{\mathrm{T}} \cdot R^{l'}_{l} \quad (8)$$

In equation 7, the observables are the GPS or INS/GPS positions $\vec{\mathrm{x}}^{\mathrm{l}}_2$ and the INS/GPS linear velocities $\vec{\mathbf{v}}^{\mathrm{l}}_2$ at epoch $\mathrm{t}_2$. The INS/GPS linear velocities at epoch $\mathrm{t}_1$, $\vec{v}^{l}_{1}$, are observational auxiliary values.

In equation 8, note the time derivative rotation matrices $\dot{\mathrm{R}}^{\mathrm{l}'}_{\mathrm{b}'}$ that can be computed after the relationship

$$\dot{R}^{l'}_{b'}(\chi_1) = R^{l'}_{b'}(\chi_1) \cdot (\Omega_1{}^{b'}_{ib'} - \Omega_1{}^{b'}_{il'}),$$

$$\dot{\mathrm{R}}^{\mathrm{l}'}_{\mathrm{b}'}(\chi_2+\vec{\mathrm{v}}_{\chi_2})=\mathrm{R}^{\mathrm{l}'}_{\mathrm{b}'}(\chi_2+\vec{\mathrm{v}}_{\chi_2})\cdot(\Omega_2{}^{b'}_{ib'}-\Omega_2{}^{b'}_{il'}),$$

where $\Omega_1{}^{b'}_{ib'}$, $\Omega_2{}^{b'}_{ib'}$, $\Omega_1{}^{b'}_{il'}$, and $\Omega_2{}^{b'}_{il'}$ are auxiliary matrices. $\Omega_1{}^{b'}_{ib'}=\Omega^{b'}_{ib'}(\omega_{\mathrm{x}_1},\omega_{\mathrm{y}_1},\omega_{\mathrm{z}_1})$ is an angular velocity matrix where $(\omega_{x_1},\omega_{y_1},\omega_{z_1})$ are the calibrated IMU angular velocities at epoch $\mathrm{t}_1$. $\Omega_2{}^{b'}_{ib'}=\Omega^{b'}_{ib'}(\omega_{\mathrm{x}_2},\omega_{\mathrm{y}_2},\omega_{\mathrm{z}_2})$ is an angular velocity matrix where $(\omega_{x_2},\omega_{y_2},\omega_{z_2})$ are the calibrated IMU angular velocities at epoch $\mathrm{t}_2$. $\Omega_1{}^{b'}_{il'}=\Omega^{b'}_{il'}(\lambda_1,\phi_1,\dot{\lambda_1},\dot{\phi_1},\omega_e)$ is an angular velocity matrix which depends on the known sensor position and on the Earth angular rate at epoch $\mathrm{t}_1$. $\Omega_2{}^{b'}_{il'}=\Omega^{b'}_{il'}(\lambda_2,\phi_2,\dot{\lambda_2},\dot{\phi_2},\omega_e)$ is an angular velocity matrix which depends on the known sensor position and on the Earth angular rate at epoch $\mathrm{t}_2$.

## 3 CONCEPT VALIDATION RESULTS

In order to analyse the overall feasibility and, somewhat, validate the concepts introduced in the previous sections, some of the newly formulated models were implemented and tested with actual data against the classical spatial absolute control models whose results played the reference role. More precisely, the functional model of equation 3 was tested against the model of equation 1 (section 3.1, "Spatial Absolute vs Spatio-temporal Absolute") and the functional models of equations 5, 6 were tested against the reference models of equations 1, 2 respectively (section 3.2, "Spatial Absolute vs Spatial Relative"). For this purpose the "Pavia block" (provided to the Institute of Geomatics by Prof. Vittorio Casella, Facoltà di Ingegneria, Università di Pavia, Italy) was used. The configuration characteristics of the block are summarized in table 2 and its layout can be seen in figure 1. The Pavia block provided all necessary data for the validation purposes mentioned with the exception of the INS/GPS-derived linear velocities and calibrated angular velocities that were not available to the author at the moment of setting up the experiments. To overcome this, the correct INS/GPS-derived velocities were approximated by numerically differentiating the INS/GPS-derived positions at the image exposure time epochs with the three-point stencil method.

| | |
|---|---|
| Scale | 1:8000 |
| Flying height | 1200 m |
| No. of strips | 11 (7+4) |
| No. of images per strip | $\approx 10$ |
| No. of photo-observations per image | $\approx 30$ |
| No. of Ground Control Points (GCP) | 8 |
| No. of Ground Check Points (CP) | 24 |
| No. of images | 131 |
| No. of photo-observations | 4167 |
| No. of tie-points | 477 |
| Overlap | $\approx 60\% \times 60\%$ |

Table 2: Pavia block configuration characteristics.

### 3.1 Spatial Absolute vs Spatio-temporal Absolute

The goal of this section is to validate whether the multi-sensor time synchronization parameter $\Delta t$ can be significantly estimated with a sufficient precision and to provide some insight on the corresponding required block configurations and, eventually, mission configurations. The validation consists on the controlled determination of a significant and precise $\Delta t$ that preserves or improves the quality of the block which is measured by the point determination accuracy at the ground check points (CPs).

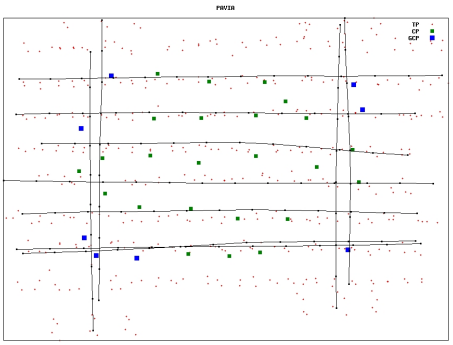

Figure 1: Pavia block layout.

| Test | Model | Shift | Velocity |
|---|---|---|---|
| A | Spatial | 1 per strip (11) | - |
| B | Spatial | 1 per block | - |
| C | Spatio-temporal | 1 per strip (11) | ct-actual |
| D | Spatio-temporal | 1 per block | ct-actual |
| E | Spatio-temporal | 1 per strip (11) | non-ct |

Table 3: Absolute spatial and spatio-temporal block configurations.

As it is to be expected (equation 3), for approximately constant velocities, the GPS positioning error calibration parameters $\vec{\mathrm{S}}^{\mathrm{l}}$ —the popular GPS "shift" parameters— and the time synchronization parameter $\Delta t$ are highly correlated if the classical block configurations of one "shift" per strip are used. This is due to the constant-computed velocities. Therefore, to a large extent, the concept validation problem reduces to the analysis of the conditions under which, the $\Delta t$ and the various $\vec{\mathrm{S}}^{\mathrm{l}}$ can be de-correlated. For this purpose, the data were perturbed with time synchronization errors and five block/mission configurations were analyzed as described in table 3. In the table, ct-actual refers to the more or less constant actual velocities and non-ct refers to the perturbed linear velocities where the strips' ends are flown at a different speed while taking the first and last images. For all these configurations or tests, the observables' precisions at the 1-$\sigma$ level are listed in table 4 where IC denotes photogrammeric image coordinates observations, P position, A attitude and V velocity. Note that for the PA control the sequence of observations is $(X,Y,Z,\psi,\vartheta,\gamma)$.

The tests results are shown in table 5. The first column

| Observable | $\sigma$ | Units |
|---|---|---|
| IC | $(5,5)$ | um |
| GCP | $(5,5,7)$ | cm |
| INS/GPS PA | $(5,5,7,8,5,5)$ | cm, mdeg |
| INS/GPS V | $(5,5,5)$ | mm/s |

Table 4: Observables' precisions.

contains the test identifier, the second one the Root-Mean-Square (RMS) of the ground coordinate differences with respect the check points (CP); the third one the estimated standard deviations of the images' exterior orientation (EO) parameters; the fourth one the estimated standard deviations of the object points (TP); and the last one the estimated standard deviation of the time synchronization parameter.

| Test | CP (mm) RMS | EO (mm) $\sigma$ | TP (mm) $\sigma$ | $\Delta T$ (ms) $\sigma$ |
|---|---|---|---|---|
| A | $(36, 27, 25)$ | $(35, 36, 32)$ | $(29, 30, 47)$ | – |
| B | $(35, 25, 28)$ | $(35, 35, 32)$ | $(29, 30, 47)$ | – |
| C | $(36, 27, 25)$ | $(35, 36, 32)$ | $(29, 30, 46)$ | 2.2 |
| D | $(34, 24, 27)$ | $(35, 35, 32)$ | $(29, 30, 47)$ | 0.1 |
| E | $(35, 26, 25)$ | $(35, 36, 32)$ | $(28, 30, 46)$ | 0.2 |

Table 5: Absolute spatial and spatio-temporal test results.

The analysis of table 5 reveals that the systematic GPS aerial control errors can be absorbed with just one shift parameter (compare rows A and B) which corresponds, for instance, to situations where the GPS reference receiver is close to the block area. This has allowed to significantly estimate (test D, functional model of equation 3) the $\Delta t$ parameter with just one shift parameter for the entire block with a precision of 0.1 ms which translates to less than 1 cm in the object space. Moreover, the estimated $\Delta t$ maintains the block quality level as proven by the correct results at the check points. If one shift parameter per strip is introduced, then the time synchronization parameter cannot be estimated at the required precision level —2.2 ms or 18 cm in the object space— and, although the CP, EO and TP columns show correct values, the configuration is labelled as "non acceptable." However, experience tells that enforcing the use of just one single shift parameter per block does not make sense in many —if not most— of cases. In order to circumvent this problem, the block data were "manipulated" to simulate the case of strips flown at different velocities at their ends while taking the first and last images (test E). In this case, the $\Delta t$ parameter and 11 shift parameters, one per strip, could be significantly and precisely estimated ($\sigma_{\Delta T} = 0.2$ ms).

The presented preliminary results are encouraging and indicate that if, as a result of windy weather or of simple aircraft velocity "maneuvers," the constant velocity limitation is broken, multi-sensor time calibration as presented in this paper is feasible. Last, note that the used velocities were not obtained from INS/GPS data and that the observation equation 4 was not used. In other words, there is room for further improvement.

### 3.2 Spatial Absolute vs Spatial Relative

The main goal of this section is to validate the aerial relative control models of equations 5 and 6. The validation consists on the comparative analysis of a standard ISO block configuration with absolute spatial aerial control and a new one with relative control via the RMS of coordinate differences at check points. For this purpose, the Pavia block was used again. The observations' precisions are described in table 6 which is largely self-explanatory.

| Observable | $\sigma$ | Units |
|---|---|---|
| IC | $(5, 5)$ | um |
| GCP | $(8, 8, 10)$ | cm |
| INS/GPS Abs PA | $(7, 7, 11, 8, 5, 5)$ | cm, mdeg |
| INS/GPS Rel PA | $(4, 4, 8, 2.7, 2.7, 2.7)$ | cm, mdeg |

Table 6: Observables' precisions.

| Test | CP (mm) RMS | EO (mm,mdeg) $\sigma$ | TP (mm) $\sigma$ |
|---|---|---|---|
| Abs | $(35, 27, 26)$ | $(39, 40, 35, 1.3, 1.3, 0.8)$ | $(32, 33, 49)$ |
| Rel | $(33, 26, 27)$ | $(39, 42, 46, 1.4, 1.2, 0.8)$ | $(35, 36, 58)$ |

Table 7: Absolute vs relative aerial control test results.

One of the advantages of the INS/GPS relative control is its high short term precision. Accordingly, the INS/GPS relative control precisions have been [conservatively] set to values consistent with the photogrammetric base and the IMU used in the Pavia block (row 'INS/GPS Rel PA' of table 6).

The results are shown in table 7. The first column contains the test configuration (Abs and Rel refer to the spatial aerial absolute and relative control models respectively); the rest of the columns are similar to those in table 5. On the one hand, the results confirm that ISO can be performed without shift and boresight calibration parameters at the price of larger estimated standard deviations in the height components of ground points (20% worse) and projection centers (30% worse). This is thought to be due to the less favorable error propagation —a somewhat weaker geometry or block *Bierbauch* effect— of relative control. The predicted errors notwithstanding, the results at the ground check points are even [insignificantly] better with relative aerial control. In the author's opinion, these are remarkable results. Indeed, for everyday practical use, the relative control formulation is simpler and less error prone than the absolute one.

Another potential expected advantage of the relative aerial control models is the mitigation of undetected GPS cycle slips effects. For this purpose, the INS/GPS-derived positions of half a central strip were largely perturbed with 50 cm shifts. Figures 2 and 3 show the coordinate differences at check points with the absolute and relative aerial control models respectively. As it can be seen, the relative aerial control models are less sensitive than the absolute aerial control models.

Moreover, the performance of the absolute aerial control models and the relative aerial control models after removed the gross-errors (detected with automated data-snooping) is shown in the table 8. The columns of this table are the same as the columns of the table 7. Again, the RMS of the coordinate differences at check points indicate that the relative control models behave better than the absolute ones.

| Test | CP (mm) RMS | EO (mm,mdeg) $\sigma$ | TP (mm) $\sigma$ |
|---|---|---|---|
| Abs | $(41, 42, 29)$ | $(40, 41, 36, 1.3, 1.3, 0.8)$ | $(33, 34, 50)$ |
| Rel | $(33, 26, 27)$ | $(39, 42, 46, 1.4, 1.3, 0.8)$ | $(35, 36, 58)$ |

Table 8: Absolute vs Relative aerial control test results.

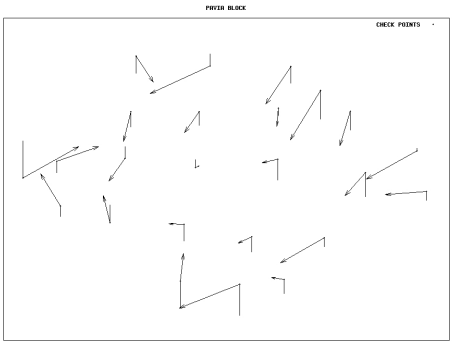


Figure 2: Absolute-estimated coordinate differences at check points of perturbed data test.

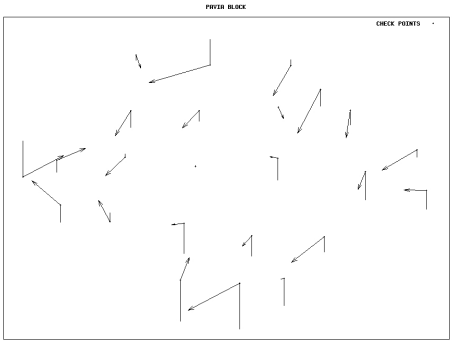


Figure 3: Relative-estimated coordinate differences at check points of perturbed data test.

These preliminary results suggest that the relative control models are more robust and reliable than the absolute aerial control model in front of undetected GPS cycle slips even if the gross-errors are removed from the data.

## 4 CONCLUSIONS AND FURTHER RESEARCH

This paper has introduced new mathematical functional models (equations 2, 3, 4, 5, 6, 7 and 8) for the spatial and spatio-temporal modeling of the GPS- and INS/GPS-derived aerial control data. Using actual data and perturbed actual data, the essential subset of the new functional models (equations 3, 4, 5 and 6) have undergone a succesful preliminary, proof-of-the-concept testing.

In the case of spatial relative aerial control models (equations 5 and 6), the expected advantages have been demonstrated with the first results using actual data. The spatial relative aerial control models eliminates the IMU-to-sensor relative orientation matrix and the GPS positioning error parameters without loss of accuracy and with a moderate loss of precision. Moreover, this model seems to mitigate the effects of undetected GPS cycle slips "better" —in the sense of reliability and robustness— than the spatial absolute aerial control models.

In the case of spatio-temporal absolute aerial control models (equations 3 and 4), the expected advantages are being tested with actual and perturbed data. The first results indicate that the time synchronization parameter can be estimated at the tenth of a milisecond precision level. New block configurations have been identified in order to estimate the multi-sensor time synchronization and the GPS positioning error parameters simultaneously.

The spatio-temporal relative aerial control models are not yet implemented. But, the results of the spatio-temporal absolute aerial control models and spatial relative aerial control models indicate that this approach could be even more reliable and robust, if a few consecutive images could be taken at different velocities. This implementation is planned together with the use of actual data to demonstrate the potential of the temporal calibration models.

## REFERENCES

Ackermann, F. and Schade, H., 1993. Application of GPS for aerial triangulation. Photogrammetric Engineering and Remote Sensing 59(11), pp. 1625–1632.

Blázquez, M. and Colomina, I., 2008. On the Use of Inertial/GPS Velocity Control in Sensor Calibration and Orientation. In: Proceedings of the EuroCOW 2008, Castelldefels, ES.

Colomina, I., 1999. GPS, INS and Aerial Triangulation: what is the best way for the operational determination of photogrammetric image orientation? In: International Archives of Photogrammetry and Remote Sensing, ISPRS Conference "Automatic Extraction of GIS Objects from Digital Imagery", Vol. 32, pp. 121–130.

Frieß, P., 1991. Aerotriangulation with gps-methods, experience, expectation. In: Proceedings of the 43rd Photogrammetric Week, Stuttgart, DE.

Jekeli, C., 2001. Inertial navigation systems with geodetic applications. Walter de Gruyter, Berlin, New York.

Lucas, J., 1987. Aerotriangulation without ground control. Photogrammetric Engineering and Remote Sensing 53(3), pp. 311–314.

Schwarz, K., Chapman, M., Cannon, M. and Gong, P., 1993. An integrated INS/GPS approach to the georeferencing of remotely sensed data. Photogrammetric Engineering and Remote Sensing 59(11), pp. 1667–1674.

## 5 AKNOWLEDGEMENTS

The models are implemented and tested with the generic network adjustment platform GENA from GeoNumerics (Barcelona, Spain). The block data were made available by Prof. Vittorio Casella (Università di Pavia). Last, but not least, the discussions held with Dr. Ismael Colomina (Institute of Geomatics) are kindly acknowledged.

# Chapter 3

# Relative INS/GNSS aerial control

This chapter features the second paper that forms part of the proposed models for a systematic approach to airborne sensor orientation and calibration. There are three essential contributions: relative aerial control models, rigorous mathematical models in a global compound mapping-geodetic coordinate system and constraint observation equations for a dual-head camera system.

The main goal of this paper is the full development and discussion of the funtional relative aerial control model for local cartesian ($l$) and global compound mapping-geodetic ($m$) coordinate systems (Figure 3.1). Its performance is evaluated with three actual independent data sets. But the paper also presents a rigorous model formulation for photogrammetric observations in $m$ frame that, as compared with current practices, eliminates the need for the projection center "height correction" and for the "azimuth correction". Finally, the paper details the constraint observation equations for multi-head camera systems that fix a constant offset and a constant relative orientation matrix between the cameras.

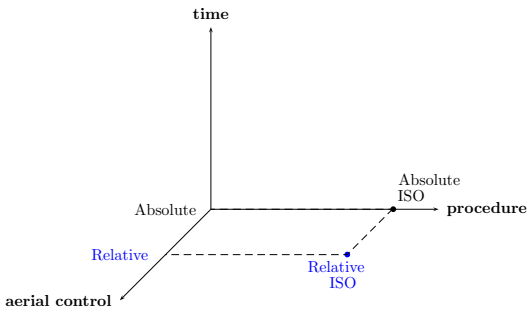


Figure 3.1: Relative aerial control models.

For this research I developed the models, programmed the GENA model toolboxes, performed the calculations and analyzed the results. I wrote the paper with Dr. Ismael Colomina who also promoted and supervised the research.

ISPRS Journal of Photogrammetry and Remote Sensing 67 (2012) 120–133

Contents lists available at SciVerse ScienceDirect

ISPRS Journal of Photogrammetry and Remote Sensing

journal homepage: www.elsevier.com/locate/isprsjprs

# Relative INS/GNSS aerial control in integrated sensor orientation: Models and performance

M. Blázquez *, I. Colomina

*Institute of Geomatics, Av. Carl Friedrich Gauss, 11 Parc Mediterrani de la Tecnologia, E-08860 Castelldefels, Spain*

ARTICLE INFO

*Article history:*
Received 15 July 2011
Received in revised form 14 November 2011
Accepted 14 November 2011

*Keywords:*
GNSS
INS
Relative
Integrated sensor orientation

ABSTRACT

In this paper we present the models and discuss the performance of relative position and attitude INS/GNSS aerial control observations in integrated sensor orientation. In relative aerial control, we use the relative position and attitude of the IMU at the exposure times of successive images instead of the usual absolute position and attitude for each image. With relative aerial control, the GNSS shift correction parameters and the IMU-to-camera boresight matrix vanish from the functional models and so does the problem of their selection. The presented models are formulated with the usual original INS/GNSS attitude parameterisation (heading, pitch and roll) to avoid unnecessary and error-prone intermediate re-parameterisation steps. Furthermore, we present a rigorous model formulation, for both aerial control and photogrammetric observations, in local mapping coordinate systems that eliminate the need of the so-called height and azimuth corrections and that guarantee geodetic correctness and consistency. The overall resulting modelling scheme allows for a direct incorporation of INS/GNSS aerial control observations into the integrated sensor orientation processing chain in a simple and robust way. The performance of the new models is evaluated with three independent data sets and the results show a comparable to better performance.


## 1. Introduction

In a series of preceding papers (Martínez et al., 2007; Blázquez and Colomina, 2008, 2010; Blázquez, 2008) we reviewed established procedures for INS/GNSS-based orientation and calibration of airborne sensors in the light of some well known but often forgotten INS, GNSS and geodetic properties and facts. In the mentioned papers we proposed a number of new concepts for integrated sensor orientation (ISO) and calibration including the use of time-position-attitude (tPA) INS/GNSS-derived aerial (in general, kinematic) control in relative mode, the use of full time-position-velocity-attitude (tPVA) INS/GNSS-derived aerial control in absolute and relative mode for 4D spatio-temporal orientation and calibration, a time-dependent relative stochastic model of tPA INS/GNSS-derived control, and an alternative use of self-calibration parameters in ISO when both static ground and kinematic aerial control are available.

In this paper we describe in detail the models and performance of tPA INS/GNSS-derived aerial control in relative mode – as introduced and initially analysed in Blázquez (2008) – with consideration of local geodetic cartesian coordinate systems and of global compound mapping – geodetic/gravimetric ones.

The couple INS/GNSS is to be found in practically all kinematic, aerial and terrestrial, image acquisition systems and it is there to stay. INS stands for inertial navigation system and encompasses the use of an inertial measurement unit (IMU) in the image acquisition system. GNSS stands for global navigation satellite system. It includes the US GPS and the Russian GLONASS and will include the coming European Galileo and Chinese Compass systems. INS/GNSS can be used for navigation, for orientation and mapping, or both. INS/GNSS belongs to the very design-based principle of imaging sensors of weak geometry (for example, line sensors) and to the very pragmatic reality of other sensors, be it for the purpose of better geometric accuracy, for more flexible mission design or, simply, to match competitors' equipment. INS/GNSS, in a wide range of quality grades, can be found in high-end and low-cost mapping systems ranging from large-format photogrammetric cameras to small-format mass-market ones. Last, INS/GNSS is flown in all types of aerial platforms, from large high-altitude pressurized airplanes to small unmanned aerial systems (UAS).

Because of the large variety of instrument grades, user backgrounds, user communities, applications, etc., INS/GNSS-based ISO shall yield *interoperability*, *flexibility*, *simplicity*, *accuracy* and *robustness*. *Interoperability*, the ability to exchange and use

* Corresponding author. Tel.: +34 93 556 92 80; fax: +34 93 556 92 92.
*E-mail addresses:* marta.blazquez@ideg.es (M. Blázquez), ismael.colomina@ideg.es (I. Colomina).

0924-2716/$ - see front matter © 2011 International Society for Photogrammetry and Remote Sensing, Inc. (ISPRS). Published by Elsevier B.V. All rights reserved.
doi:10.1016/j.isprsjprs.2011.11.003

information between different systems, refers, in our context, to the exchange and use of INS/GNSS-based ISO results. *Flexibility*, the quality of being adaptable or variable, mainly refers to the geometry of the data acquisition mission that should be constrained as little as possible by the INS/GNSS characteristics. *Simplicity* refers to uncomplicated ISO computational procedures. *Accuracy*, a measure of the absence of systematic errors, in our performance analysis, will include the actual accuracy as well as precision. *Robustness* refers here to the capacity to withstand errors, not only in the observations but also in the procedures. One necessary condition for these requirements to be met is that ISO mathematical models be functionally rigorous and properly capture the sensor stochastic properties. The main purpose of the paper is to describe in detail new ISO models that meet the above requirements.

Strictly speaking, integrated sensor orientation and calibration is the method and process of using a set of heterogeneous observations in a grand bundle block adjustment to estimate image orientation, camera calibration and object point parameters. Colloquial, unless otherwise stated, ISO refers to the use of photogrammetric, ground control and INS/GNSS-derived tPA aerial control observations. In the following, INS/GNSS-derived tPA aerial control observations will be referred to as aerial control observations or simply as aerial control.

The ideas behind ISO are relatively simple. They originated in the nineteen eighties with GPS aerial triangulation (Lucas, 1987) and evolved over the next decade with the extension to INS/GPS (Schwarz et al., 1993). In the context of the topic of this paper, we highlight the contributions of (Friess, 1991) (kinematic GPS processing, the concept of GPS shift parameters and the use of cross-strips), (Blázquez, 2008) (spatio-temporal relative and absolute approaches), some major testing exercises (Heipke et al., 2000; Cramer, 2010) and the extension to airborne laser scanning (Kager, 2004; Friess, 2006; Skaloud and Lichti, 2006).

This paper addresses four main contributions that bring simplicity, flexibility, interoperability, accuracy and robustness to ISO:

– elimination of system calibration parameters;
– stationary time dependent stochastic model for relative aerial control;
– new photogrammetric observation models for horizontal map-projected coordinates;
– new attitude aerial control observation models to avoid re-parameterisations steps.

The first paper contribution extends our previous work on the use of aerial control observations in relative mode; i.e., relative position and attitude of the IMU at the exposure times of two successive images. With this approach, the GNSS linear shift and the IMU-to-camera relative orientation matrix – the so-called boresight – parameters vanish from the aerial control model. And so does the problem of their selection, a frequent source of mistakes, particularly under time pressure conditions or with inexperienced operators. Relative aerial control observations bring simplicity to ISO.

The second contribution is a consequence of the first one. In the usual ISO formulation the absolute aerial control observations error is modelled as a time series of independent random variables. This assumption is a rather crude approximation of the actual behaviour of INS/GNSS positioning where, depending on the trajectory dynamics and on the GNSS update rates, the tPVA errors are more or less time correlated and, roughly speaking, grow larger with time. For relative aerial control we propose a stationary time dependent stochastic model. Thanks to this model, images at the end/start of successive survey segments can be related by a relative aerial control observation thus adding strength to the ISO adjustment – i.e., contributing flexibility to the mission design geometry and accuracy to the results.

The third contribution fixes a problem that dates back to the early days of GPS aerial triangulation. In fact, the use of aerial control observations has uncovered a known fact of classical aerial photogrammetry, that had been either forgotten or simply ignored [or absorbed by the GNSS shift parameters], namely, that in compound mapping ($E$,$N$)-geodetic ($h$) coordinate systems, the height component is affected by the scale factor of the map projection making inconsistent the correct heights of the GNSS- and INS/GNSS-derived positions. Up to now, the common practice has been to rescale the aerial control heights. In the paper we propose new photogrammetric observation models that take into account this fact and allow use of original aerial control observations while delivering correct and consistent horizontal and vertical results. This contribution serves the interoperability, simplicity and accuracy requirements.

The fourth and last key contribution of the paper is related to a combined coordinate system and aerial control observations parameterisation issue. The common practice is to re-parameterise the attitude Euler angles in the aerial control observations from the INS/GNSS convention into the photogrammetric one and then to correct (sic) the third angle $\kappa$ so the sensor attitude is given with respect to the mapping coordinate system. It goes without saying and experience confirms that, in addition to being troublesome, these transformation steps are unnecessary if, as we show, the appropriate models are used. This approach adds robustness and simplicity to the overall ISO procedure.

The paper is organized in two main sections: mathematical models and performance analysis. They correspond to the main tasks of the research. In the mathematical section, the functional and the stochastic models are presented. In the performance analysis section, before presenting and discussing the results, the data and analysis methods are described. Finally, after the conclusions, an appendix with the mathematical models and results of a multi-head camera system with inter-head relative orientation constraints is included.

## 2. Mathematical models

From a modelling point of view, the paper's contributions can be summarized in the derivation of functional and stochastic models for the relative aerial control observations and in the derivation of functional models appropriate for the compound mapping-geodetic coordinate systems. In all cases, the observations, photogrammetric or aerial control, are the original ones as delivered by photogrammetric measuring systems and by INS/GNSS post-processing programmes.

This modelling approach is, in turn, derived from one obvious fact (item 1 below) and one simple modelling principle (item 2).

1. *If a sensor and an IMU are rigidly attached, the sensor relative attitude between any two epochs is the same as the IMU relative attitude between the same two epochs* (Blázquez, 2008).
2. The *"do not touch the observations"* principle; i.e., rather than modifying the actual observations with "corrections" so they fit into coarse models, we write models closer to reality so that observations better fit in them.

From a mathematical point of view, this translates into functional estimation models for sensor orientation, sensor calibration and point determination that use the original INS/GNSS-derived aerial control observations and that do not include the usual GNSS linear shift and IMU-to-camera relative orientation matrix parameters (Sections 2.2.3 and 2.3.3). It also translates into a simple and natural way to stochastically model the time correlated errors of

INS/GNSS-derived trajectories (Section 2.4). Last, we do not only use the original aerial control observations but also the original photogrammetric ones thus concentrating the modelling effort in the models and neither in additional preprocessing software nor in users.

All in all, in the rest of this section, we will identify, and where appropriate, develop in detail one stochastic model and six functional models: the photogrammetric collinearity observation equations, the absolute aerial control observation equations and the relative aerial ones; both for local cartesian coordinate systems and for global compound mapping-geodetic ones.

### 2.1. Reference frames, notation and naming conventions

For the sake of clarity and correctness, the type of reference frames and coordinate systems – i.e., of coordinate reference frames (CRF) or, simply, *frames* – used in the models is described next. As already mentioned, we will develop our functional models for two frame types, $l$ and $m$. A frame of the $l$-type is a local level geodetic [terrestrial] reference frame together with local cartesian coordinates in some right-handed system. Two frames of the $l$-type will be used, $l$ and $l'$, with coordinate sequences east-north-up $(e, n, u)$ and north-east-down $(n, e, d)$, respectively. A frame of the $m$-type is a global terrestrial reference frame together with horizontal map-projected coordinates $E$, $N$ (easting and northing) and vertical ellipsoidal or gravimetric heights $h$. Just one frame of the $m$-type will be used and called $m$ as well. In addition to the frames $l$, $l'$ and $m$, three instrumental frames are required: $c$ for the camera; $b$ (forward-left-up) and $b'$ (forward-right-down) for the IMU.

In the observation equations we will use superscripts to indicate the frame of vectors like in $P^m$; superscripts and subscripts to indicate the "to" and "from" frames, respectively, of rotation matrices and scale factors like in $R_c^b$ and $s_l^m$; the superscript $T$ to transpose vectors like in $[(E, N, h)^m]^T$ and vector subscripts to distinguish two different vectors like $P^m$ and $P_o^m$. For the sake of clarity, if $X^m$ is a vector, we will write $X^m = (x, y, z)^m$ instead of the formally correct notation $X^m = [(x, y, z)^m]^T$ and when rotation matrices are explicitely parameterised by, say, $\chi_b^l$ we will use $R_b^l(\chi)$ instead of $R(\chi_b^l)$.

### 2.2. Functional models for the l frame

#### 2.2.1. Collinearity

The model for image measurements whose object space is represented in the $l$ frame is the set of traditional collinearity equations. They are well known and not reproduced in this paper (Mugnier et al., 2004).

#### 2.2.2. Absolute spatial aerial control

The absolute aerial control observation equations in the $l$ frame are described in (Blázquez, 2008). We reproduce them here for the sake of completeness. They consist of a positional and an attitude part (Eqs. (1) and (2) below, respectively). The positional part is

$$X^l + V_X^l = P^l + R_c^l(\Gamma) \cdot (A^c + N^c) + S^l \tag{1}$$

where $P^l$ is the camera projection centre, $R_c^l(\Gamma)$ is the camera attitude matrix (usually parameterised by Euler angles $\Gamma = (\omega, \varphi, \kappa)$), $A^c$ is the camera-to-IMU lever arm, $N^c = (0, 0, n)$ is the camera nodal vector, $n$ is the nodal distance, and $S^l$ is the GNSS shift correction vector. $X^l$ and $V_X^l$ are the vectors of aerial position observations and residuals, respectively.

The attitude part is

$$R_c^l(\Gamma) = R_b^l(\chi + V_\chi) \cdot R_c^b \tag{2}$$

where $R_b^l(\chi + V_\chi)$ is the IMU attitude matrix and $R_c^b$ the IMU-to-camera relative attitude (boresight) matrix. $\chi = (\psi, \theta, \gamma)$ are the aerial attitude angular observations heading $(\psi)$, pitch $(\theta)$ and roll $(\gamma)$ and $V_\chi$ is the angular residuals vector.

Note that, in the INS field, it is customary that the angles in $\chi$, as obtained from INS and INS/GNSS programmes, be used to parameterise the matrix $R_{b'}^{l'}(\chi)$ which is related to $R_b^l(\chi)$ as

$$R_b^l(\chi) = R_{l'}^l \cdot R_{b'}^{l'}(\chi) \cdot R_b^{b'}$$

where $R_{l'}^l$ and $R_b^{b'}$ are constant matrices.

#### 2.2.3. Relative spatial aerial control

Relative aerial control observation equations relate the orientation parameters of two [consecutive] images through their corresponding absolute aerial control observations (Blázquez, 2008). In the $l$ frame they are

$$X_1^l - X_2^l + V_{\Delta X}^l = P_1^l - P_2^l + \left(R_c^l(\Gamma_1) - R_c^l(\Gamma_2)\right) \cdot (A^c + N^c) \tag{3}$$

and

$$R_c^l(\Gamma_1) \cdot R_l^c(\Gamma_2) = R_b^l(\chi_1) \cdot R_l^b(\chi_2 + V_{\Delta\chi}) \tag{4}$$

where the subscripts 1 and 2 distinguish the orientation elements $(P^l, \Gamma_c^l)$ of the two involved images and the INS/GNSS-derived position $X^l$ and attitude $\chi_b^l$ at the respective image acquisition time epochs.

Note, that parameters $S^l$ (GNSS shifts) and $R_c^b$ (boresight matrix) have vanished in Eqs. (3) and (4), as compared to Eqs. (1) and (2), respectively. As discussed in (Blázquez, 2008), this is one of the advantages of using relative control, namely that the ISO software user does not need to care about GNSS shifts and IMU-to-camera relative attitude issues.

It also bears mentioning that relative aerial control can be applied to the last and first images of two consecutive strips, regardless of whether the aerial control applied to images of the same strip is absolute or relative aerial control. This means that, in an ISO procedure, the INS/GNSS-derived information of each image can be modelled with absolute aerial control (Eqs. (1) and (2)) or with relative aerial control (Eqs. (3) and (4)), but the INS/GNSS-derived information of the last image of each strip and the first image of the next strip can always be modelled with relative aerial control (Eqs. (3) and (4)) adding more control information to the ISO procedure.

In Eq. (3) above we have written the explicit position $X_1^l - X_2^l + V_{\Delta X}^l$ difference by using the absolute position $X_1^l$, $X_2^l$ observations instead of already differentiated ones $\Delta X^l + V_{\Delta X}^l$. Similarly, in Eq. (4) for the relative attitude aerial control we have written $R_b^l(\chi_1) \cdot R_l^b(\chi_2 + V_{\Delta\chi})$ instead of $R_l^l(\Delta\chi + V_{\Delta\chi})$. This is done on purpose in order to facilitate the use of the INS/GNSS trajectory output. Note, however, that in both Eqs. (3) and (4) the residual position and attitude vectors $V_{\Delta X}^l$, $V_{\Delta\chi_b}^l$ refer to actual relative residuals to apply a correct stochastic model to actual relative observations. We claim (Section 2.4) that the stochastic model for relative aerial control observations is more natural than the stochastic model for the absolute ones.

### 2.3. Functional models for the m frame

In the next three sections we introduce the functional models for image, absolute aerial and relative aerial observations in the $m$ frame. The combined use of the models offers a simple interface to the ISO software user as no corrections need to be applied to the measurements and, analogously to the $l$ frame case, there is no need to deal with GNSS shift and boresight parameters if relative aerial control is used. In contrast to other approaches, the horizontal scale factor of map projections is modelled on the collinearity equations and neither on the aerial control observations nor on the camera calibration constants (the so-called height and focal

length corrections). We claim that this is the natural way of modelling since the horizontal-vertical scale inconsistency affects the collinearity models and not the aerial control ones, see also the independent approaches of Alamús et al. (2002) and Skaloud and Legat (2008).

*2.3.1. Collinearity*

For the $m$ frame, we provide a modified version of the traditional collinearity equations where the scale factor $s_l^m$ between the horizontal and the vertical coordinates is taken into account

$$\begin{aligned}(x-x_0)+\delta x+v_x &= -f\frac{m_{11}(E_o-E)+m_{12}(N_o-N)+m_{13}s_l^m(h_o-h)}{m_{31}(E_o-E)+m_{32}(N_o-N)+m_{33}s_l^m(h_o-h)}\\ (y-y_0)+\delta y+v_y &= -f\frac{m_{21}(E_o-E)+m_{22}(N_o-N)+m_{23}s_l^m(h_o-h)}{m_{31}(E_o-E)+m_{32}(N_o-N)+m_{33}s_l^m(h_o-h)}\end{aligned} \tag{5}$$

where $P_o^m=(E_o,N_o,h_o)^m$ is the object point, $P^m=(E,N,h)^m$ is the camera projection centre, $(m_{ij})_{1\leqslant i,j\leqslant 3}=R_m^c(\Gamma)$ is the camera attitude matrix, $s_l^m$ is the scale factor of conformal map projections that depends on $P^m$, $(x_0,y_0)^c$ is the camera principal point, $f^c$ the camera constant and $(\delta x,\delta y)^c$ the total effect of atmospheric refraction and Earth curvature modelling. $(x,y)^c$ and $(v_x,v_y)^c$ are the image observations and their residuals, respectively (for the sake of simplicity and clarity, the frames are only specified in the description of the terms of Eq. (5), but not in the explicit equations.).

The actual final model further extends Eq. (5) with self-calibration functions (for example, Ebner or Gruen self-calibration functions).

We note that modelling of refraction and Earth curvature effects is included in $(\delta x,\delta y)^c$ and, therefore, the typical image "corrections" for refraction and Earth curvature need not to be applied to the original observations before the adjustment. Therefore, the ISO software user avoids the problem of "what corrections have to be or have been applied."

*2.3.2. Absolute spatial aerial control*

Since $s_l^m$ in Eq. (5) already accounts for the scale ratio between the horizontal and vertical coordinates in an $m$ frame, there is no need to modify the altitude provided by the aerial control observations. Therefore, simple observation equations can also be written for the positional part of the absolute aerial control in the $m$ frame:

$$X^m+V_X^m=P^m+R_c^m(\Gamma)\cdot(A^c+N^c)+S^m, \tag{6}$$

where $X^m$ is the aerial control position observation, $V_X^m$ its residual vector, and $S^m$ is the GNSS shift parameter in the $m$ frame.

The attitude part is

$$R_c^m(\Gamma)=R_l^m(\eta)\cdot R_b^l(\chi+V_\chi)\cdot R_c^b \tag{7}$$

where $\eta_l^m$ is the meridian convergence angle of conformal map projections at $P^m$, and $R_l^m(\eta)$ is the three dimensional rotation matrix – rotation around the normal line to the ellipsoid through $P^m$ – that brings the local frame $l$ to the mapping frame $m$.

Note that the inclusion of $R_l^m(\eta)$ in the model allows use of the original aerial control attitude observation vector $\chi$ with no external "heading correction."

*2.3.3. Relative spatial aerial control*

From Eqs. (6) and (7) for absolute position and attitude aerial control respectively, new observation Eqs. (8) and (9) for relative aerial control can be easily deduced. The equation for the positional part is

$$X_1^m-X_2^m+V_{\Delta X}^m=P_1^m-P_2^m+\left(R_c^m(\Gamma_1)-R_c^m(\Gamma_2)\right)\cdot(A^c+N^c) \tag{8}$$

where the subscripts 1 and 2 distinguish the orientation elements $(P^m,\Gamma_c^m)$ of two [consecutive] images and their associated aerial control positions.

Analogously, the observation equation for the attitude part is

$$R_c^m(\Gamma_1)\cdot R_m^c(\Gamma_2)=R_l^m(\eta_1)\cdot R_b^l(\chi_1)\cdot R_l^b(\chi_2+V_{\Delta\chi})\cdot R_m^l(\eta_2) \tag{9}$$

where the subscripts 1 and 2 distinguish, as well, the meridian convergence angles ($\eta=\eta(P^m)$) of conformal map projections at projection centres $P^m$ and their corresponding aerial control angles $\chi_l^b$.

As for the $l$ frame, one of the advantages of using relative control, is that the parameters $S^m$ (GNSS shifts) and $R_c^b$ (boresight matrix) have vanished in Eqs. (8) and (9), respectively. Also note, that the use of the original $\chi=(\psi,\theta,\gamma)$ INS/GNSS angular parameterisation together with the $R_l^m(\eta)$ rotations, both in the absolute and relative aerial control approaches, allow the use of the original angular aerial control observations with no need to re-parameterise to the conventional photogrammetric angular sequences.

*2.4. Stochastic model*

Since the IMU calibration is not perfect and since inertial error measurements propagate in a cumulative way – even in the presence of GNSS and filtering – the INS/GNSS-derived position, velocity and attitude errors are time correlated. Similarly, albeit of lesser impact, GNSS delivers time correlated errors. Absolute GNSS-derived positions are affected by remaining unmodelled tropospheric, ionospheric, satellite orbit, satellite clock and other GNSS system errors. Locally generated GNSS errors, at the receiver, like incorrectly estimated carrier phase ambiguities or multipath effects also generate time correlated errors. Differential GNSS techniques remove the former to a large extent but cannot deal with the latter. Thus, from a stochastic point of view, as it is well known, the strict absolute aerial control models are incorrect because they are based on the assumption that aerial control observations at different epochs are stochastically independent. Traditionally this has been mitigated by extending the models with shift parameters (almost invariably for the position models and less frequently for the attitude ones). On the contrary, the proposed relative approach correctly translates the INS/GNSS error characteristics into the relative aerial control stochastic model.

Next, we describe the criteria to establish the relative aerial control stochastic models. For pragmatical reasons we derive them from the usually available error estimates provided by the INS/GNSS system vendors (Applanix, 2011): absolute and relative precision and accuracy figures to describe the quality of attitude and absolute figures for position. Since INS/GNSS position errors are dominated by the GNSS errors, we model the relative aerial control position errors according to the GNSS error information. Relative aerial control attitude errors are modelled according to the INS/GNSS error information.

The precision of relative attitude aerial control ($\sigma_a^2(\Delta t)$) is computed in terms of a random walk process (precision) and [remaining uncalibrated] drift (accuracy) as

$$\sigma_a^2(\Delta t)=\left(\omega\cdot\sqrt{\Delta t}\right)^2+(b\cdot\Delta t)^2 \tag{10}$$

where $\omega$ and $b$ are the angular driving white noise and the angular drift, respectively, as specified by the manufacturers up to a maximum value defined by the absolute precision figures. Typical value intervals for $\omega$ and $b$ are

$$[0.005,0.1]\,\mathrm{deg}/\sqrt{\mathrm{h}}\quad\text{and}\quad[0.01,0.5]\,\mathrm{deg/h}$$

respectively (Applanix, 2011). From our experience in processing INS/GNSS trajectories we claim that, while $\omega$ is usually the same for the three attitude parameters, $b$ may have to be assigned two

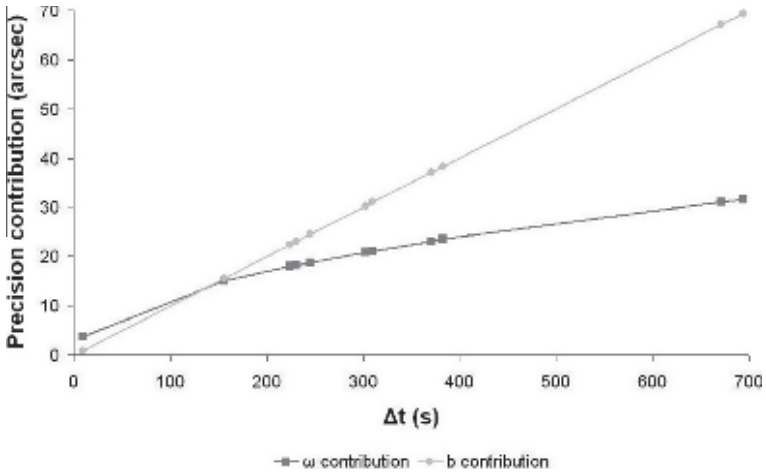


**Fig. 1.** Contribution of $\omega$ and $b$ to relative attitude control precision ($\omega = 0.02$ deg/$\sqrt{\text{h}}$, $b = 0.1$ deg/h).

**Table 1**
P block: accuracy results for different $k(\Delta t)$ values ($\sigma(e,n)_p = 35$ mm, $\sigma(u)_p = 55$ mm).

| Within strip $k(\Delta t)$ | Between strips $k(\Delta t)$ | MEAN ChP (mm) | | | RMS ChP (mm) | | |
|---|---|---|---|---|---|---|---|
| | | e | n | u | e | n | u |
| 1/16 | 64 | 2 | −7 | 10 | 34 | 26 | 33 |
| 1/4 | – | 1 | −9 | 8 | 33 | 26 | 31 |
| 1/4 | 64 | 0 | −9 | 6 | 32 | 25 | 30 |
| 1/4 | 4 | −1 | −8 | 6 | 33 | 24 | 30 |
| 1/4 | 3 | −1 | −7 | 6 | 33 | 23 | 30 |
| 1/4 | 1 | −1 | −7 | 6 | 33 | 22 | 30 |
| 1/2 | 2 | −2 | −7 | 2 | 32 | 22 | 29 |
| 1 | 1 | −4 | −9 | −2 | 32 | 22 | 30 |

different values, one for heading and one for pitch and roll (see next section).

Fig. 1 illustrates the contribution of the $\omega$ and $b$ terms of Eq. (10) for $\omega = 0.02$ deg/$\sqrt{\text{h}}$ and $b = 0.1$ deg/h corresponding to the heading angular component.

The precision of relative position aerial control ($\sigma_p^2(\Delta t)$) is a subtle issue because, in the practice of airborne photogrammetry and remote sensing, it depends on the GNSS features as well as on the processing strategies, for instance, on the approach to solve the double differenced ambiguities. Thus, GNSS trajectory processing strategies may treat the various flight lines or strips as independent data sets; i.e., may try to use the same satellites within a flight line but not necessarily for two different though consecutive ones (note that this level of freedom is not available in INS trajectory

**Table 2**
Test blocks: geometric configuration.

| Test block | Pavia (P) | Salou (S) | Vaihingen/Enz (V) |
|---|---|---|---|
| Equipment | Leica RC30 | Z/I DMC | IGI Dual-DigiCAM-H/39<br>Roll Angle Left H/39 −14.8°<br>Roll Angle Right H/39 +14.8° |
| | Applanix POS AV 510 | Applanix POS AV 510 | AEROControl II-D |
| Image size | 23 × 23 cm<br>16329 × 16329 px | 9 × 17 cm<br>7680 × 13824 px | 2 × 5 × 4 cm<br>2 × 7216 × 5412 px |
| Image size (along flight direction) | 23 cm | 9 cm | 4 cm |
| Image size (across flight direction) | 23 cm | 17 cm | 2 × 5 cm |
| Pixel size | 14 μm | 12 μm | 6.8 μm |
| Camera constant | 153 mm | 120 mm | 82 mm |
| Flying height above ground (≈) | 1200 m | 1000 m | 1150 m |
| Scale (≈) | 1:8000 | 1:8800 | 1:14000 |
| Ground sampling distance (GSD) (≈) | 11 cm | 11 cm | 10 cm |
| No. of strips | 11 (7 + 4) | 7 (5 + 2) | 6 (3 + 3) |
| No. of images | 131 | 112 | 2 × 120 |
| No. of images per strip (≈) | 10 | 15 | 2 × 20 |
| No. of photo-observations | 4167 × 2 | 6049 × 2 | 7910 × 2 |
| No. of photo-observations per image (≈) | 30 × 2 | 50 × 2 | 30 × 2 |
| No. of ground control points (GCP) | 8 | 10 | 8 |
| No. of ground check points (ChP) | 25 | 38 | 14 |
| No. of tie-points (TP) | 478 | 1151 | 1106 |
| Overlap (≈) | 60 × 60% | 60 × 30% | 60 × 76% |
| Coordinate reference frame | *l* | *m* | *m* |

processing.). Therefore, we empirically investigated and found that $\sigma_p^2(\Delta t)$ can be expressed as a function of the precision of absolute position control ($\sigma_p^2$) as

$$\sigma_p^2(\Delta t) = k(\Delta t) \cdot \sigma_p^2. \quad (11)$$

where $k(\Delta t)$ is almost constant. After analysing the GNSS shift parameter ($S^l$ and $S^m$) estimates in ISO blocks and testing their performance, the recommended values for $k(\Delta t)$ are in the following ranges: $k(\Delta t) \in [1/4,1]$ for consecutive images of the same strip and $k(\Delta t) \in [1,4]$ for consecutive images in different, consecutive strips.

As an example, Table 1 shows the ground point accuracy results of different relative ISO adjustments of the Pavia block (P) (see the block characteristics in Section 3). Each row of the table corresponds to one relative ISO adjustment of the P block where the relative position aerial control precision is computed with Eq. (11) for a selected $k(\Delta t)$ value for consecutive images of the same strip (first column) and another $k(\Delta t)$ value for consecutive images in different, consecutive strips (second column). The ground point accuracy is measured by the mean (third column) and Root-Mean-Square (fourth column) of the coordinate differences with respect to the Check Points (ChP).

In spite of the table results, with the everyday operational conditions in mind, for the sake of robustness and even at the price of slightly worsening our results we propose and have used $k(\Delta t) = 4$ for consecutive images of the same strip and $k(\Delta t) \approx 64$ (instead of any recommendable value $k(\Delta t) \in [1,4]$) for consecutive images in different, consecutive strips.

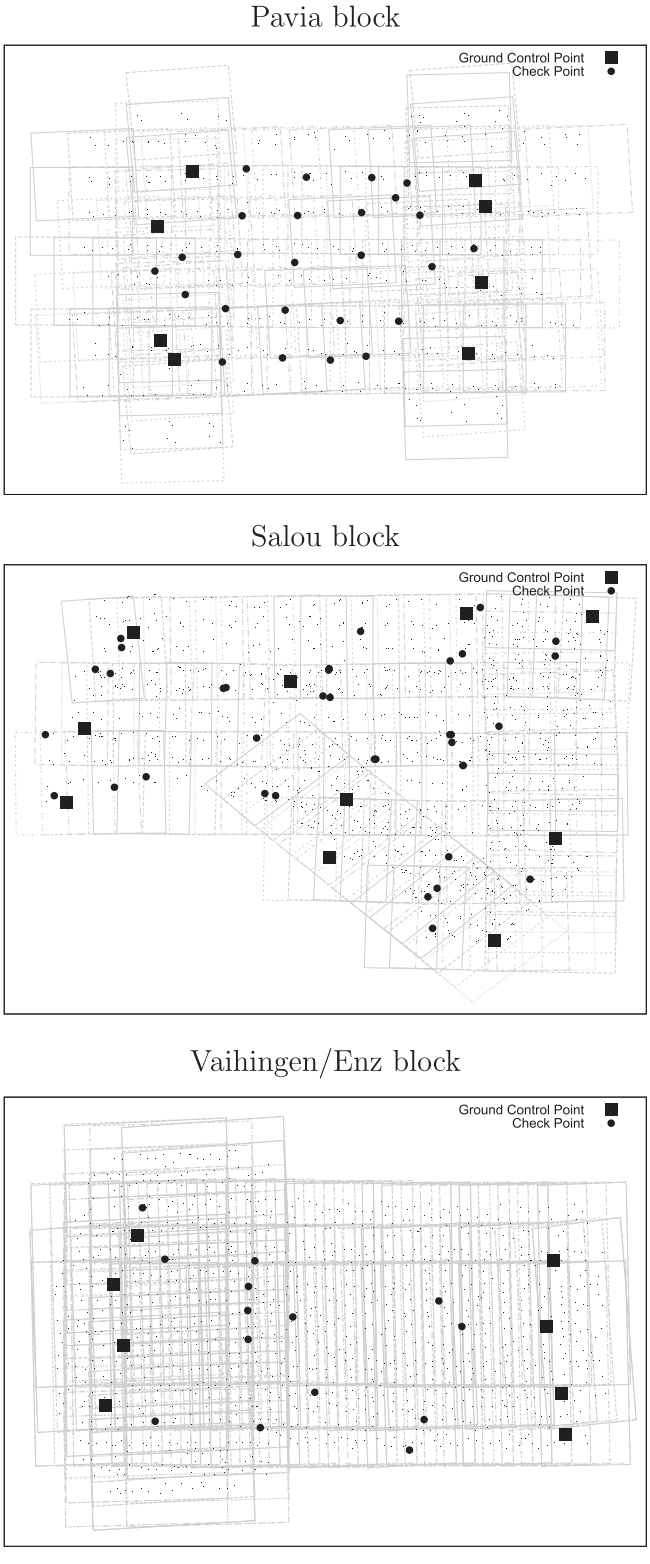


**Fig. 2.** Test blocks: layouts.

## 3. Performance analysis

In the following paragraphs, the properties and performance of relative spatial aerial control are investigated for analogue, digital large format and multiple-head medium format cameras. In the computations, depending on the test block, the *l* or *m* frame and models are used.

### 3.1. Test data

We selected three test blocks of similar flying altitude for each one of the camera types mentioned above: a block captured with an analogue Leica RC30 camera (the Pavia block), a block captured with a digital large format Zeiss/Intergraph (Z/I) DMC (DMC1-0026) camera (the Salou block), and a block captured with a digital dual-head medium format, IGI Dual-DigiCAM-H/39, camera (the Vaihingen/Enz block). The blocks are intended to represent the main types of frame cameras currently in use and their control configurations (ground control distribution and INS/GPS trajectory processing). Details on the geometric configuration of the blocks,

**Table 3**
Test blocks: precision of observables.

| Observables | Block | | | Units |
|---|---|---|---|---|
| | P | S | V | |
| *Image coordinates* | | | | |
| – $\sigma_{x,y}$ | 4.8 | 1.5 | 1.4 | μm |
| | 0.34 | 0.13 | 0.21 | px |
| *Ground control points* | | | | |
| – $\sigma_{E,N}$ | 8 | 5 | 2 | cm |
| – $\sigma_h$ | 10 | 6 | 2 | cm |
| *Absolute aerial control* | | | | |
| – $\sigma_{E,N}$ | 3.5 | 3.5 | 3.5 | cm |
| – $\sigma_h$ | 5.5 | 5.5 | 5.5 | cm |
| – $\sigma_{\gamma,\theta}$ | 5 | 5 | 5 | mdeg |
| – $\sigma_\psi$ | 8 | 8 | 8 | mdeg |
| *Relative aerial control* | | | | |
| – $\sigma_{\Delta E,\Delta N}$ (within strips) | 1.75 | 1.75 | 1.75 | cm |
| – $\sigma_{\Delta h}$ (within strips) | 2.75 | 2.75 | 2.75 | cm |
| – $\sigma_{\Delta E,\Delta N}$ (between strips) | 28 | 28 | 28 | cm |
| – $\sigma_{\Delta h}$ (between strips) | 44 | 44 | 44 | cm |
| – $\omega$ | 0.02 | 0.02 | 0.010 | deg / $\sqrt{\text{h}}$ |
| – $b_{\gamma,\theta}$ | 0.01 | 0.01 | 0.005 | deg/h |
| – $b_\psi$ | 0.10 | 0.10 | 0.050 | deg/h |

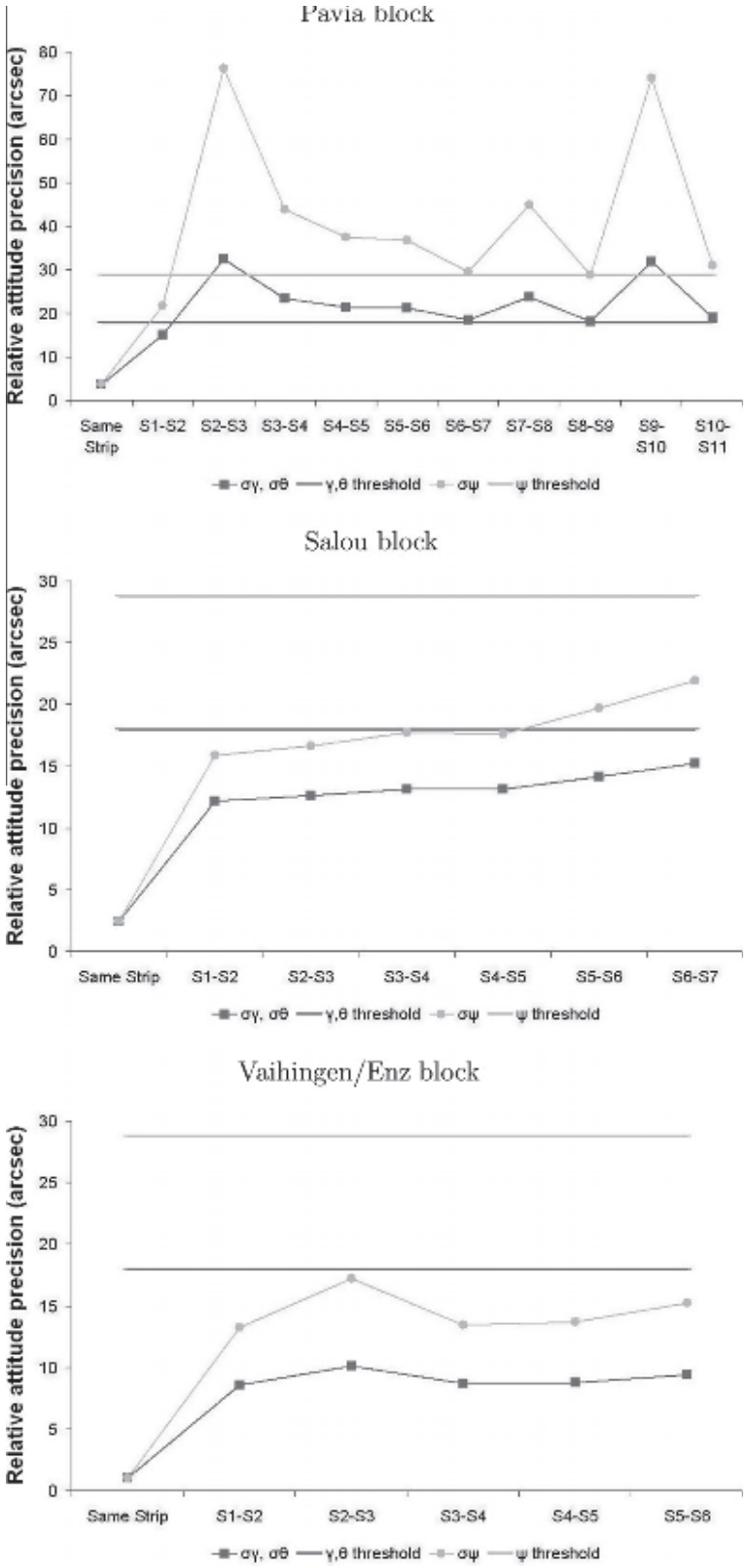


**Fig. 3.** Precision of relative attitude control as derived from Eq. (10) thresholded by 18″ ($\gamma$, $\theta$) and 28.8″ ($\psi$) absolute precision values.

general layouts and the precision of their observations are given in Table 2, Fig. 2 and Table 3, respectively.

The photogrammetric measurements, the ground control measurements and distribution, the INS/GPS-derived trajectories and lever arm values were used as given by the three block providers in order to stick to actual ISO operational conditions.

Table 3, together with Eqs. (10) and (11), describe the precision of the measurements of the P, S and V test blocks following the

**Table 4**
Test block configurations for general positioning and orientation performance analysis; P, S and V blocks.

| Test | INS/GNSS aerial control | Control BS | Cross strips |
|---|---|---|---|
| A-pa-woros-wcs | Absolute tPA | No | Yes |
| A-pa-woros-wocs | Absolute tPA | No | No |
| R-pa-wros-wcs | Relative tPA | Yes | Yes |
| R-pa-wros-wocs | Relative tPA | Yes | No |

BS: between strips.

**Table 5**
Test block configurations for the illustration of recommendable mission configurations.

| Test | INS/GNSS aerial control | Control BS | Cross strips |
|---|---|---|---|
| A-p-woros-wcs | Absolute tP | No | Yes |
| A-p-woros-wocs | Absolute tP | No | No |
| A-pa-wros-wocs | Absolute tPA | Yes | No |
| R-p-wros-wcs | Relative tP | Yes | Yes |
| R-p-wros-wocs | Relative tP | Yes | No |
| R-pa-woros-wcs | Relative tPA | No | Yes |
| R-pa-woros-wocs | Relative tPA | No | No |

BS: between strips.

rationale of Section 2.4. Fig. 3 further illustrates the precision of relative attitude control for the three test blocks. Its values have been computed from the angular driving white noise $\omega$, angular drifts $b_\gamma$, $b_\theta$, $b_\psi$, time intervals between consecutive images $\Delta t$ and thresholded by the absolute precision values as proposed in Section 2.4.

### 3.2. Analysis targets and selected block configurations

For all block configurations a self-calibrating ISO adjustment has been computed. In the case of absolute aerial control, a linear shift per strip and a boresight per block parameters have been estimated. In all cases, the 12-parameter Ebner self-calibration function (4 sets in the case of the Z/I DMC) has been used (the Ebner function has been selected because of its widespread use and its proven acceptable performance. Admittedly, for some cameras better results could be achieved using other self-calibration functions).

#### 3.2.1. Relative versus absolute configurations

The main analysis target is the point positioning and orientation performance of the relative aerial control models, in *l* and *m* frames, with respect to the absolute ones for the same ground control configurations.

In order to support the above analysis targets two sets of block configurations were selected out of the many configurations analysed in our research. The first set (Table 4) will serve the main analysis target; i.e., for given sparse ground control configurations of the existing P, S and V blocks, we will compare the point positioning and orientation performance with absolute and relative aerial control (*A* and *R* codes), with INS/GNSS-derived position and attitude aerial control (*pa* code), with and without cross strips (*wcs* and *wocs* codes) and with and without relative orientation control between consecutive strips (*wros* and *woros* codes). Clearly, this paper does not address every possible combination of the above codes.

#### 3.2.2. Relative optimal mission configuration

The second analysis target is the identification of optimal and/or recommendable mission configurations – i.e., block geometries – for relative aerial control. The latter target is relevant since the INS/GNSS absolute aerial control contributions to ISO – as compared, for instance, to GNSS absolute aerial control – go beyond the reduction of ground control to the relaxation of block design regularity and fixed flight pattern (cross strips) requirements.

The second set (Table 5) contains some key block configurations that illustrate and support our recommendations for operational block configurations. In this case, the scope of the analysis will include absolute and relative aerial control (*A* and *R* codes), INS/GNSS-derived position and INS/GNSS-derived position and attitude aerial control (*p* and *pa* codes), with and without cross strips (*wcs* and *wocs* codes) and with and without relative orientation control between consecutive strips (*wros* and *woros* codes). As for Table 4, only a subset of the possible test combinations has been selected.

### 3.3. Performance indicators, results and discussion

The performance of the new models is analysed through a main indicator, the empirical accuracy of ground point determination, and through an auxiliary one, the predicted precision of both ground point and orientation parameters determination. Ground point accuracy is measured by the Root-Mean-Square (RMS) of the coordinate differences with respect to the Check Points (ChP) which is a measure of both random and systematic effects. The mean of the coordinate differences with respect to the Check Points is also provided to complement the RMS figures. Precision is measured by the mean of the estimated standard deviations of

**Table 6**
Accuracy and precision results for Table 4 test blocks.

| Block | Test | Accuracy | | | | | | Precision | | | | | | | | |
|---|---|---|---|---|---|---|---|---|---|---|---|---|---|---|---|---|
| | | MEAN ChP (mm) | | | RMS ChP (mm) | | | MEAN $\sigma$ TP (mm) | | | MEAN $\sigma$ EO (mm/") | | | | | |
| | | *e*/*E* | *n*/*N* | *u*/*h* | *e*/*E* | *n*/*N* | *u*/*h* | *e*/*E* | *n*/*N* | *u*/*h* | *e*/*E* | *n*/*N* | *u*/*h* | $\omega$ | $\phi$ | $\kappa$ |
| P | Reference | – | – | – | – | – | – | 26 | 27 | 42 | 31 | 32 | 26 | 4 | 4 | 3 |
| | A-pa-woros-wcs | −4 | −9 | 10 | 36 | 27 | 32 | 36 | 37 | 53 | 39 | 39 | 40 | 4 | 4 | 3 |
| | A-pa-woros-wocs | −7 | −19 | 14 | 39 | 28 | 41 | 42 | 45 | 54 | 43 | 46 | 42 | 5 | 4 | 3 |
| | R-pa-wros-wcs | 0 | −9 | 6 | 32 | 25 | 30 | 38 | 39 | 57 | 38 | 39 | 44 | 4 | 3 | 2 |
| | R-pa-wros-wocs | −3 | −17 | 4 | 38 | 29 | 33 | 46 | 48 | 63 | 43 | 53 | 50 | 6 | 3 | 3 |
| S | Reference | – | – | – | – | – | – | 13 | 14 | 29 | 26 | 25 | 17 | 4 | 5 | 2 |
| | A-pa-woros-wcs | 12 | −1 | −4 | 32 | 29 | 54 | 20 | 21 | 36 | 30 | 29 | 26 | 5 | 5 | 2 |
| | A-pa-woros-wocs | 15 | 2 | 6 | 36 | 31 | 53 | 22 | 23 | 42 | 33 | 37 | 29 | 6 | 5 | 3 |
| | R-pa-wros-wcs | 16 | 1 | −1 | 33 | 28 | 52 | 22 | 23 | 39 | 28 | 31 | 31 | 4 | 4 | 2 |
| | R-pa-wros-wocs | 20 | 3 | 15 | 37 | 30 | 50 | 24 | 25 | 47 | 31 | 43 | 35 | 7 | 4 | 3 |
| V | Reference | – | – | – | – | – | – | 12 | 16 | 38 | 22 | 22 | 16 | 5 | 5 | 3 |
| | A-pa-woros-wcs | 3 | 1 | −12 | 18 | 24 | 58 | 15 | 18 | 41 | 23 | 23 | 19 | 5 | 5 | 3 |
| | A-pa-woros-wocs | 2 | 6 | −33 | 18 | 30 | 68 | 17 | 25 | 50 | 25 | 26 | 21 | 6 | 6 | 4 |
| | R-pa-wros-wcs | −5 | 6 | −4 | 17 | 23 | 57 | 15 | 18 | 42 | 20 | 21 | 21 | 4 | 3 | 2 |
| | R-pa-wros-wocs | −1 | 7 | −14 | 15 | 19 | 62 | 17 | 25 | 51 | 22 | 32 | 24 | 7 | 4 | 3 |

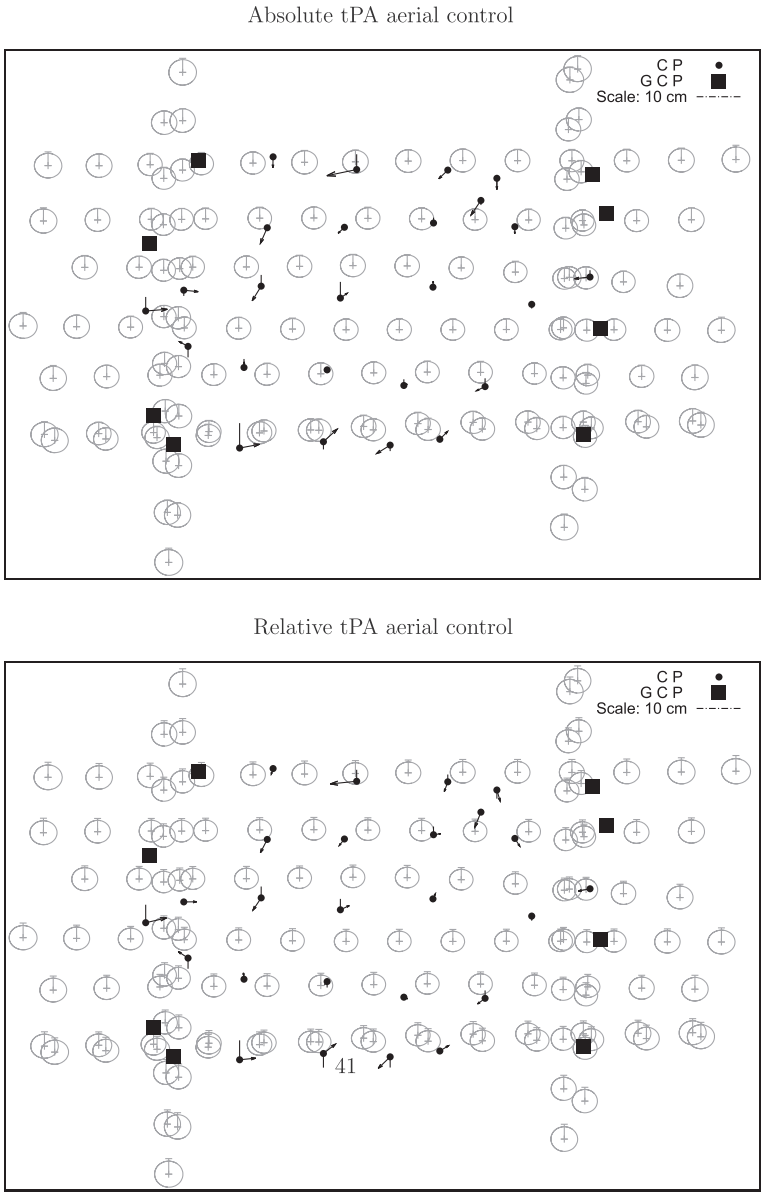


**Fig. 4.** P block: absolute and relative tPA aerial control with cross strips.

the object points (TP) and the mean of the estimated standard deviations of the exterior orientation parameters (EO). In order to facilitate the precision performance analysis, for each test block, a reference solution has been computed by using all available observations: photogrammetric, ground control (including all GCP and ChP) and aerial control.

Table 6 contains the accuracy and precision indicators for the selected test block configurations of Table 4. In general terms, all configurations deliver excellent results. The same could be said for the relative aerial control models as witnessed by the vertical-error-to-flying-height ratios $0.28 \times 10^{-4}$, $0.52 \times 10^{-4}$ and $0.54 \times 10^{-4}$ or their equivalent vertical-error-to-GSD ratios 0.30, 0.47 and 0.62 for the P, S and V blocks, respectively.

In the table, in order to compare the performance of absolute and relative aerial control under the same conditions, for each test block, rows coded *A-pa-woros-wcs* are compared against rows *R-pa-wros-wcs* and rows coded *A-pa-woros-wocs* against rows *R-pa-wros-wocs*. The comparison is performed by computing the ratios of homologous indicators. Thus, for instance, to compare the overall accuracy performance of *A-pa-woros-wocs* and *R-pa-wros-wocs*, the sum of the 18 RMS values of the *A-pa-woros-wocs* rows for the three blocks is divided by the corresponding sum of the *R-pa-wros-wocs*. The more the ratio deviates from 1, the better the performance of one solution with respect to the other one.

If this is done to analyse the ground point accuracy of Table 6 configurations, the accuracy indicators (RMS of the ChPs) of overall relative aerial control are slightly better (9%) than the absolute ones, and the test block that best benefits from relative aerial control is the V block (17%) followed by the P block (8%) and the S block (2%). If the comparison is restricted to blocks without cross strips, ground point accuracy indicators of relative aerial control are better than absolute ones (13%). Table 6 also contains the means of the coordinate differences between ground estimated and check points. If the absolute values of the means are compared, relative aerial control performs better for the P (62%) and the V (54%) blocks and worse for the S (30%) block. On average, relative aerial control suffers less from systematic errors (21%) than absolute control.

Analysing the estimated precision of the object points and exterior orientation parameters of the Table 6 configurations, those for

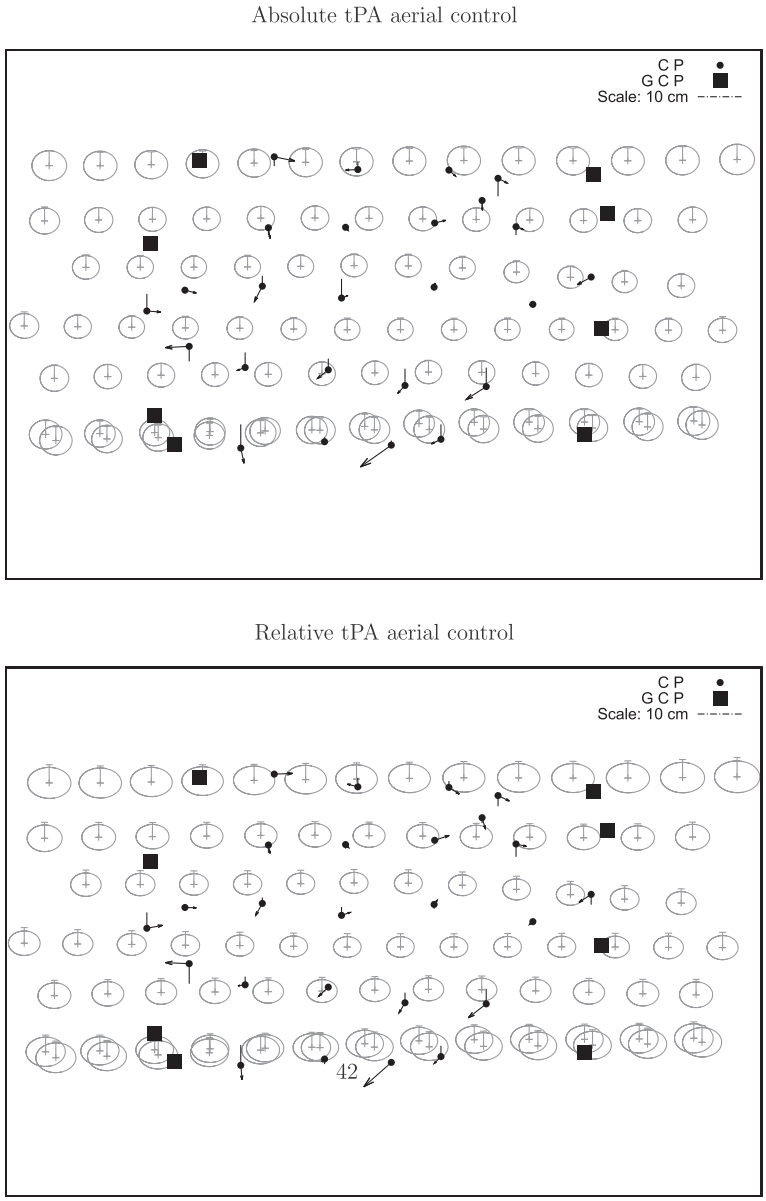


**Fig. 5.** P block: absolute and relative tPA aerial control with no cross strips.

**Table 7**
Exterior orientation elements precision losses (negative) and gains (positive) of relative aerial control with respect to absolute in the absence of cross strips (in %).

| | e/E | n/N | u/h | $\omega$ | $\phi$ | $\kappa$ |
|---|---|---|---|---|---|---|
| Largest | 14 | −19 | −17 | −17 | 50 | 33 |
| Average | 7 | −15 | −15 | −15 | 36 | 11 |

**Table 8**
Precision results of the use of relative aerial control between strips combined with absolute aerial control within strips.

| Block | Test | MEAN $\sigma$ EO (mm/") | | | | | |
|---|---|---|---|---|---|---|---|
| | | e/E | n/N | u/h | $\omega$ | $\phi$ | $\kappa$ |
| P | A-pa-woros-wocs | 38 | 39 | 41 | 4 | 4 | 3 |
| | A-pa-wros-wocs | 38 | 38 | 40 | 4 | 4 | 3 |
| S | A-pa-woros-wocs | 33 | 37 | 29 | 6 | 5 | 3 |
| | A-pa-wros-wocs | 26 | 27 | 25 | 4 | 4 | 2 |
| V | A-pa-woros-wocs | 25 | 26 | 21 | 6 | 6 | 4 |
| | A-pa-wros-wocs | 24 | 23 | 21 | 6 | 5 | 4 |

relative aerial control are slightly worse than absolute for point precision (6%) and for exterior orientation position precision (4%). On the contrary, the relative aerial control precision indicators are slightly better (21%) for exterior orientation attitude precision, particularly for the V block (35%).

Figs. 4 and 5 illustrate the accuracy and precision results of Table 6 configurations for the Pavia block. Both figures plot the coordinate differences of the check points (e/n components as a vector and u component as a straight line) and the ellipse errors of the exterior orientation parameters. Fig. 4 plots the accuracy and precision results of the *A-pa-woros-wcs* and *R-pa-wros-wcs* configurations and Fig. 5 plots the accuracy and precision results of the *A-pa-woros-wocs* and *R-pa-wros-wocs* configurations. In both cases, the figures illustrate similar results, with no significant differences, between the absolute and relative aerial control.

From the results and discussion above, under the same conditions, relative aerial control seems to perform comparably (insignificant differences around 2%) to slightly better (significant differences around 21%) than absolute control. From this, we

**Table 9**
Accuracy and precision results for Table 5 test blocks.

| Block | Test | Accuracy | | | | | | Precision | | | | | | | | |
|---|---|---|---|---|---|---|---|---|---|---|---|---|---|---|---|---|
| | | MEAN ChP (mm) | | | RMS ChP (mm) | | | MEAN $\sigma$ TP (mm) | | | MEAN $\sigma$ EO (mm/") | | | | | |
| | | *e*/*E* | *n*/*N* | *u*/*h* | *e*/*E* | *n*/*N* | *u*/*h* | *e*/*E* | *n*/*N* | *u*/*h* | *e*/*E* | *n*/*N* | *u*/*h* | $\omega$ | $\phi$ | $\kappa$ |
| S | A-p-woros-wcs | 11 | 0 | -5 | 33 | 30 | 54 | 21 | 22 | 38 | 31 | 32 | 28 | 5 | 5 | 2 |
| | A-p-woros-wocs | 15 | 7 | 24 | 36 | 32 | 55 | 23 | 24 | 50 | 34 | 52 | 38 | 9 | 6 | 3 |
| | R-p-wros-wcs | 11 | 1 | 4 | 33 | 31 | 50 | 23 | 24 | 45 | 36 | 39 | 37 | 6 | 6 | 3 |
| | R-p-wros-wocs | 15 | 5 | 23 | 35 | 32 | 52 | 25 | 26 | 54 | 38 | 56 | 43 | 10 | 6 | 3 |
| V | R-pa-woros-wcs | −2 | 6 | −11 | 17 | 23 | 59 | 15 | 18 | 43 | 22 | 27 | 23 | 5 | 4 | 2 |
| | R-pa-woros-wocs | −1 | 5 | −7 | 16 | 19 | 70 | 17 | 25 | 54 | 23 | 52 | 27 | 12 | 4 | 3 |
| | R-pa-wros-wcs | −5 | 6 | −4 | 17 | 23 | 57 | 15 | 18 | 42 | 20 | 21 | 21 | 4 | 3 | 2 |
| | R-pa-wros-wocs | −1 | 7 | −14 | 15 | 19 | 62 | 17 | 25 | 51 | 22 | 32 | 24 | 7 | 4 | 3 |

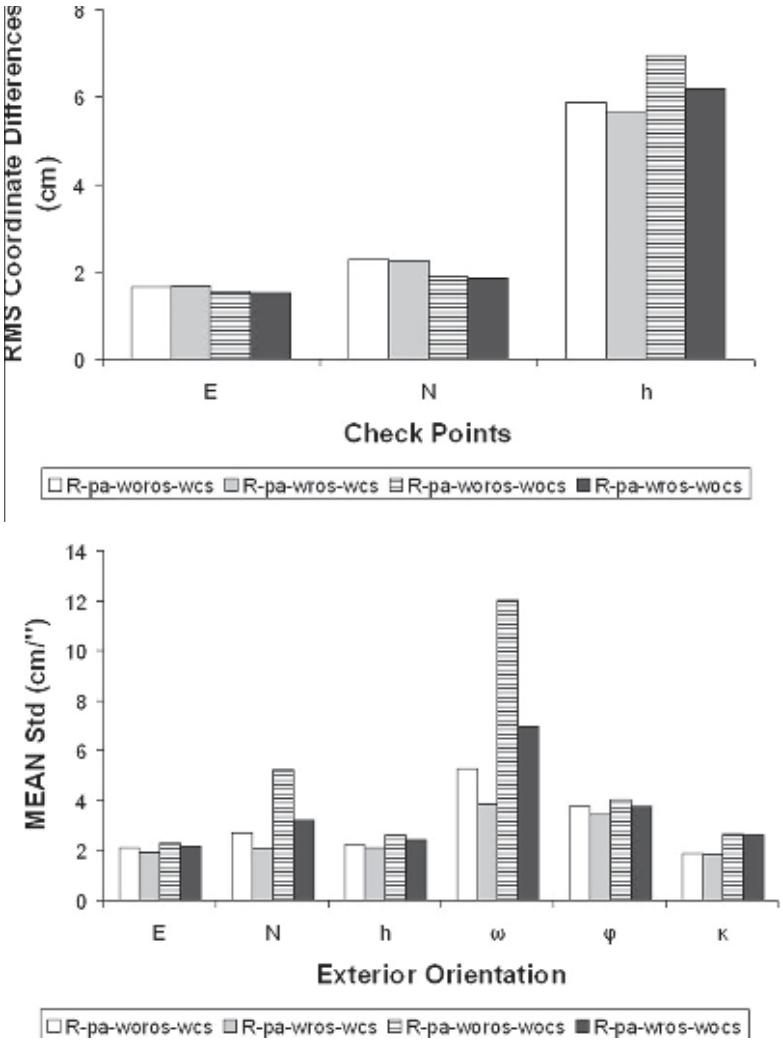


**Fig. 6.** V block: accuracy and precision with relative INS/GNSS tPA aerial control; impact of relative observations between strips.

conclude that the recommendations for block geometry design with relative aerial control should be the same as for absolute aerial control. In order to empirically confirm this statement, results in Table 6 can be combined with those in Table 9 which contain the accuracy and precision indicators for the selected additional test block configurations of Table 5.

The contribution of cross strips for relative aerial control is, as per the results in Table 6, limited. Deterioration of accuracy results – there are also improvements – after removing cross strips reaches up to 16% and 9% maximum values in the horizontal and vertical components, respectively (rows *R-pa-wros-wcs* versus rows *R-pa-wros-wocs*). On average, the contribution of cross strips yields a modest 2% and 4% improvement. Similar analysis for absolute position and attitude aerial control yields 20% and 22% maximum and 8% and 12% average accuracy worsening for the horizontal and vertical components respectively (rows *A-pa-wros-wcs* versus rows

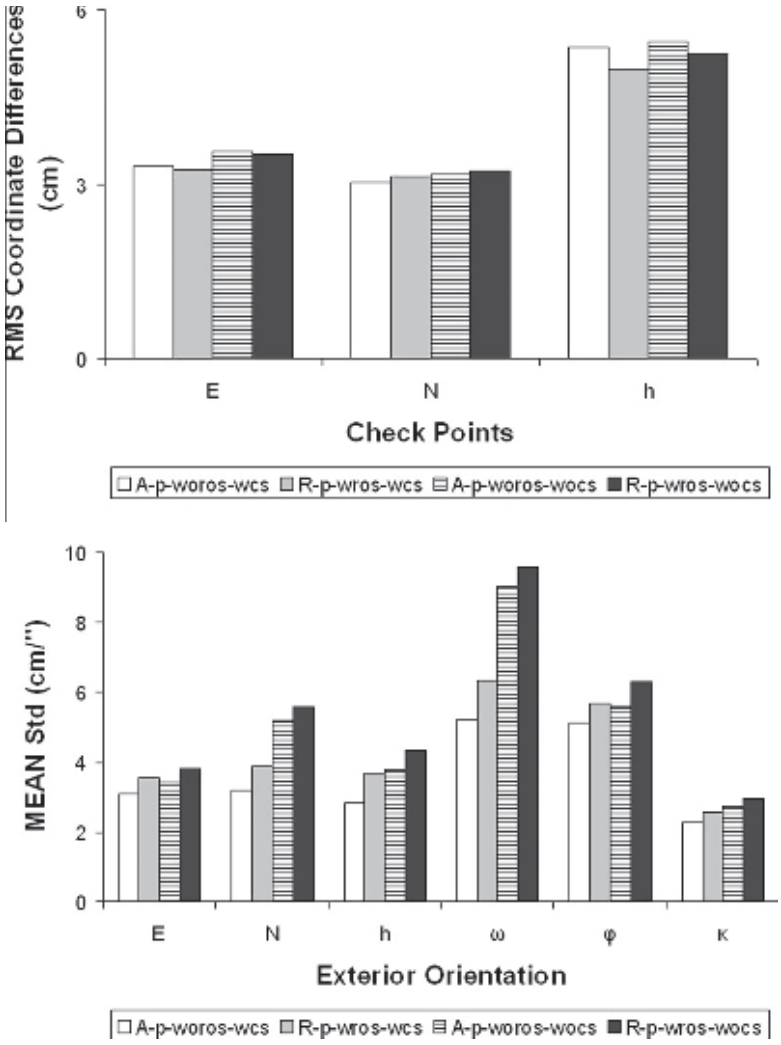


**Fig. 7.** S block: accuracy and precision with INS/GNSS tP aerial control.

*A-pa-wros-wocs*). Further to this, in the absence of cross strips, relative aerial control yields better accuracy results than absolute aerial control: 13% average accuracy improvement in both the horizontal and vertical components (rows *A-pa-woros-wocs* versus rows *R-pa-wros-wocs*). According to this, relative position and attitude aerial control is more resilient to the absence of cross strips than absolute control. However, these results have to be interpreted carefully as the number of photogrammetric observations contributing to the determination of ground check points differs from one case to the other. If the contribution of cross strips is analysed through the exterior orientation parameters indicators (rows *A-pa-woros-wocs* versus rows *R-pa-wros-wocs*) component-dependent gains and losses can be found as presented in Table 7 where the horizontal flying direction, $\phi$ and $\kappa$ components are more precisely estimated with relative aerial control and, the other three components are more precisely estimated with absolute aerial control. This is the result of the combined contribution of block geometry and relative orientation aerial control properties. While absolute aerial control tends to "favour" overall block geometry – i.e., across track directions and $\omega$ angles – relative aerial control does it locally – i.e., along track direction and $\phi$, $\kappa$ angles. Therefore, the use of cross strips tends to compensate for the "weaknesses" of each, absolute or relative, control approach. Equivalently, the elimination of cross strips tends to uncover their "weaknesses." Last, we recall that relative aerial control between strips can be combined with the traditional absolute control to contribute to block flexibility as illustrated through the precision estimates of exterior orientation parameters in Table 8.

In all of our relative aerial control configurations we have linked consecutive strips with relative aerial control. This is a natural thing to do as the observations are available and it does not make much sense not to use them. Rows *R-pa-wros-wcs* and *R-pa-wros-wocs* in Table 6, rows *R-pa-woros-wcs* and *R-pa-woros-wocs* in Table 9, and Fig. 6 illustrate their relevance, particularly in the absence of cross strips.

Last, Table 9 and Fig. 7 illustrate the performance of relative position aerial control. We leave the interpretation of these results to the reader, as they are rather similar to those of relative position and attitude relative control. As expected and as happens with absolute position control, cross strips are advisable.

One further advantage of relative aerial control models is that the detection of outliers in the aerial control observations becomes easier. Examples thereof can be sudden position jumps which result from changes in the selected GNSS satellite configurations or from incorrectly resolved carrier phase ambiguities. In order to roughly validate this claim, we introduced errors in INS/GNSS

trajectories that resembled actual ones. In all cases, outlier detection for relative control observations performed better than for absolute observations. This has been reported in Blázquez (2008) with simulated data.

All in all, relative aerial control can be used as an alternative to absolute control. To correctly do so, only two design principles need to be followed: design the blocks as for absolute aerial control and connect consecutive strips with relative aerial control observations. In other words, on the one hand, cross strips are only required – or at least recommendable – in the case of position aerial control. On the other hand, relative aerial control observations should be applied to the last and first images of consecutive strips.

## 4. Summary and conclusions

We have provided models and described in detail the relative approach to the use of INS/GNSS-derived position and attitude observations for aerial control in ISO. The approach has advantages over the traditional, absolute, one: the stochastic model for the INS/GNSS-derived relative aerial control better represents the actual INS/GNSS trajectory error features; the GNSS linear shift and boresight unknown parameters vanish from the models and no longer need to be estimated which, in turn, avoids the typical errors associated with their selection and use. We have also introduced new models, in the *l* and *m* frames, for the main ISO observables: photogrammetric; and INS/GNSS-derived aerial control, both absolute and relative. The new models use original observations thus eliminating angular re-parameterisations, height and azimuth "corrections" and guarantee geodetic correctness and integration with other systems.

We have validated the new models with three independent data sets from different manufacturers, with different mission patterns and for various block configurations. The new relative models lead from comparable to better ground point accuracy behaviour as compared to the absolute ones under identical conditions. In particular, ISO blocks with INS/GNSS-derived relative aerial control can be designed with no shape regularity and cross strip requirements. Therefore, ISO blocks with INS/GNSS-derived absolute and relative aerial control can be designed in the same way.

The above contributions also show that it is possible to increase the robustness and to reduce the complexity of INS/GNSS-based integrated sensor orientation by concentrating the modelling effort on the models and letting the user concentrate on their use.

## Acknowledgments

The data sets Pavia block, Salou block and Vaihingen/Enz block were provided by Prof. Vittorio Casella (Università di Pavia, Italy), Josep L. Colomer (Institut Cartogràfic de Catalunya, Spain) and Dr. Jens Kremer (IGI GmbH, Germany) and Dr. Michael Cramer (Institut für Photogrammetrie, Universität Stuttgart, Germany), respectively. Many thanks for these contributions. The models were implemented and the results were obtained with the Generic Extensible Network Approach (GENA) platform from GeoNumerics (Barcelona, Spain). This support for our research is greatly appreciated. The research reported in this paper has been funded by the Spanish projects LIRA (Ref. P 44/08, Ministerio de Fomento, Spain) and Geo-Land-Models (Ref. PET2008_071, Ministerio de Ciencia e Innovación, Spain).

## Appendix A. Mathematical model for dual-head cameras

"*The Dual-DigiCAM-H/39 consists of two DigiCAM-H/39 medium format digital cameras rigidly connected to ensure a fixed relative orientation inbetween the two cameras.*" (Kremer and Cramer, 2008). This is the common situation in multi-sensor acquisition systems and it is, therefore, natural to model the constant [up to system instabilities] relative orientation between each pair of instruments. In the particular case of the V block, in the course of a mission, the relative orientation (position and attitude) between the left (instrumental frame $c_1$) and the right (instrumental frame $c_2$) cameras is constant. To use this knowledge in the ISO adjustment, unknown system interior orientation parameters $(A_{12}^{c_1}, \Gamma_{12c_1}^{c_2})$ are introduced through the following observation equations for position (Eq. (A.1)) and attitude (Eq. (A.2)), formulated in the *m* frame,

$$P_2^m = P_1^m + R_{c_1}^m(\Gamma_1)\cdot(A_{12}^{c_1} + a_{12}^{c_1} + v_a^{c_1}), \tag{A.1}$$

$$R_{c_1}^{c_2}(\Gamma_{12})\cdot R_{c_1}^{c_1}(\gamma_{12} + v_\gamma) = R_m^{c_2}(\Gamma_2)\cdot R_{c_1}^m(\Gamma_1) \tag{A.2}$$

where the subscripts 1 and 2 distinguish the orientation elements $(P^m, \Gamma_c^m)$ of the two images taken at the same time with the left and the right DigiCAM-H/39 cameras, respectively. $A_{12}^{c_1}$ and $\Gamma_{12c_1}^{c_2}$ are parameters to be estimated: $A_{12}^{c_1}$ is the camera left to the camera right lever arm in the $c_1$ frame and $R_{c_1}^{c_2}(\Gamma_{12})$ is the camera left to camera right relative attitude matrix. Both $A_{12}^{c_1}$ and $\Gamma_{12c_1}^{c_2}$ can be initialized with approximate values and/or related to previously measured or estimated values with simple observation equations. $a_{12}^{c_1}$ and $\gamma_{12c_1}^{c_2}$ are 3D vectors of spatial and angular observations both set to $(0,0,0)$ so that the stability of the system interior orientation can be stochastically modelled (Tommaselli et al., 2009) through their input covariance matrices. Their respective residuals, $v_a^{c_1}$ and $v_{\gamma\ c_1}^{c_2}$, once adjusted, provide information on the camera system vibrations at every exposure time. The estimated covariance of $(A_{12}^{c_1}, \Gamma_{12c_1}^{c_2})$ describes the overall stability of the sensor system.

Our results for the dual-head camera system of block V presented in this paper were obtained by including the system orientation constraints A.1 and A.2. Because of the high mechanical stability (Kremer and Cramer, 2008) of the dual head assembly, each of the observations $(0,0,0)$ for $a_{12}^{c_1}$ and $\gamma_{12c_1}^{c_2}$ was assigned diagonal covariance matrices of standard deviations $\sigma_{a_{12}} = 1$ mm and $\sigma_{\gamma_{12}} = 1$ mdeg, respectively. These values led to the best results.

To illustrate the impact of the inner geometric restrictions, Table A.10 shows, for the V block, the precision performance of indirect sensor orientation (InSO) – i.e., classical bundle block adjustment with no aerial control and regular ground control – and the precision and accuracy of ISO (configuration A-pa-woros-wcs, Table 4) with (w-dh) and without (wo-dh) interior orientation constraints. Accuracy for InSO cannot be reliably

**Table A.10**
V block: performance indicators with (w-dh) and without (wo-dh) dual-head constraints.

| Test | Accuracy | | | | | | Precision | | | | | | | | |
|---|---|---|---|---|---|---|---|---|---|---|---|---|---|---|---|
| | MEAN ChP (mm) | | | RMS ChP (mm) | | | MEAN $\sigma$ TP (mm) | | | MEAN $\sigma$ EO (mm/") | | | | | |
| | *E* | *N* | *h* | *E* | *N* | *h* | *E* | *N* | *h* | *E* | *N* | *h* | $\omega$ | $\phi$ | $\kappa$ |
| InSO (w-dh) | – | – | – | – | – | – | 14 | 19 | 47 | 60 | 52 | 27 | 12 | 13 | 5 |
| InSO (wo-dh) | – | – | – | – | – | – | 16 | 20 | 54 | 103 | 100 | 47 | 24 | 24 | 6 |
| A-pa-woros-wcs (w-dh) | 18 | 24 | 58 | 3 | 1 | −12 | 15 | 18 | 41 | 23 | 23 | 19 | 5 | 5 | 3 |
| A-pa-woros-wcs (wo-dh) | 18 | 28 | 60 | 1 | −2 | −15 | 16 | 20 | 42 | 32 | 32 | 25 | 7 | 7 | 4 |

assessed as there are not enough GCPs to only keep some of them as GCP and spare the rest as ChP.

Note, that in Table A.10, precision is presented in terms of the average precision of tie points and exterior orientation parameters. As can be seen, even when aerial control observations are available, constraints Eqs. (A.1) and (A.2) improve parameter estimation. As was to be expected, in the case of the InSO adjustment and for the estimation of the exterior orientation parameters, the precision improvement is significantly higher. Last, we note that changing the stochastic model (values $\sigma_{a_{12}}$ and $\sigma_{\gamma_{12}}$) within reasonable limits ($\sigma_{a_{12}} \in [1,10]$ mm and $\sigma_{\gamma_{12}} \in [1,10]$ mdeg) – and even beyond, up to $\sigma_{a_{12}} = 10$ cm – does not significantly impact the results.

We believe that the convenience of modelling the system interior orientation parameters of multi-sensor systems is clear and the models are straightforward. Therefore, the topic deserves no further discussion other than to state that Eqs. (A.1) and (A.2), or their equivalents, should be included into all InSO and ISO multi-head adjustments.

## References


Alamús, R., Barón, A., Talaya, J., 2002. Integrated sensor orientation at ICC, mathematical models and experiences. OEEPE Official Publication 43, 153–162.

Applanix, 2011. POS AV Specifications: performance specifications, <http://www.applanix.com/media/downloads/products/specs/POSAV_SPECS.pdf> (Accessed 25.5.2011).

Blázquez, M., Colomina, I., 2008. On the use of inertial/GPS velocity control in sensor calibration and orientation. In: Proceedings of EuroCOW 2008, Castelldefels, Spain, 30 January–01 February, 8p. (on CDROM).

Blázquez, M., 2008. A new approach to spatio-temporal calibration of multi-sensor systems. International Archives of the Photogrammetry: Remote Sensing and Spatial Information Sciences 37 (Part B1), 481–486.

Blázquez, M., Colomina, I., 2010. On the role of self-calibration functions in integrated sensor orientation. In: Proceedings of EuroCOW 2010, Castelldefels, Spain, 10–12 February, 7p. (on CDROM).

Cramer, M., 2010. The DGPF-test on digital airborne camera evaluation overview and test design. PFG Photogrammetrie, Fernerkundung, Geoinformation 2010 (2), 73–82.

Friess, P., 1991. Aerotriangulation with GPS-methods, experience, expectation. In: Proceedings of 43rd Photogrammetric Week, Stuttgart, Germany, 9–14 September, pp. 43–49.

Friess, P., 2006. Toward a rigorous methodology for airborne laser mapping. In: Proceedings of EuroCOW 2006, Castelldefels, Spain, 25–27 January, 7p. (on CDROM).

Heipke, C., Jacobsen, K., Wegmann, H., Andersen, O., Nilsen, B., 2000. Integrated sensor orientation – an OEEPE test. International Archives of the Photogrammetry, Remote Sensing and Spatial Information Sciences 33 (Part B3), 373–380.

Kager, H., 2004. Discrepancies between overlapping laser scanning strips – simultaneous fitting of aerial laser scanner strips. International Archives of Photogrammetry, Remote Sensing and Spatial Information Sciences 35 (Part B1), 555–560.

Kremer, J., Cramer, M., 2008. Results of a performance test of a dual mid-format digital camera system. International Archives of the Photogrammetry, Remote Sensing and Spatial Information Sciences 37 (Part B1), 1051–1058.

Lucas, J., 1987. Aerotriangulation without ground control. Photogrammetric Engineering and Remote Sensing 53 (3), 311–314.

Martínez, M., Blázquez, M., Gómez, A., Colomina, I., 2007. A new approach to the use of position and attitude control in camera orientation. In: Proceedings of Seventh International Geomatic Week, Barcelona, Spain, 20–23 February, 5 p. (on CDROM).

Mugnier, C.J., Förstner, W., Wrobel, B., Paderes, F., Munjy, R., 2004. The mathematics of photogrammetry. In: McGlone, J.C., Mikhail, E.M., Bethel, J., Mullen, R. (Eds.), Manual of Photogrammetry, fifth ed. American Society of Photogrammetry and Remote Sensing, Bethesda, MA, pp. 181–316.

Schwarz, K., Chapman, M., Cannon, M., Gong, P., 1993. An integrated INS/GPS approach to the georeferencing of remotely sensed data. PE&RS Photogrammetric Engineering and Remote Sensing 59 (11), 1667–1674.

Skaloud, J., Lichti, D., 2006. Rigorous approach to bore-sight self-calibration in airborne laser scanning. ISPRS Journal of Photogrammetry and Remote Sensing 61 (1), 47–59.

Skaloud, J., Legat, K., 2008. Theory and reality of direct georeferencing in national coordinates. ISPRS Journal of Photogrammetry and Remote Sensing 63, 272–282.

Tommaselli, A.M.G., Galo, M., Bazan, W.S., Ruy, R.S., Marcato Junior, J., 2009. Simultaneous calibration of multiple camera heads with fixed base constraint. In: Proceedings of Sixth International Symposium on Mobile Mapping Technology, Presidente Prudente, SP, Brazil, 21–24 July, 6p. (on CDROM).

# Chapter 4

# INS/GNSS-based synchronization

This paper is the third of this series and it contributes to the proposed systematic approach to airborne sensor orientation and calibration with the review and extension of the spatio-temporal absolute aerial control model for local cartesian and global compound mapping-geodetic coordinate systems (Figure 4.1).

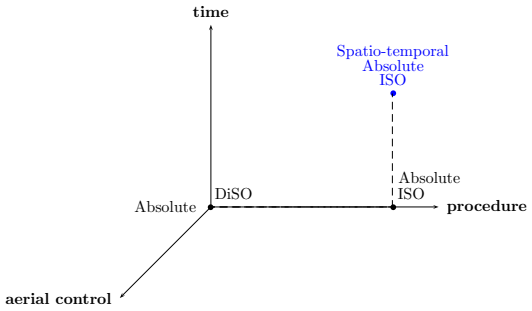


Figure 4.1: Spatio-temporal absolute aerial control model.

The spatio-temporal absolute aerial control model calibrates a constant time shift parameter between the sensor and the INS/GNSS system through its impact in the position. To do this, the proposal is to use the available INS/GNSS-derived linear velocities in addition to the traditional INS/GNSS position and attitude observations. This paper does not only provide the observation equations, it also discusses the decorrelation of time errors from space errors, proposes appropriate geometries and presents the results for various actual data sets.

For this research I developed the models, programmed the GENA model toolboxes, performed the calculations and analyzed the results. I wrote the paper with Dr. Ismael Colomina who also promoted and supervised the research.

*Blázquez, M., Colomina, I., 2012. On INS/GNSS-based time synchronization in photogrammetric and remote sensing multi-sensor systems. Photogrammetrie, Fernerkundung und Geoinformation 2012(2), pp. 91–104.*

PFG 2012 / 2, 0091 – 0104
Stuttgart, February 2012

Article

# On INS/GNSS-based Time Synchronization in Photogrammetric and Remote Sensing Multi-Sensor Systems

Marta Blázquez & Ismael Colomina, Castelldefels, Spanien

**Keywords:** Synchronization, orientation, self-calibration, INS/GNSS, Multi-sensor systems

**Summary:** We propose a method to estimate time calibration parameters in the frame of a space-time integrated sensor orientation concept for the purpose of correct instrumental synchronization or synchronization verification in multi-sensor photogrammetric and remote sensing systems. The new method is based on the use of the INS/GNSS-derived velocities in addition to the commonly used INS/GNSS-derived positions and attitudes for aerial control. We present the corresponding mathematical models for local geodetic and global map-projected coordinate systems, discuss the separability between spatial and temporal calibration parameters, deduce various appropriate block configurations, and assess their behaviour with actual data. The results show that, for a number of block configurations, it is possible to correctly estimate synchronization calibration parameters with a precision of few tenths of a millisecond.

**Zusammenfassung:** *Über INS/GNSS-basierte Synchronisation von Multisensor-Systemen in der Photogrammetrie und Fernerkundung.* Im Beitrag wird eine Methode zur Schätzung von zeitlichen Kalibrierparametern vorgestellt, die bei Verfahren zur gemeinsamen räumlichen und zeitlichen Sensororientierung von Multisensor-Systemen eine Rolle spielen, und die entweder der richtigen Gerätesynchronisation oder deren Verifikation dienen. Der neue Ansatz berücksichtigt auch die aus den INS/GNSS-Beobachtungen abgeleitete Geschwindigkeit und nicht nur die bislang meist verwendeten Positionen und Neigungen. Der Beitrag entwickelt die mathematischen Modelle für lokale dreidimensionale kartesische und für globale projizierte Koordinatenreferenzsysteme, befasst sich mit der Trennbarkeit von räumlichen und zeitlichen Parametern, leitet daraus eine Reihe geeigneter Blockgeometrien ab und zeigt deren Verhalten mit realen Daten. Die Ergebnisse belegen, dass es bei bestimmten Blockgeometrien möglich ist, die zeitlichen Kalibrierparameter mit einer Genauigkeit von fast einer Zehntel Millisekunde zu schätzen.

## 1 Introduction

This paper is about the calibration of synchronization errors among the instruments of multi-sensor systems.

Synchronization errors are common in multi-sensor systems. They originate in the clocks that drive the instrumental temporal reference frames and in the delays that hardware and software introduce in the time transfer interfaces. In aerial photogrammetry and remote sensing, synchronization errors are obviously harmful in Direct Sensor Orientation (DiSO), are simply non-existent in classical aerial triangulation (Indirect Sensor Orientation, InSO), and are harmless in Integrated Sensor Orientation (ISO) because they are absorbed by the INS/GNSS per strip shifts. In the latter case they are recognizable through the usual pattern showing their flying sense dependency (Fig. 3). In terrestrial kinematic photogrammetry e.g., mobile mapping systems (Graham 2010), the various sensors are mutually and critically related by an overall system clock, usually a subsystem of an INS/GNSS-based time-Position-Velocity-Attitude (tPVA) server.


www.schweizerbart.de
DOI: 10.1127/1432-8364/2012/0104
1432-8364/12/0104 $ 3.50

Synchronization issues are usually dealt with at the hardware level by original equipment manufacturers and by system integrators. A system that is "internally well synchronized" is one in which all relevant subsystems have access to a common time reference frame within a given time error threshold. Synchronization of electrical devices and, in general, timekeeping are vast and complex engineering disciplines. Today, using off-the-shelf computer components, it is possible to design and build systems that are internally well synchronized down to 1 μs (microsecond) with a resolution of 0.1 μs. However, the resources required for correct time transfer and synchronization are not always available. Further, it is not always possible to synchronize internally well synchronized instruments to others. These situations, and possibly others, lead to what we call synchronization errors; i.e., to different time coordinates – time tags – being assigned to simultaneous events or to simply incorrect time coordinates being assigned to events. Here we assume that, contrary to the dictates of modern physics, simultaneity is an absolute concept and does not depend on the observer's reference frame.

As opposed to spatial errors, to the best of our knowledge, synchronization errors are not modelled as such and therefore can not be estimated in photogrammetric and remote sensing orientation and calibration software. Even if Integrated Sensor Orientation (ISO) can deal with them implicitly it may be better to model them explicitly. Consider, for instance, an ideal airborne ISO block consisting of $n$ strips, affected by a constant synchronization error, with a perfectly calibrated camera and perfectly determined INS/GNSS aerial control. In this case 3 x $n$ INS/GNSS shift unknowns could be replaced with just 1 calibration unknown; the temporal $\delta t$ calibration one.

(Unfortunately, ideal blocks do not exist and there are always, small or large, original or remaining, camera calibration and INS/GNSS aerial control errors that have an influence similar to synchronization errors. As we shall see, the challenge of synchronization calibration is to distinguish between the $\delta t$ calibration parameter or family of parameters from the camera calibration ones and GNSS or INS/GNSS shifts.)

The key idea behind our approach to spatio-temporal orientation and calibration is based on the observation that an INS/GNSS system delivers aerial control of the tPVA type and not just of the time-Position-Attitude (tPA) type. The use of the INS/GNSS 3D velocity estimates, in addition to those for position and attitude, makes it possible to relate time and space and consequently, allows for $\delta t$ calibration in the context of spatial observations. More precisely, we will explore the combined determination of the images' orientation parameters and of the instruments' calibration parameters including the estimation of synchronization errors in an ISO block adjustment. Note that, when dealing with time, we face both orientation and calibration tasks as we have to estimate transformation parameters between different time reference frames, an orientation problem, and correction parameters – a calibration problem. Admittedly, many times, there is no essential difference between orientation and calibration.

Despite the relevance of synchronization in multi-sensor systems, in our geomatic literature research we found no discussion related to sensor synchronization calibration at the ISO or comparable levels. In robotics, where both machine vision grade and consumer grade sensors are commonly used, the synchronization problem seems to be more acute and there is a wealth of publications on the topic. However, their vast majority are unfeasible for our purposes since they require the implementation of specific communication features between the sensors like in Harrison & Newman (2011). A nice exception is the algorithm proposed in Olson (2010). However, its context is rather different from ours where we count on an INS/GNSS system and on motion. In our previous research (Blázquez & Colomina 2008) we introduced the use of INS/GNSS-derived linear and angular velocities for the estimation of constant $\delta t$ in local geodetic ($e$, $n$, $u$) coordinate systems ($l$-type systems). In Blázquez (2008) actual ISO data and simulated linear velocities were combined to validate the concept. In this paper we provide detailed mathematical models for constant $\delta t$ calibration with INS/GNSS-derived linear velocities in local geodetic $l$-type systems and in global compound mapping-geodetic ($E$, $N$, $h$)

coordinate systems (*m*-type systems) as well as the first analyses and validation tests with actual data. We concentrate on the determination of multi-sensor system time calibration or, in other words, time orientation between the various instruments of a multi-sensor system for the case of GNSS receivers, inertial measurement units (IMUs) and frame cameras.

The paper does not tackle the exploitation of INS/GNSS-derived rotational and angular velocities for $\delta t$ determination because of the importance of properly understanding the linear velocity case. Further, the paper does not cover the case of time dependent $\delta t(t)$ synchronization errors or the similar case of internal temperature dependent or other instrumental clock $\delta t(t)$ instabilities because in many cases instrumental clocks are slaved to the few ns (nanosecond) precise output synchronization signals of GNSS receivers, thus guaranteeing stable internal time reference frames just affected by a $\delta t$ time offset inaccuracy. The estimation of $\delta t(t)$ would require its modelling as a stochastic process and a dynamic observation model in the form of a stochastic differential equation or differential observation equation involving $\delta t(t)$.

Our research on time calibration in multi-sensor systems is not directly motivated by the improvement of point or orientation determination accuracy, but rather by the general progress in sensor calibration. The result of accurate time calibration is more accurate geometric calibration as geometric calibration parameters are no longer contaminated by synchronization errors. Moreover, an independent method to check the correctness of hardware instrument synchronization would be of interest to original equipment manufacturers, equipment integrators and advanced users.

The paper is organized as follows: section 2 presents the observation equations for the estimation of $\delta t$, section 3 discusses the geometry of space-time Integrated Sensor Orientation, section 4 introduces the validation criteria for the models and the overall space-time calibration concept, section 5 describes the validation data and the experiments conducted, and section 6 presents and discusses the results.

## 2 Mathematical Models

As mentioned, this paper introduces a new mathematical model to calibrate synchronization errors in global compound mapping-geodetic *m*-type coordinate systems and, for the sake of completeness, reviews the mathematical model in local geodetic *l*-type systems (Blázquez 2008). Both models are based on the idea presented in Blázquez (2008) "The sensor calibration and orientation problem is not a 3D spatial problem, it is a 4D spatio-temporal one. Moreover, the INS/GNSS-derived data contain not only positions and attitudes, they also contain velocities."

In *l*-type coordinate systems, the aerial control observation equations that relate the $\delta t$ synchronization parameter to the position and velocity aerial observations are

$$X^l + v^l_X = P^l + R^l_c(\Gamma)\cdot(A^c + N^c) + S^l - (V^l + v^l_V)\cdot\delta t \quad (1)$$

The position control aerial equation above is complemented with the usual equation for attitude aerial control

$$R^l_c(\Gamma) = R^l_b(\chi + v_\chi)\cdot R^b_c \quad (2)$$

In *m*-type coordinate systems, the above equations become

$$X^m + v^m_X = P^m + R^m_c(\Gamma)\cdot(A^c + N^c) + S^m - M(s^m_t)\cdot R^m_l(\eta)\cdot(V^l + v^l_V)\cdot\delta t \quad (3)$$

$$R^m_c(\Gamma) = R^m_t(\eta)\cdot R^l_b(\chi + v_\chi)\cdot R^b_c \quad (4)$$

The coordinate reference frames and variables involved in (1) to (4) are described in Tabs. 1 and 2.

**Tab. 1:** Coordinate Reference Frames.

| | |
|---|---|
| *m* | Compound mapping-geodetic global terrestrial frame (Easting-Northing-height) |
| *l* | Cartesian local terrestrial frame (east-north-up) |
| *b* | IMU instrumental frame (forward-left-up) |
| *c* | Camera instrumental frame |

**Tab. 2:** Variables.

| | |
|---|---|
| $X^m = (x, y, z)^m$ | aerial position observation in *m*-frame |
| $v_{X}{}^m = (v_x, v_y, v_z)^m$ | aerial position observation residuals in *m*-frame |
| $X^l = (x, y, z)^l$ | aerial position observation in *l*-frame |
| $v_{X}{}^l = (v_x, v_y, v_z)^l$ | aerial position observation residuals in *l*-frame |
| $R_b^l(\chi)$ | INS/GNSS attitude matrix |
| $\chi_b^l = (\psi, \theta, \gamma)_b^l$ | aerial attitude observation (parameterized by the traditional Euler $\psi$ heading, $\theta$ pitch and $\Gamma$ roll angles) |
| $v_\chi = (v_\psi, v_\theta, v_\gamma)$ | aerial attitude observation residuals |
| $V^l = (v_e, v_n, v_u)^l$ | aerial velocity observation |
| $v_V{}^l = (v_{v_e}, v_{v_n}, v_{v_u})^l$ | aerial velocity observation residuals |
| $P^m = (E, N, h)^m$ | camera projection centre in *m*-frame |
| $P^l = (e, n, u)^l$ | camera projection centre in *l*-frame |
| $R_c^m(\Gamma)$ | camera attitude matrix (parameterized by the Euler angles $\Gamma_c{}^m = (\omega, \varphi, \kappa)_c{}^m$) |
| $R_c^l(\Gamma)$ | camera attitude matrix (parameterized by the traditional Euler angles $\Gamma_c^l = (\omega, \varphi, \kappa)_c^l$) |
| $A^c = (a_x, a_y, a_z)^c$ | camera-to-IMU lever arm |
| $N^c = (0, 0, n)^c$ | camera nodal vector (*n* is the camera nodal distance) |
| $S^m = (s_E, s_N, s_h)^m$ | GNSS shift correction vector in *m*-frame |
| $S^l = (s_e, s_n, s_u)^l$ | GNSS shift correction vector in *l*-frame |
| $\delta t$ | multi-sensor synchronization calibration parameter |
| $R_c^b$ | camera-to-IMU relative attitude (boresight) matrix (parameterized by the Euler angles $\Upsilon_c^b = (v_x, v_y, v_z)_c^b$) |
| $s_l^m$ | scale factor of conformal map projections that depends on $P^m$ with $M(s_l^m) = diag(s_l^m, s_l^m, l)$ |
| $\eta_l{}^m, R_l{}^m(\eta)$ | meridian convergence angle of conformal map projections at $P^m$ and its three-dimensional rotation matrix – rotation around the normal line to the ellipsoid through $P^m$ – that aligns the local frame *l* to the mapping frame *m* |

## 3 The geometry of space-time Sensor Orientation and Calibration Networks

The mathematical models introduced in the previous section together with the usual ISO models such as collinearity (photogrammetric observations), ground control (point position observations) and aerial control (tPA observations) as presented, for instance, in Blázquez & Colomina (2012) lead to a new type of photogrammetric network in which both space and time, orientation and calibration parameters are estimated. As with previously existing photogrammetric networks, like bundle self-calibrating or ISO blocks, a space-time ISO network exhibits a "geometry" that is a function of the number, quality and distribution of observations, of the models in use and of the number and distribution of unknown parameters. A "strong" geometry makes it possible to estimate more parameters than a "weak" geometry, or to better estimate them. A network's geometry is largely influenced by the block configuration; i.e. the number, distribution, length and flying sense of strips; the degree of image overlap and the ground control point distribution.

Understanding space-time network geometries makes it possible to properly configure blocks and select the models and observations required for accurate $\delta t$ determination. For this purpose, we will now discuss the impact of synchronization and other related systematic errors – like camera calibration and GNSS or INS/GNSS aerial control position errors – on some relevant parameters.

A constant synchronization error $\Delta t$ causes a 3D error $\Delta t \cdot V(t)$ in the aerial control position coordinates at time $t$ and, therefore, on the ground point coordinates. In a typical aerial photogrammetric mission and within a strip, the velocity vector $V(t)$, if $V(t) = (v_E(t),v_N(t),v_h(t))^T$, is almost constant with $v_h(t) \approx 0$ and images are horizontally stabilized. Thus, the impact of the $\Delta t$ error is a horizontal shift $\Delta t \cdot (v_E(t),v_N(t))^{\mathrm{T}}$ where the velocity vector $(v_E(t),v_N(t))^{\mathrm{T}}$ describes the instantaneous direction and sense of the trajectory. We note that the error $\Delta t \cdot (v_E(t),v_N(t))^{\mathrm{T}}$ is independent from the flying height and that the size of $\Delta t$ depends on the instrument and system (a 1 ms error at a flying speed of 300 km/h results in a spatial error of 8.3 cm).

It is also known that an error $(\Delta x_0,\Delta y_0)^T$ in the coordinates of the camera principal point $(x_0,y_0)^T$ results in an approximate horizontal ground shift $R_h(\kappa) \cdot m \cdot (\Delta x_0,\Delta y_0)^T$ where $m$ is the image scale factor and $R_h(\kappa)$ is a 2D horizontal rotation of angle $\kappa$ . This error is flying height-dependent and, if the camera reference frame is aligned to the forward-left-up directions of the aircraft, then the component of the error $R_h(\kappa) \cdot m \cdot (\Delta x_0,0)^T$ behaves similarly to $\Delta t \cdot (v_E(t),v_N(t))^{\mathrm{T}}$.

Errors in the camera-to-IMU and IMU-to-GNSS antenna relative positions (lever arms), and even in the calibration of the GNSS receiver's antenna phase centre, have similar, flying strip sense-dependent and height-independent, effects. These errors are in the order of up to a few centimetres.

Last, the systematic errors in the GNSS or INS/GNSS aerial control observations are highly dependent on the navigation instrument quality and the observation and processing strategies. When the satellites' measurements are processed consistently, either in the differential GNSS or Precise Point Positioning (PPP) modes, the positional systematic errors are almost constant within strips or within blocks. Velocity errors can be ignored in our application because their impact is at the $10^{-5}$ m level. INS/GNSS systematic angular errors, contrary to what is sometimes assumed in photogrammetric modelling, are not constant due to the nature of angular velocity error propagation (triple integration) and the nature of INS/GNSS sensor fusion (errors concentrating on poor signal-to-noise ratio trajectory intervals).

Tab. 3 summarizes the identified sources of systematic errors in a space-time ISO network.

With the exception of the INS/GNSS velocities and angles, each error, e.g. $\Delta e$, discussed above can be modelled by the corresponding calibration parameter $\delta e$ leading to a set of physical error models that include the parameter $\delta e$. The physical error models extend the collinearity, ground control and aerial control

**Tab. 3:** Main systematic error sources influencing orientation and calibration.

| Error type | Scale-dependent impact | Strip sense-dependent impact | Velocity-dependent impact | Typical size | |
|---|---|---|---|---|---|
| Synchronization | no | yes | yes | < 1 | ms |
| principal point, camera constant | yes | yes | no | 1–2 | px |
| other camera distortions | yes | - | no | ** | |
| GNSS antenna centre | no | yes | no | 1–5 | cm |
| IMU-to-GNSS antenna | no | yes | no | 0.2–2 | cm |
| camera-to-IMU vector | no | yes | no | 0.2–2 | cm |
| camera-to-IMU rotation | yes | yes | no | 0.002 | deg |
| INS/GNSS hor. position | no | no* | no | < 5 | cm |
| INS/GNSS ver. position | no | no* | no | <15 | cm |
| INS/GNSS velocity | no | no* | yes | <0.01 | m/s |
| INS/GNSS $\theta$, $\gamma$ attitude | yes | yes | no | <0.01 | deg |
| INS/GNSS $\psi$ attitude | yes | yes | no | <0.02 | deg |

*: depends on GNSS processing strategy and satellite geometry
**: depends on camera quality

ISO models with the $\delta e$'s and the appropriate formulas. However, some of these calibration parameters are strongly correlated and tend to over-parameterize the estimation process leading to numerical singularities or inaccurate estimates. As is customary in these cases, simplified estimation error models, i.e. a set of observation equation models, are deduced from the complex physical error model equations. The new estimation models are adequate for the network geometries encountered in real life situations.

At this point, based on the above discussion and preliminary network adjustments, we propose a number of realistic block configurations (Tab. 4), and the corresponding calibration parameters to be estimated, or equivalently, the simplified estimation models to be used.

With the exception of configuration (a) the selected block configurations are based on typical "space ISO blocks". By "space ISO block" we understand a regular rectangular block with or without cross strips, with standard (yet camera type-dependent) forward and lateral overlaps, flown at a constant height and speed, with sparse ground control concentrated at the block ends and tPVA aerial control. The boresight matrix angles and self-calibration parameters, i.e. Ebner or Grün models, are always left as unknowns and estimated.

In all block configurations we assume correctly measured lever-arms (camera-to-IMU and IMU-to-GNSS antenna vectors), nodal vectors $A^c$ and correctly calibrated GNSS receiver antenna phase centres.

Block configuration (a) is considered for the sake of completeness and to highlight the contribution of velocity differences to decorrelate scale-dependent and eventual INS/GNSS strip-dependent systematic errors. This configuration will not be analyzed in this paper due to a lack of actual data conforming to its requirements. Refer to Blázquez (2008) for the performance of the (a) configuration with a combination of actual and simulated data.

Block configuration (b) corresponds to the situation in which INS/GNSS positional errors are similar for the whole block and where reliable camera calibration data are available. In both (a) and (b) cases, we expect INS/GNSS positional error corrections to be separable from the $\delta t$ parameter.

Block configuration (c) includes cross-strips and considers the often-encountered situation in which strips flown in different senses exhibit different velocities. While INS/

**Tab. 4:** Block configurations for the determination of the time calibration parameter $\delta t$.

| | Block strip configuration | Block velocity configuration | Camera calibration $(\delta x_0, \delta y_0, \delta f)^c$ | Time calibration $\delta t$ | INS/GNSS correction $(s_E, s_N, s_h)^m$ |
|---|---|---|---|---|---|
| a | alt. flying sense | velocity differences within strips | no | per system | per strip |
| b | alt. flying sense | approximate constant velocity in block | no | per system | per block |
| c | alt. flying sense and cross-strips | velocity differences among strips | only $\delta x_0$, $\delta y_0$ | per system | per block |
| d | alt. flying sense<br>---<br>2 blocks different altitudes | approximate constant velocity within blocks | only $\delta x_0$, $\delta y_0$ | per block or system | per block |
| e | alt. flying sense<br>---<br>2 blocks different altitudes | approximate constant velocity within blocks | yes | per block or system | 1 shift for the 2 blocks |

alt.: alternating

GNSS shift parameters cannot be estimated per strip, the velocity differences make it possible to separate the $(\delta x_0, \delta y_0)^{cT}$ calibration parameters from $\delta t$.

Block configurations (d) and (e) correspond to the ideal situation of two blocks for the same camera, flown at different altitudes for the purpose of decorrelating the calibration parameters that exhibit a scale-dependent impact on the parameters of interest. In this way, $\delta t$ only needs to be decorrelated from the INS/GNSS shift parameters.

## 4 Concept Validation Criteria

A comprehensive validation of space-time ISO network calibration and orientation according to the previous network geometry discussion requires datasets that are not readily available. Fortunately (section 5), we had access to a set that, although not specifically designed for $\delta t$ calibration analysis, was close enough to some of the identified Tab. 4 configurations. Given these circumstances, we will concentrate on the (b), (c), (d) and (e) block configurations since case (a) was already investigated in Blázquez (2008). Further, the validation of the space-time ISO block adjustment concept is designed as follows. Space-time ISO adjustments according to block configurations (b) to (e) will be performed. The results of the adjustment will be inspected for precision (through the standard deviations of the exterior orientation parameters (EO) and tie points (TP)), determinability (through the covariance matrices of the estimated parameters) and accuracy (by comparison to ground check point coordinates). The adjustment will be accepted if precision and accuracy are achieved and if the calibration parameters are determinable. We consider that accuracy is met if the root-mean-square error (RMSE) of the ground check points (ChP) is comparable to the RMSE of the ChPs obtained in a classical space tPA ISO adjustment. Analogously, we consider that precision is met if the mean of the standard deviations of the estimated exterior orientation (EO) and tie point (TP) parameters is similar to the classical space tPA ISO adjustment. Finally, we consider that the $\delta t$ calibration parameter is well determined if there are no suspicious (according to our experience) correlations greater than 0.75 with the other estimated calibration parameters. In addition to this, with $\delta t$ and $\sigma(\delta t)$ the routine significance testing can be performed.

Last, once the precision, accuracy and determinability criteria are met, a final tPA space ISO adjustment will be conducted with a free INS/GNSS shift per strip and the rest of calibration parameters fixed to the estimated values in the tPVA spatio-temporal adjustment. If the estimated INS/GNSS shifts are not stochastically significant and/or do not exhibit a strip flying sense dependency, we will declare the block well calibrated, in space and time.

## 5 Test Data

As mentioned, datasets to test the performance of the proposed space-time ISO method are not readily available. The Vaihingen/Enz dataset described in Kremer & Cramer (2008), although not specifically designed for the purpose, has a number of interesting features related to Tab. 4 configurations (velocity differences between strips – though moderate – and two blocks flown at different altitudes) that make it possible to derive conclusions relevant to this research. We used three blocks of the Vaihingen/Enz dataset: the Vaihingen/Enz-7 (V-7), the Vaihingen/Enz-20 (V-20) and their combination into a single two-altitude block (V-7-20). The blocks were flown in 2008, on the same day, one after the other, with IGI's Dual-DigiCAM-H/39 system and are named respectively after the nominal ground sample distance (GSD); V-7 for the 7 cm GSD block and V-20 for the 20 cm GSD

**Tab. 5:** Precision of observations.

| Observables | V-7 & V-20 blocks |
|---|---|
| Image coordinates | $\sigma_x = \sigma_y = 1.4$ µm |
| Ground Control | $\sigma_E = \sigma_N = \sigma_h = 2$ cm |
| Aerial Control | $\sigma_E = \sigma_N = 3.5$ cm<br>$\sigma_h = 5.5$ cm<br>$\sigma_{ve} = \sigma_{vn} = 5$ mm/s<br>$\sigma_{vu} = 5$ mm/s<br>$\sigma_\gamma = \sigma_\theta = 5$ mdeg<br>$\sigma_\psi = 8$ mdeg |

one. The precision of the observations and block configurations are described in Tabs. 5 and 6 respectively. General block layouts are presented in Figs. 1 and 2.

Reference tPA space ISO adjustment results for precision and accuracy analysis are to be found in Blázquez & Colomina (2012) and Kremer & Cramer (2008). Thus, for the V-7

**Tab. 6:** Vaihingen/Enz-7 and Vaihingen/Enz-20 block configurations.

| Test block | Vaihingen/Enz-7 | Vaihingen/Enz-20 |
|---|---|---|
| Equipment | IGI Dual-DigiCAM-H/39<br>Roll Angle Left H/39 -14:8<br>Roll Angle Right H/39 +14:8<br>AEROControl II-D | |
| Image size | 2 x 5 cm x 4 cm<br>2 x 7216 x 5412 px | 2 x 5 cm x 4 cm<br>2 x 7216 x 5412 px |
| Image size (along flight direction) | 4 cm | 4 cm |
| Image size (across flight direction) | 2 x 5 cm | 2 x 5 cm |
| Pixel size | 6.8 µm | 6.8 µm |
| Camera constant | 82 mm | 82 mm |
| Exposure time | 1/800 s | 1/350 s |
| Flying height above ground (≈) | 1150 m | 2750 m |
| Horizontal speed range (≈) | 60-80 m/s | 53-68 m/s |
| Scale (≈) | 1:14000 | 1:33500 |
| Ground sample distance (GSD) (≈) | 10 cm | 23 cm |
| No. of strips | 6 (3+3) | 3 (3+0) |
| No. of images | 2 x 120 | 2 x 60 |
| No. of images per strip (≈) | 2 x 20 | 2 x 20 |
| No. of photo-observations | 7910 x 2 | 11781 x 2 |
| No. of photo-observations per image (≈) | 30 x 2 | 100 x 2 |
| No. of ground control points (GCP) | 8 | 8 |
| No. of ground check points (ChP) | 14 | 85 |
| No. of tie-points (TP) | 1106 | 2258 |
| Overlap (≈) | 60% x 76% | 60% x 64% |
| Coordinate reference frame | m-type | m-type |

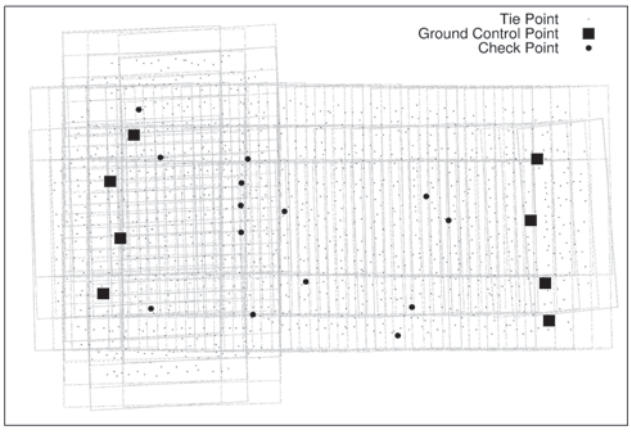


**Fig. 1:** Vaihingen/Enz-7 block layout.

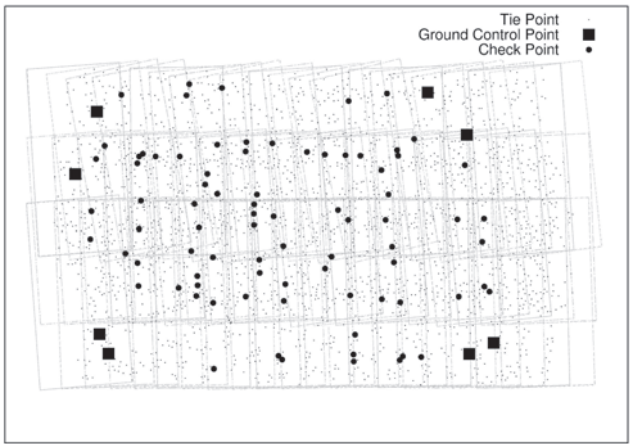


**Fig. 2:** Vaihingen/Enz-20 block layout.

block ChPs, accuracy (RMSE) is at the 2, 4 and 7 cm level for the two horizontal and vertical components and precision is slightly better. For the V-20 block, the RMSE of ChPs is at the 4, 7 and 17 cm level and precision is also slightly better. Precision of the images' exterior orientation parameters, also from tPA space ISO adjustments, is at the 3, 2 cm (horizontal and vertical) and 5, 3 arc sec ($\omega$, $\varphi$ and $\kappa$) level for V-7 and at the 6, 4 cm (horizontal and vertical) and 5, 3 arc sec ($\omega$, $\varphi$ and $\kappa$) level for V-20. More details on the reference precision and accuracy values are not necessary as the obtained results (section 6) are not affected by accuracy and precision problems.

Last, when dealing with synchronization of multi-head systems, there is always the question of how many $\delta t$ shall be estimated: one per head or one per the combined multi-head system. In principle, both approaches are correct as long as the network geometries are strong enough and the choice is consistent with the system design. In our case, we decided to estimate one common $\delta t$ for the two cameras because the dual head-system was designed for simultaneous shutter opening leaving any synchronization uncertainty as a common synchronization error (Kremer 2011).

## 6 Results

Tabs. 7 to 9 contain the main results of our research. All block configurations have been tested: (b) and (c) for the two blocks resulting in four test cases numbered 1 to 4; (d) and (e) for the combined V-7-20 block with a single $\delta t$ parameter corresponding to test cases 5, 6 and (d) and (e) for the combined V-7-20 block with two $\delta t$ parameters, for the images of the V-7 and V-20 blocks resulting in two more test cases 7, 8. For the test cases 3 to 5 and 7, the camera constants have been set and kept fixed to their nominal values; in test cases 1 and 2, the cameras' interior orientation elements have been set and kept fixed to known calibration values.

Tab. 7 describes the mean accuracy of the ground check points (ChP columns), the mean precision of the exterior orientation parameters (EO columns), the mean precision of the ground tie points (TP columns) and the precision of the camera-to-IMU [boresight] angles ($\Upsilon$ column). Note that in test cases 5 to 8, the accuracy estimates are given separately for the V-7 ChPs (first row) and the V-20 ones (second row). All values are well within the acceptable ranges provided in section 5 and therefore all test cases pass the accuracy and precision validation criteria with the exception of the Northing component of the V-20 ChPs of test cases 6 and 8 (due to the global common INS/GNSS shift). As we will conclude later on, the two

cameras of the IGI Dual-DigiCAM-H/39 are already well synchronized and therefore no significant differences between the various test configurations are to be expected in the ground check point results when the $\delta t$ calibration parameter is estimated.

Tab. 7 also contains the precision estimates for the camera-to-IMU, $\Upsilon_c^b$, angles which are all well determined at the arc sec level and with correlations with the camera interior orientation elements of less than 0.7 and exceptionally between 0.7 and 0.8.

Tab. 8 provides bounding information on the correlation of $\delta t$ with the rest of the calibration parameters. With the exception of test case 4, all test cases lead to determinable $\delta t$ estimates according to the criteria set in section 4. Total correlation values $b(\delta t)$ are provided for the sake of completeness. At this point of time, the interpretation of $b(\delta t)$ is not clear; however, the $b(\delta t)$ correlations seem to indicate a stronger V-7 than V-20 geometry. This is thought to be a consequence of V-7 being a larger dataset and having cross-strips, or because of its slightly larger velocity differences.

The actual calibration results are presented in Tab. 9 where parameters significantly different from 0 are boldfaced (In Tab. 9, the standard deviation of each estimated parameter is indicated following the value of the calibrated parameter with a ± symbol.). The test case 4 will not be discussed as it did not pass the $\delta t$ determinability criteria. In the table, for the test cases 3 to 8, double rows within cells of the $\delta f$, $\delta x_0$ and $\delta y_0$ columns correspond to the two cameras. Double rows within cells of the $s_E$, $s_N$ and $s_h$ columns correspond to the two INS/GNSS shifts (one per each V-7 and V-20 blocks, in the test cases 5 and 7) whereas a single row corresponds to a common shift (test cases 1 to 4, 6 and 8). A similar convention is used for the double rows within cells of the $\delta t$ column for the test cases 7 and 8 where two $\delta t$ calibration parameters were used (one per each V-7 and V-20 blocks).

INS/GNSS shift parameters are not significantly different from 0. This is an independent confirmation of the quality of the GNSS aerial control that, after the calibration in space and time, does not exhibit significant systematic errors.

Test cases 1, 2, 3, 7 and 8 show a remarkable consistency in the determination of a block dependent $\delta t$. If we now analyze the interior orientation elements, $\delta f$, $\delta x_0$ and $\delta y_0$, of the 3,

**Tab. 7:** Accuracy and precision results for the block configurations (b) to (e).

| No. | Config. & Block | ChP RMSE (cm) | | | EO MEAN σ (cm, arc sec) | | | | | TP MEAN σ (cm) | | | $\Upsilon$* σ (arc sec) | |
|---|---|---|---|---|---|---|---|---|---|---|---|---|---|---|
| | | E | N | h | $E_0$ | $N_0$ | $h_0$ | ω φ | κ | E | N | h | $\upsilon_x$ $\upsilon_y$ | $\upsilon_z$ |
| 1 | b V-7 | 1.9 | 2.4 | 5.7 | 2.2 | 2.1 | 1.8 | 5 | 3 | 1.5 | 1.8 | 4.1 | 3 | 2 |
| 2 | b V-20 | 3.8 | 7.1 | 12.3 | 3.9 | 3.0 | 4.8 | 3 | 3 | 3.1 | 5.3 | 14.1 | 3 | 3 |
| 3 | c V-7 | 1.8 | 2.4 | 5.6 | 2.3 | 2.1 | 1.9 | 5 | 3 | 1.5 | 1.8 | 4.0 | 3 | 2 |
| 4 | c V-20 | 3.8 | 7.2 | 12.7 | 6.0 | 3.0 | 4.9 | 4 | 3 | 3.1 | 5.4 | 14.1 | 4 | 3 |
| 5 | d V-7-20 | 2.0<br>3.3 | 2.5<br>6.3 | 6.0<br>11.3 | 2.5 | 2.4 | 2.7 | 4 | 3 | 2.6 | 4.2 | 10.8 | 2 | 2 |
| 6 | e V-7-20 | 2.0<br>3.3 | 2.9<br>9.5 | 6.0<br>11.6 | 2.3 | 2.1 | 3.0 | 4 | 3 | 2.5 | 4.1 | 10.8 | 3 | 2 |
| 7 | d V-7-20 | 1.9<br>3.4 | 2.5<br>6.2 | 6.0<br>11.1 | 2.9 | 2.4 | 2.7 | 4 | 3 | 2.6 | 4.2 | 10.7 | 2 | 2 |
| 8 | e V-7-20 | 1.9<br>3.3 | 2.9<br>9.4 | 6.0<br>11.3 | 2.7 | 2.1 | 3.0 | 4 | 3 | 2.5 | 4.1 | 10.8 | 3 | 2 |

*: $\Upsilon_c^b = (\upsilon_x, \upsilon_y, \upsilon_z)_c^{bT}$ is the vector of boresight (camera-to-IMU) angles.

7 and 8 test cases we will see that the results of the test cases 7, 8 are consistent with each other and inconsistent with test case 3, particularly for the second camera. This may be an indication that the velocity differences between strips of the dataset used are not large enough to accurately separate $\delta f$, $\delta x_0$ and $\delta y_0$ from $\delta t$.

In principle, because of the larger number of observations and the two different block altitudes, test cases 5, 6, 7 and 8 should lead to the best results, and those most consistent among themselves. On the contrary, Tab. 9 shows that the $\delta t$ and $\delta x_0$ estimates are inconsistent between the test cases 5, 6 and 7, 8. The reason for this (Kremer 2011) is the DualDigiCAM-H/39 time tagging convention (at the time of shutter opening) that differs from the tagging convention assumed in the paper (at the mid exposure time). According to this and to Tab. 6, a correctly synchronized DualDigiCAM-H/39 head with the manufacturer's convention should lead (test cases 1, 2, 3, 7 and 8) to half of 1/800 s ($\delta t$ = 0.625 ms) and half of 1/350 s ($\delta t$ = 1.43 ms) for the V-7 and V-20 blocks respectively. These figures are consistent with and not significantly different from the results of test cases 2, 7 and 8. They explain the differences with test cases 5, 6 and empirically confirm that block configurations (b), (d) and (e) are appropriate for tPVA space and time ISO orientation and calibration. The result is remarkable if one considers that the datasets used were not originally designed for $\delta t$ calibration (A further consequence of this

**Tab. 8:** $\delta t$ correlation bounds with the rest of calibration parameters ($\rho(\delta t, -)$) and total correlation ($b(\delta t)$).

| | 1 | 2 | 3 | 4 | 5 | 6 | 7 | 8 |
|---|---|---|---|---|---|---|---|---|
| $\rho(\delta t, -) \leq 0.7$ | yes | yes | yes | no<br>$\rho(\delta t, \delta x_0) = 0.8$ | yes | yes | yes | Yes |
| $b(\delta t)$ | 0.934 | 0.984 | 0.961 | 0.996 | 0.956 | 0.945 | 0.950<br>0.986 | 0.943<br>0.986 |

**Tab. 9:** Precision and determinability results for the block configurations (b) to (e).

| No. | Config. & Block | Interior orientation: (μm) | | | INS/GNSS shifts (cm) | | | Time (ms) |
|---|---|---|---|---|---|---|---|---|
| | | $\delta f$ | $\delta x_0$ | $\delta y_0$ | $s_E$ | $s_N$ | $s_h$ | $\delta t$ |
| 1 | b V-7 | - | - | - | -0.1 ±1.0 | -2.5 ±1.0 | 2.7 ±1.5 | -0.1 ±0.1 |
| 2 | b V-20 | - | - | - | 0.5 ±1.8 | 3.5 ±2.1 | -3.1 ±4.4 | **1.4** ±0.4 |
| 3 | c V-7 | - | -2 ±1<br>5 ±2 | **14** ±1<br>**-10** ±1 | 0.0 ±1.0 | -2.5 ±1.0 | 4.5 ±1.5 | 0.0 ±0.2 |
| *4** | *c V-20* | - | *-3 ±2*<br>*-2 ±2* | ***15*** *±2*<br>*4 ±2* | *1.3 ±1.9* | *3.2 ±2.1* | *-3.8 ±4.5* | *0.4 ±0.8* |
| 5 | d V-7-20 | - | -3 ±1<br>**-4** ±1 | **11** ±1<br>-1 ±1 | -0.0 ±1.0<br>1.6 ±1.8 | -2.7 ±1.0<br>6.1 ±2.1 | 2.6 ±1.6<br>-0.1 ±3.9 | **-0.5** ±0.1 |
| 6 | e V-7-20 | -2 ±2<br>0 ±2 | **-4** ±1<br>-3 ±1 | **12** ±1<br>-3 ±1 | 0.3 ±0.9 | -1.1 ±0.9 | 4.1 ±2.6 | **-0.5** ±0.1 |
| 7 | d V-7-20 | - | 1 ±1<br>-1 ±1 | **11** ±1<br>-1 ±1 | -0.4 ±1.0<br>0.8 ±1.8 | -2.6 ±1.0<br>6.1 ±2.1 | 2.7 ±1.6<br>-0.3 ±3.9 | 0.0 ±0.2<br>**1.4** ±0.4 |
| 8 | e V-7-20 | -2 ±2<br>0 ±2 | 0 ±1<br>0 ±1 | **12** ±1<br>-3 ±1 | -0.1 ±0.9 | -1.0 ±0.9 | 4.4 ±2.6 | 0.0 ±0.2<br>**1.3** ±0.4 |

*: row 4 is provided just for completeness as $\delta t$ did not pass the determinability criteria; it is not considered in the discussion of results.

is that block configuration (c) could be neither validated nor disregarded as the velocity differences were apparently too small.).

To conclude, as proposed in section 4, we conduct a tPA space ISO adjustment with a free INS/GNSS shift per strip and the rest of calibration parameters fixed to the estimated values in the tPVA space-time adjustment of test case 7. The results of this adjustment for the V-20 block show that the shifts are not significantly different from 0. They are depicted in Fig. 4 (All the images of the same strip have the same estimated INS/GNSS shift of the strip associated with them.). Fig. 3 shows the analogous pattern of the INS/GNSS shifts before tPVA space-time ISO orientation and calibration. As can be seen in Fig. 3, the INS/GNSS shift parameters were contaminated

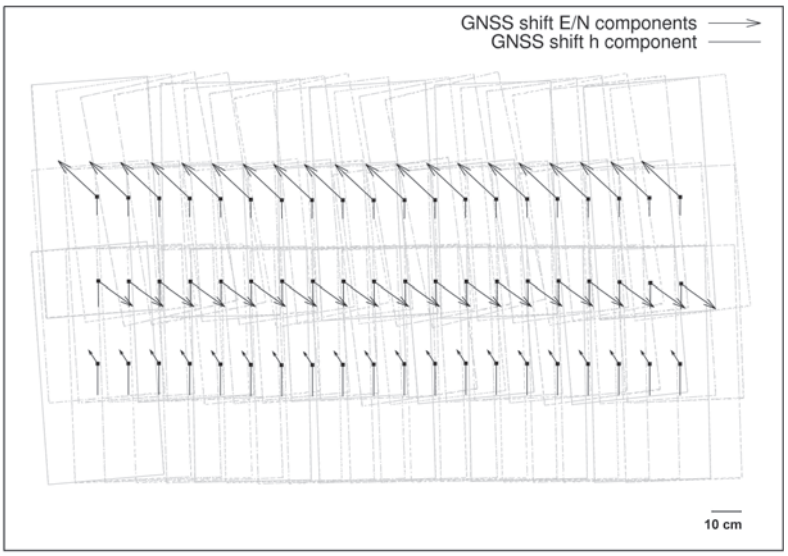


**Fig. 3:** V-20 INS/GNSS linear shifts before time calibration.

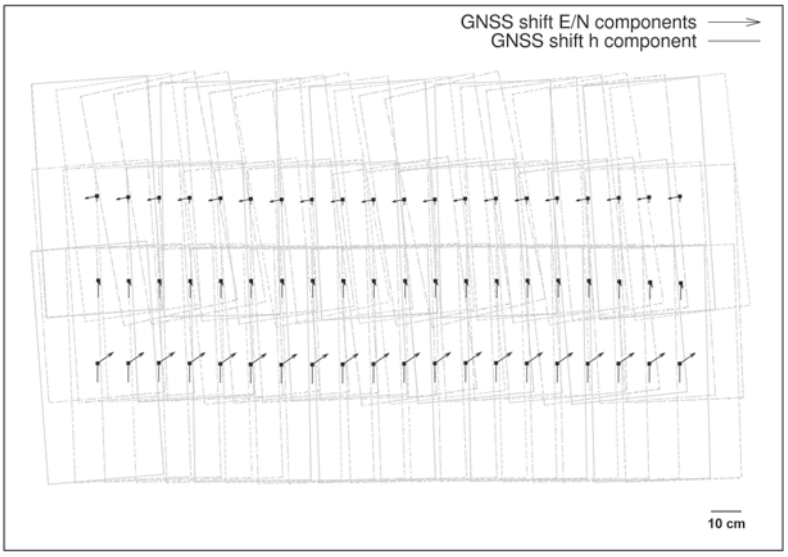


**Fig. 4:** V-20 INS/GNSS linear shifts after time calibration.

by flying sense-dependent spatial calibration errors. The effect of these errors vanishes in Fig. 4.

## 7 Conclusions

We have presented and discussed in detail the concept of spatio-temporal integrated sensor orientation for the case of constant $\delta t$ synchronization calibration parameters between frame cameras and the temporal reference frame materialized by the on-board INS/GNSS system. The concept is based on the use of INS/GNSS-derived control velocities and on the decorrelation of the $\delta t$ unknown parameter from other camera, system and aerial control calibration unknown parameters. Indeed, we have shown that a realistic – accurate – estimation of $\delta t$ requires the careful separation between it and other calibration parameters through the appropriate block configuration. We have found that valid block configurations can be based on different altitude strips (d and e) or on standard blocks with pre-calibrated cameras (b). With the available data, we were not able to confirm that moderate velocity differences between strips (c) make it possible to separate the camera fundamental geometric calibration parameters ($\delta f$, $\delta x_0$ and $\delta y_0$) from the temporal ones $\delta t$. Cross strips are advisable because they add more data and contribute to a better determination of the camera geometric calibration parameters.

Some block configurations are more appropriate for the situation of a manufacturer's field calibration mission prior to delivery to customers; others are better suited to operational, on-the-job self-calibrating ISO. Some configurations (one INS/GNSS shift per block) are more advisable for small-area blocks and accurate short-range differential GNSS processing; others (INS/GNSS shifts per strip and velocity differences within strips) would perform better for large-area blocks and precise – though probably less accurate – long-range differential or non-differential PPP GNSS processing.

We do not claim that the mentioned and tested block configurations are the only possible ones. However, we do state that an accurate determination of $\delta t$ requires separation from the camera internal geometric calibration parameters, from system calibration ones and from INS/GNSS shifts. If this is achieved by any appropriate block configuration, then the INS/GNSS-derived velocities allow for $\delta t$ precisions at the tenth of a millisecond level.

We envision two main scenarios where the proposed time calibration method can be of practical interest. The first one is on the manufacturers' side for system verification and calibration purposes. In this case, the configuration of geometric test flights can be fine tuned to serve also the needs of time calibration. The second scenario is that of end users. In this case, systems that require some sort of on-the-job synchronization, high demanding specifications, the need to verify the system performance for whatever reason or pre-calibration for DiSO can benefit from our method. In the latter scenario, at least initially, we recommend a conservative approach to block configuration where scale and/or velocity differences are big. For high-end geodata acquisition systems, considering their current status and foreseen progress, system verification and calibration purposes may probably dominate its applications. For simpler systems with lower cost off-the-shelve components the method may lead to routine procedures for both verification, calibration and production purposes.

The principle of the method, using INS/GNSS-derived velocities to link space and time, can be applied to other acquisition instruments or combinations of instruments like line cameras or laser scanners. Of course, new sensing geometries may require different block configurations than those discussed in this paper.

Last, we confirm that the Dual-DigiCAM, which integrates two independent cameras, behaved as indicated by the manufacturer as what we recovered from our estimated synchronization calibration parameters was the difference between the initial (IGI convention) and mid (our convention) exposure times.

## Acknowledgements

The datasets Vaihingen/Enz blocks were provided by Dr. Jens Kremer (IGI GmbH, Ger-

many) and Dr. Michael Cramer (Institut für Photogrammetrie, Universität Stuttgart, Germany). The models were implemented and the results were obtained with the Generic Extensible Network Approach (GENA) platform from GeoNumerics (Barcelona, Spain). This support for our research is greatly appreciated. The research reported in this paper has been funded by the Spanish projects LIRA (Ref. P 44/08, Ministerio de Fomento, Spain) and GeoLandModels (Ref. PET2008 071, Ministerio de Ciencia e Innovación, Spain).

## References

Blázquez, M. & Colomina, I., 2008: On the Use of Inertial/GPS Velocity Control in Sensor Calibration and Orientation. – EuroSDR, ISPRS, Proceedings of the EuroCOW 2008, Castelldefels, Spain, 8 p. (on CDROM).

Blázquez, M., 2008: A New Approach to Spatio-Temporal Calibration of Multi-Sensor Systems. – International Archives of the Photogrammetry, Remote Sensing and Spatial Information Sciences **37** (B1): 481–486.

Blázquez, M. & Colomina, I., 2012: Relative INS/GNSS aerial control in integrated sensor orientation: models and performance. – ISPRS Journal of Photogrammetry and Remote Sensing **67:** 120–133.

Graham, L.I., 2010: Mobile Mapping Systems overview. – Photogrammetric Engineering and Remote Sensing **76:** 222–228.

Harrison, A. & Newman, P., 2011: TICSync: knowing when things happened. – Proceedings of the IEEE International Conference on Robotics and Automation **ICRA2011:** 356–363, Shanghai, China.

Kremer, J. & Cramer, M., 2008: Results of a performance test of a dual mid-format digital camera system. – International Archives of the Photogrammetry, Remote Sensing and Spatial Information Sciences **37** (B1): 1051–1057.

Kremer, J., 2011: Private communication.

Olson, E., 2010: A passive solution to the sensor synchronization problem. – Proceedings of the IEEE/RSJ International Conference on Intelligent Robots and Systems (IROS): 1059–1064, Taipei, Taiwan.

Address of the Authors:

Marta Blázquez, Ismael Colomina, Institute of Geomatics, Av. Carl Friedrich Gauss 11, Parc Mediterrani de la Tecnologia, E-08860 Castelldefels, Tel.: +34-93-5569280, Fax: +34-93-5569292, e-mail: {marta.blazquez}{ismael.colomina}@ideg.es

Manuskript eingereicht: Dezember 2011
Angenommen: Januar 2012

# Chapter 5

# Fast AT

The contribution of this last paper is not the presentation or development of any new mathematical model. Its contribution is the proposal of a new integrated sensor orientation procedure: "fast aerotriangulation" (Fast AT).

Fast AT is an integrated sensor orientation procedure based on the use of a limited number of ground control points, their mapping sensor measurements and INS/GNSS-derived aerial control data for all images. It is a particular case of the traditional ISO with fewer measurements. Figure 5.1 shows how Fast AT lies between DiSO and ISO.

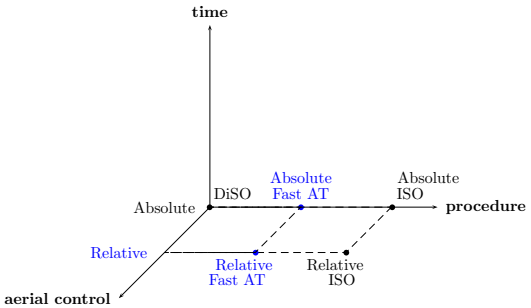


Figure 5.1: Fast AT

This paper introduces the concept and discusses its performance for absolute and relative aerial control with three actual independent data sets. All these data sets are regularly-shaped blocks, but the performance of Fast AT for corridor aerial mapping is discussed in [Blázquez and Colomina, 2012d].

For this research I performed the calculations and analyzed the results. I wrote the paper with Dr. Ismael Colomina who also promoted and supervised the research.

ISPRS Journal of Photogrammetry and Remote Sensing 71 (2012) 1–11

Contents lists available at SciVerse ScienceDirect

ISPRS Journal of Photogrammetry and Remote Sensing

journal homepage: www.elsevier.com/locate/isprsjprs

# Fast AT: A simple procedure for quasi direct orientation

M. Blázquez *, I. Colomina

*Institute of Geomatics, Av. Carl Friedrich Gauss, 11, Parc Mediterrani de la Tecnologia, E-08860 Castelldefels, Spain*

ARTICLE INFO

*Article history:*
Received 26 March 2012
Received in revised form 19 April 2012
Accepted 20 April 2012

*Keywords:*
GNSS
INS
Orientation
Calibration
Camera
Adjustment

ABSTRACT

Over the past two decades, the development of Global Navigation Satellite System (GNSS) technology, inertial navigation technology and Inertial Navigation Systems (INS) and their application to sensor orientation in photogrammetry and remote sensing has led to more precise, accurate, reliable and cost efficient orientation and calibration methods and procedures. Today, most airborne photogrammetric and remote sensing systems are equipped with GNSS receivers and inertial sensors. To a large extent and more or less independently from the imaging geometry and sensor type, orientation is performed with the "direct" and "integrated" methods. In this paper we introduce a new orientation method that we call "Fast AT" for frame images. The new method combines image measurements, ground control and aerial control observations in novel quantitative and qualitative ways. Depending on project specifications, Fast AT can be a robust alternative to direct orientation and, at the very least, a fast quality control tool for any orientation task. We analyze the performance of Fast AT with analogue and digital frame imagery and draw conclusions on its general properties.


## 1. Introduction and motivation

Airborne sensor orientation has evolved from classical aerial triangulation – restricted to frame or matrix sensors – to modern GNSS and INS/GNSS based sensor orientation – extended to practically all types of mapping sensors. After the initial period when the fundamental concepts of aerial triangulation itself, self-calibration and gross error detection were established, the development of sensor orientation has been driven by the introduction of GNSS and INS/GNSS (Schwarz et al., 1993) -derived position and position–attitude aerial control, respectively. Today, the majority of medium- and high-end mapping sensor systems are equipped with a geodetic grade GNSS receiver and a tactical- or higher grade Inertial Measurement Unit (IMU). INS/GNSS systems – possibly complemented with other navigation sensors – have become time, Position, Velocity and Attitude (tPVA) servers able to provide kinematic tPVA control observations to airborne and terrestrial mapping data acquisition systems. The tPVA control observations can be used to perform Direct Sensor Orientation (DiSO) or, together with measurements made on the mapping sensor data and/or on the ground, perform Integrated Sensor Orientation (ISO). Orientation performed without tPVA aerial control will be referred to as Indirect Sensor Orientation (InSO). Classical aerial triangulation is a particular case of InSO.

In the case of frame cameras, the time, Position and Attitude (tPA) control subset of the tPVA set is used in the DiSO and ISO orientation modes. More specifically, DiSO is performed by using tPA observations together with previously obtained IMU-to-camera relative orientation values (boresight matrices and lever arm vectors) treated as constants or observations. ISO is performed by using the same tPA observations together with a large number of image observations. From those, usually, image observations for ground control points are measured manually by specialized operators whereas the rest of image observations are obtained automatically with digital image matching software. The properties of DiSO and ISO are currently well understood for the existing sensors (Heipke et al., 2002; Ip et al., 2007; Skaloud and Lichti, 2006) and, as new sensor configurations and geometries appear, their performance is either implicitly or explicitly being re-evaluated (Cramer, 2009; Haala et al., 2010). DiSO is faster than ISO as it does not require the measurement of image coordinates. It is also more flexible as it does not depend on image texture or flight geometry. However, it cannot benefit from self-calibration and relies critically on the accuracy of GNSS and IMU-to-camera relative orientation. ISO can include sensor self-calibration and can correct GNSS inaccuracies if few ground control points are available. However, it takes longer. ISO enjoys the self-diagnosis properties of geodetic network adjustment; DiSO does not. And while it is always advisable to check the ISO results with independently determined ground check points, this is the only means of quality control for DiSO.

* Corresponding author. Tel.: +34 93 556 92 80; fax: +34 93 556 92 92.
*E-mail addresses:* marta.blazquez@ideg.es (M. Blázquez), ismael.colomina@ideg.es (I. Colomina).

0924-2716/$ - see front matter © 2012 International Society for Photogrammetry and Remote Sensing, Inc. (ISPRS) Published by Elsevier B.V. All rights reserved.
http://dx.doi.org/10.1016/j.isprsjprs.2012.04.005

We note that the mathematical models and procedures of DiSO and ISO were established in the late eighties and early nineties (Ackermann and Schade, 1993; Colomina, 1993; Schwarz et al., 1993) and that, other than testing the performance of GNSS and INS/GNSS, no significant development has since taken place in the field, as pointed out in Colomina (2007). Recently we have proposed new concepts and methods to use the tPVA observations for ISO (Blázquez, 2008): the use of tPA control observations in relative mode and the full use of tPVA control observations in both absolute and relative modes. The use of tPA relative control in ISO eliminates the need for IMU-to-camera relative rotation parameters and for those of GNSS shift (3D-vector parameter that absorbs the INS/GNSS errors as those due to incorrect ambiguities) (Blázquez and Colomina, 2012a). The full use of tPVA control – i.e., the use of velocity observations in addition to positions and angles – allows the estimation of IMU-to-camera synchronization parameters (Blázquez and Colomina, 2012b).

In this paper we introduce a new ISO mode that we call "fast aerial triangulation" (Fast AT). Fast AT is loosely related to F. Ackermann's early idea of simplified aerial triangulation from the late 1980s (Friess, 2012). In a simplified aerial triangulation, the goal is to reduce the number of tie points to a few per image. Fast AT is closer to the concept of "minimal aerial triangulation" (Alamús et al., 2002; Barón et al., 2003) for regularly-shaped blocks where the number of photogrammetric measurements is significantly reduced by concentrating them in the cross strips.

The goal of Fast AT is to provide a sensor orientation method and procedure that is almost as fast as DiSO, does not suffer from GNSS inaccuracies or reference frame uncertainties and that, with relative tPA control, does not require the attention of the user with respect to IMU-to-camera relative orientation and GNSS shift parameters. In this paper we concentrate on the analysis of rectangular-shaped Fast AT blocks because, as we will discuss in the next section, their geometry differs little from that of regular blocks. For an initial analysis of corridor blocks, the reader is referred to Blázquez and Colomina (2012c).

The paper is organized in two main sections: Fast AT and performance analysis. In the next section, we introduce the concept, the potential applications and the geometry of the Fast AT method. In the performance analysis section, the test data, the block configurations and the results are discussed. Last, we present the conclusions.

## 2. Fast AT

### 2.1. The concept

Fast AT is a particular case of ISO characterized by the use of the following observations:

- tPA aerial control observations, either in the absolute or relative mode, for all images.
- Ground control point observations for a limited number (in principle) of points and images.
- Image coordinate observations for the ground control points only.

In other words, a Fast AT block is an ISO block when all Tie Points (TPs) are Ground Control Points (GCPs) and where the number of GCPs is small. The concept is simple and can be performed with existing software with no or minimal modifications.

As compared to the "minimal aerial triangulation" concept (Alamús et al., 2002; Barón et al., 2003). Fast AT uses far fewer measurements (no digital matching needed) at the expense of being less accurate and robust. While Fast AT only requires photogrammetric measurements for GCPs, "minimal aerial triangulation" also requires photogrammetric measurements for images either belonging to or overlapping cross strips.

**Table 1**
Observations of InSO, ISO, Fast AT and DiSO.

| Observations | InSO | ISO | Fast AT | DiSO |
|---|---|---|---|---|
| tPA/tPVA aerial control | NO | YES | YES | YES |
| Ground control points | YES<br>many | YES<br>few | YES<br>few | NO |
| Image coordinates | YES<br>many | YES<br>many | YES<br>few | NO |

**Table 2**
Properties of ISO, Fast AT and DiSO.

| Properties | ISO | Fast AT | DiSO |
|---|---|---|---|
| Precision | + | 0 | 0 |
| Accuracy | + | 0 | – |
| Reliability | + | 0 | – |
| Cost | + | 0 | – |
| Time | + | 0 | – |

+: high. 0: average. –: low.

Fast AT lies between DiSO and ISO, as it uses more observations than DiSO and fewer than ISO. Our view is that Fast AT shares its application context and scope with DiSO; therefore, we will analyze its properties under conditions similar to those of DiSO. Tables 1 and 2 and Fig. 1 compare the concepts of InSO, ISO, Fast AT and DiSO. Notice that in Fig. 1, there are missing images for Fast AT and DiSO to point out that these orientation methods do not require physical overlap between images not including GCPs. For the sake of thoroughness, Fig. 2 represents an InSO block layout.

### 2.2. Potential applications

In general, Fast AT is of interest in situations where ISO is not feasible or required and where DiSO is not accurate or reliable enough. For instance, it may be used for ill-textured areas like forested regions, deserts, wetlands or the vicinity of rivers and lakes where image matching is difficult. Note, however, that Fast AT is not necessarily a lower-cost alternative to DiSO, as difficult areas for image matching tend to also be difficult areas for the establishment of ground control. Fast AT may also be of interest for applications currently relying on DiSO, where accuracy and reliability matter, and that, for some reason, cannot afford the time and/or cost required by ISO and where the measurement or use of existing GCPs makes sense in the context of the application. In emergency situations like natural or man-made disasters that require rapid mapping or georeferencing, Fast AT can be the orientation and calibration method of choice.

Fast AT can be used in combination with standard ISO procedures in various ways. One possibility is that a small ISO block be used for camera calibration and that Fast AT be applied for larger blocks. The data acquisition for the ISO block can take place at any time, before, in between or after the Fast AT blocks are acquired. Sensor calibration parameters can then be computed and, later on, used as constants or observations in the Fast AT blocks. In this combination, the ISO block estimates camera and possibly system calibration parameters while the Fast AT blocks estimate reference frame inconsistencies, INS/GNSS errors and possibly, system calibration parameters.This combination of ISO and Fast AT only makes sense as long as the calibration parameters estimated in the ISO block are stable for their period of use

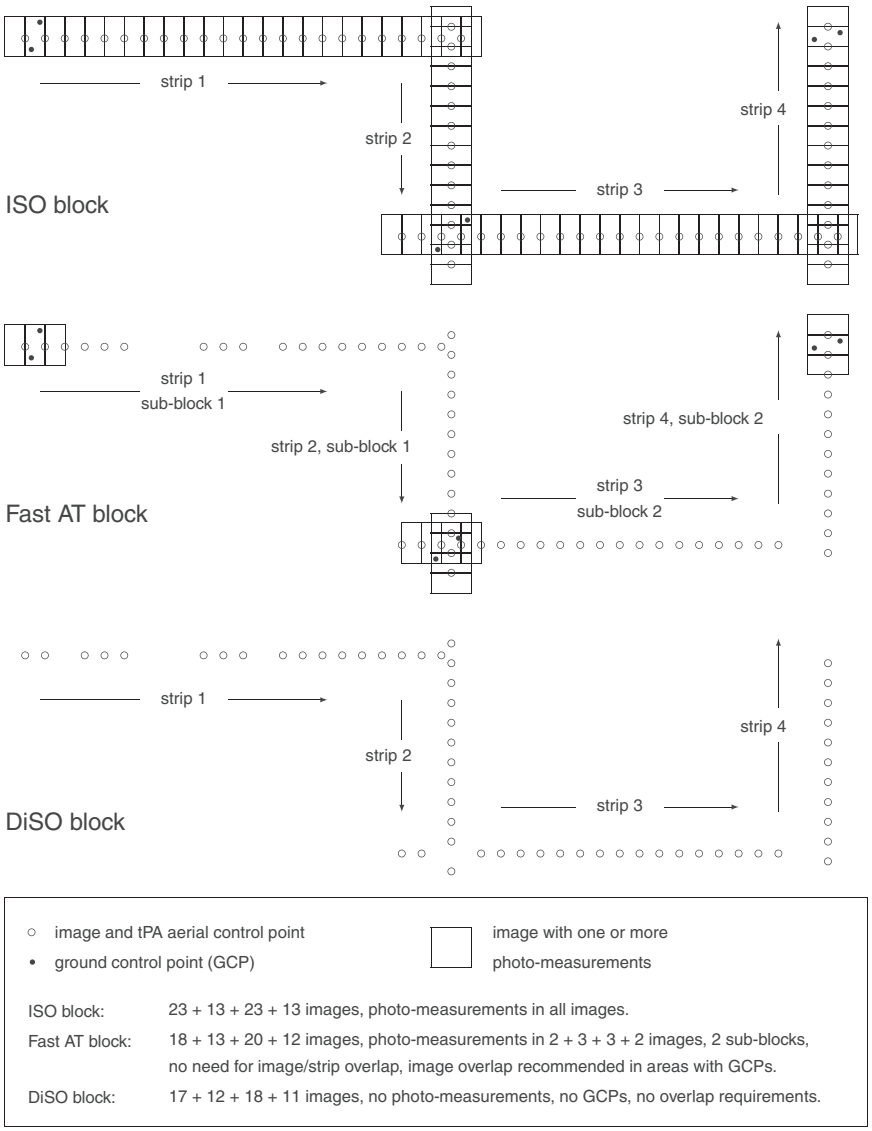


**Fig. 1.** Conceptual layout of a classical ISO, Fast AT and DiSO blocks.

in Fast AT. One example is the calibration of small- and medium-format cameras with the Conrady–Brown model where the coefficients of the radial distortion terms tend to be quite stable as opposed to the corrections to the camera constant and principal point coordinates. In this case, Fast AT will benefit from the stable radial calibration parameters, will mostly absorb the vertical error generated by any camera constant parameter and will partially absorb the horizontal errors generated by any principal point parameters.

A second possibility is that, in a single block, a subset of images be measured and processed under the classical ISO paradigm with the usual tie point density while the complementary subset can be measured under the Fast AT paradigm with no (or minimal) tie points and image measurements only for GCPs, if any. This type of mixed blocks is suited for complex terrain scenarios where Fast AT can be used to bridge low-textured areas not suitable for image matching or irregular ones like coast lines, river banks or islands. In some cases, the majority of images will be oriented under the standard ISO procedure and in other cases the Fast AT procedure will be predominant.

Last, Fast AT can be applied to rapid quality control of photogrammetric flights and INS/GNSS trajectory validation processes.

### 2.3. Mathematical models

Strictly speaking, the Fast AT concept is independent from the particular functional models of the observation equations for image coordinate, ground control and aerial control observations.

Considering the classical use of tPA aerial control observations in absolute mode, differences in the functional models are mainly due to the choice of coordinate systems and, to a lesser degree, the personal preferences of the model authors. Clearly, the features and behaviour of Fast AT shall be independent from the former choices and preferences.

In the frame of the presented research, the new sensor orientation and calibration procedure is tested with the functional and stochastic models presented and validated in Blázquez and Colomina (2012a). In this case, we differentiate between the classical use of tPA aerial control observations in absolute mode, absolute Fast AT, and the proposed use of tPA aerial control observations in relative mode, relative Fast AT.

### 2.4. The geometry

A Fast AT block is a particular type of ISO block and, indeed, from a qualitative point of view, meets standard ISO criteria as it

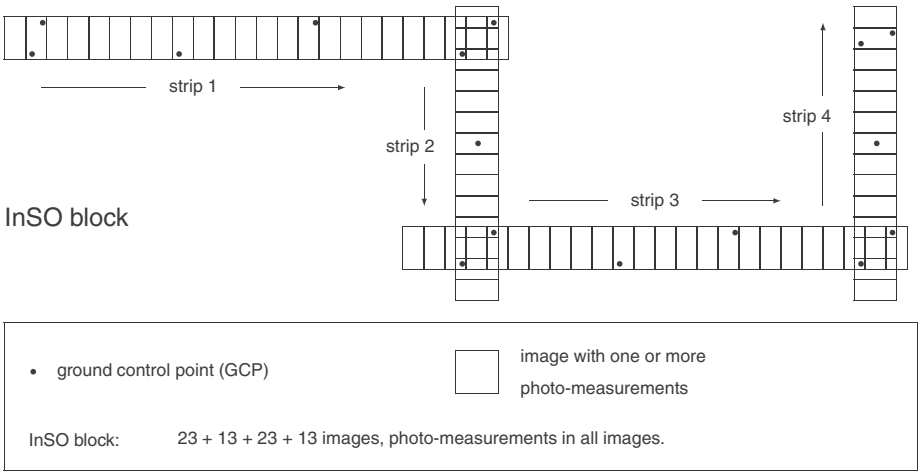


**Fig. 2.** Conceptual layout of a classical InSO block.

**Table 3**
Test blocks: geometric configuration.

| Test block | P | V-7 | V-20 |
|---|---|---|---|
| Equipment | Leica RC30 | IGI Dual-DigiCAM-H/39<br>Roll Angle Left H/39 −14.8°<br>Roll Angle Right H/39 +14.8° | IGI Dual-DigiCAM-H/39<br>Roll Angle Left H/39 −14.8°<br>Roll Angle Right H/39 +14.8° |
| | Applanix POS AV 510 | AEROControl II-D | AEROControl II-D |
| Image size | 23 cm × 23 cm<br>16329 px × 16329 px | 2 × 5 cm × 4 cm<br>2 × 7216 × 5412 px | 2 × 5 cm × 4 cm<br>2 × 7216 × 5412 px |
| Image size (along flight direction) | 23 cm | 4 cm | 4 cm |
| Image size (across flight direction) | 23 cm | 2 × 5 cm | 2 × 5 cm |
| Pixel size | 14 μm | 6.8 μm | 6.8 μm |
| Camera constant | 153 mm | 82 mm | 82 mm |
| Flying height above ground (≈) | 1200 m | 1150 m | 2750 m |
| Scale (≈) | 1:8000 | 1:14000 | 1:33500 |
| Ground Sampling Distance (GSD) (≈) | 11 cm | 10 cm | 23 cm |
| No. of strips | 11 (7 + 4) | 6 (3 + 3) | 3 (3 + 0) |
| No. of images | 131 | 2 × 120 | 2 × 60 |
| No. of images per strip (≈) | 10 | 2 × 20 | 2 × 20 |
| No. of Ground Control Points (GCPs) | 8 | 8 | 8 |
| No. of Ground Check Points (ChPs) | 25 | 14 | 63 |
| Overlap (≈) | 60% × 60% | 60% × 76% | 60% × 64% |
| Coordinate reference frame | *l* | *m* | *m* |

includes exactly the same type of observations: photogrammetric, ground control and aerial control. Like any geodetic or photogrammetric network, the "geometry" of a Fast AT block is a function of the number, quality and distribution of observations, of the mathematical models in use and the number and distribution of unknown parameters. A "strong" geometry makes it possible to estimate more parameters than a "weak" one and/or to better estimate them. The geometry of a Fast AT block is weaker than that of its correspondent standard ISO block because of the latter's higher number of photogrammetric observations.

In general, a block's geometry is dominated by the block configuration; i.e., the number, distribution, length and flying direction of strips; the degree of image overlap and the GCP distribution (also in general, block geometry for a given sensor orientation and calibration concept can be investigated, for the various configurations of interest, through simulated data sets and the corresponding covariance analysis. This method is not pursued in this paper). In the particular case of a Fast AT block, since the number of photogrammetric measurements is low, the degree of image overlap has a correspondingly small – even negligible – impact on the geometry and is no longer one of the characteristic parameters of a block's configuration.

In order to understand the geometry of a Fast AT block, we partition the block in sub-blocks; i.e., in subsets of images that share a common INS/GNSS 3D-vector shift parameter. Thus, in a Fast AT block there are as many sub-blocks as INS/GNSS shift parameters. Since shift parameters, in principle, absorb INS/GNSS errors, the number of sub-blocks depends on the stability of the INS/GNSS errors which, in turn, depends on the constancy of the visible GNSS satellite configuration, the flying style and the INS/GNSS processing method. Typical block configurations are those based on 1 shift-per-strip and 1 shift-per-block. However, in general – and in particular for large blocks – the sub-blocks' configurations depend on the duration and dates of the flights. Note that an interruption of the INS/GNSS observation streams will result in the termination or beginning of sub-blocks, respectively.

In the above paragraph we use the shift parameters to characterize sub-blocks. In the case of aerial relative control (Blázquez and Colomina, 2012a), because shift parameters are avoided, sub-blocks are characterized by the images that belong to strips that are interconnected with relative aerial control observations.

The two previous definitions of sub-blocks are consistent: relative aerial control between consecutive strips makes sense if and only if there are no significant differences between the INS/GNSS

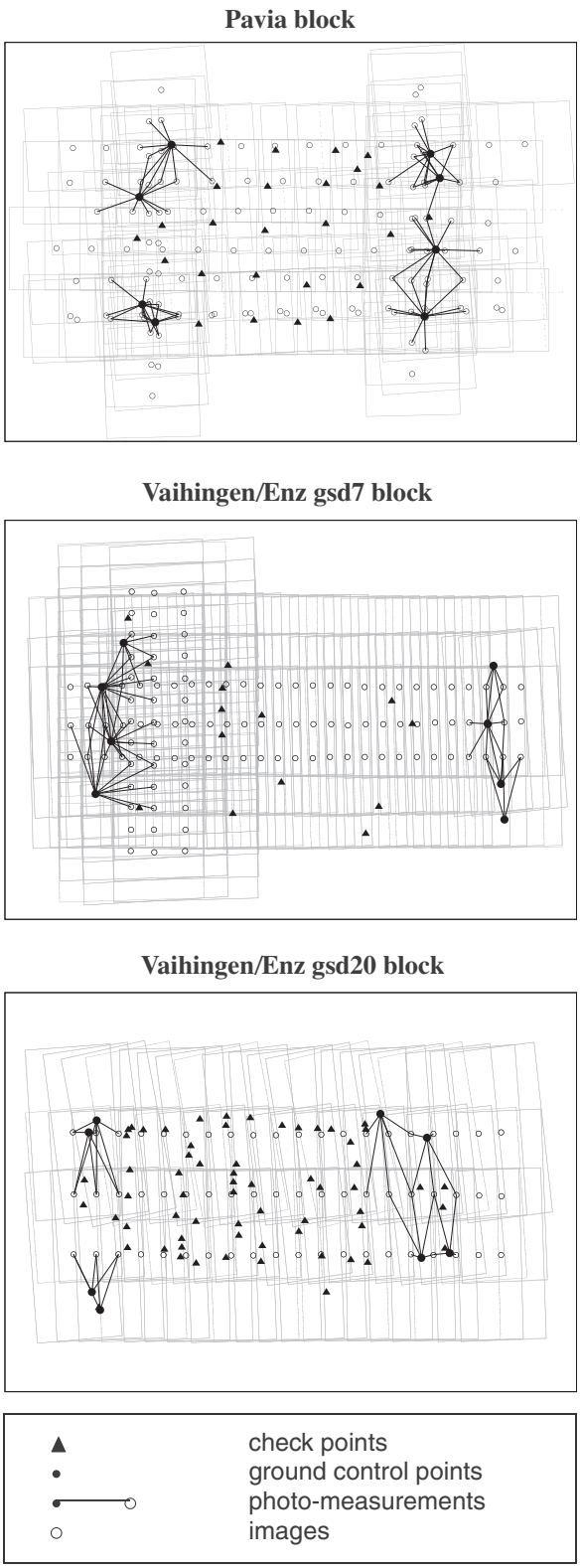


**Fig. 3.** Test blocks: layouts.

systematic errors affecting both strips, which is the criterion to set a common shift parameter for those two strips.

In Fast AT, as in any other type of ISO block, GCPs can be shared by more than one sub-block. In spite of this, to a large extent, sub-blocks are independent from each other. The correction of possible INS/GNSS errors, local geodetic reference frame differences, camera constant, principal point and synchronization errors depend on the GCPs; that is, on their quality and on the quality of the related photogrammetric measurements. Therefore, as empirical testing has confirmed, a GCP should be measured on all images where it belongs. Moreover, for obvious error propagation, reliability and cost issues, redundant GCPs per sub-block shall be used and placed at the ends (also at intersections) of the sub-blocks so that contiguous (also intersecting) sub-blocks can benefit from the same GCPs.

According to the preceding discussion, a Fast AT block configuration can be described correctly with:

- the number of images, strips and sub-blocks;
- the average number of images per strip and strips per sub-block;
- the average number of GCPs per sub-block; and
- the average number of images where a GCP is observed.

**Table 4**
Test blocks: precision of observables.

| Observables | Block | | Units |
|---|---|---|---|
| | P | V-7<br>V-20 | |
| Image coordinates | | | |
| – $\sigma_{x,y}$ | 4.8<br>0.34 | 1.4<br>0.21 | μm<br>px |
| Ground control points | | | |
| – $\sigma_{E,N}$ | 8 | 2 | cm |
| – $\sigma_h$ | 10 | 2 | cm |
| Absolute position aerial control | | | |
| – $\sigma_{E,N}$ | 3.5 | 3.5 | cm |
| – $\sigma_h$ | 5.5 | 5.5 | cm |
| Absolute attitude aerial control | | | |
| – $\sigma_{\gamma,\theta}$ | 5 | 5 | mdeg |
| – $\sigma_\psi$ | 8 | 8 | mdeg |
| Relative position aerial control | | | |
| – $\sigma_{\Delta E,\Delta N}$ (within strips) | 4 | 4 | mm |
| – $\sigma_{\Delta h}$ (within strips) | 6 | 6 | mm |
| – $\sigma_{\Delta E,\Delta N}$ (between strips) | 3.5 | 3.5 | cm |
| – $\sigma_{\Delta h}$ (between strips) | 5.5 | 5.5 | cm |
| Relative attitude aerial control | | | |
| – $\sigma_{\Delta\gamma,\Delta\theta}$ (average within strips) | 1 | 0.4 | mdeg |
| – $\sigma_{\Delta\psi}$ (average within strips) | 1 | 0.4 | mdeg |
| – $\sigma_{\Delta\gamma,\Delta\theta}$ (average between strips) | 5 | 2.5 | mdeg |
| – $\sigma_{\Delta\psi}$ (average between strips) | 8 | 4 | mdeg |

$\sigma_{x,y}$: $x$ and $y$ precisions. $\sigma_{E,N}$, $\sigma_h$: easting ($E$), northing ($N$) and height ($h$) precisions. $\sigma_{\gamma,\theta}$, $\sigma_\psi$: roll ($\gamma$), pitch ($\theta$) and heading ($\psi$) precisions. $\sigma_{\Delta E,\Delta N}$, $\sigma_{\Delta h}$: easting, northing and height difference precisions. $\sigma_{\Delta\gamma,\Delta\theta}$, $\sigma_{\Delta\psi}$: roll, pitch and heading difference precisions.

**Table 5**
Test blocks: number of Image Coordinate observations (ic) and Tie Points (TPs).

| Test block | ISO | | Fast AT | |
|---|---|---|---|---|
| | No. of ic | No. of TPs | No. of ic | No. of TPs |
| P | $4167 \times 2$ | 478 | $93 \times 2$ | 8 |
| V-7 | $7910 \times 2$ | 1106 | $73 \times 2$ | 8 |
| V-20 | $11781 \times 2$ | 2258 | $44 \times 2$ | 8 |
| V-20* | $11781 \times 2$ | 2258 | $28 \times 2$ | 8 |

**Table 6**
Test block configurations.

| Mode | tPA control | Self-calibration | GNSS shift | Boresight matrix |
|---|---|---|---|---|
| DiSO | Absolute | No | No | Known |
| ISO | Absolute | Ebner | Block | Yes |
| ISO | Relative | Ebner | – | – |
| Fast AT | Absolute | No | Block | Yes |
| Fast AT | Relative | No | – | – |

**Table 7**
RMSE of ChPs of Table 6 configurations for the P, V-7 and V-20 blocks.

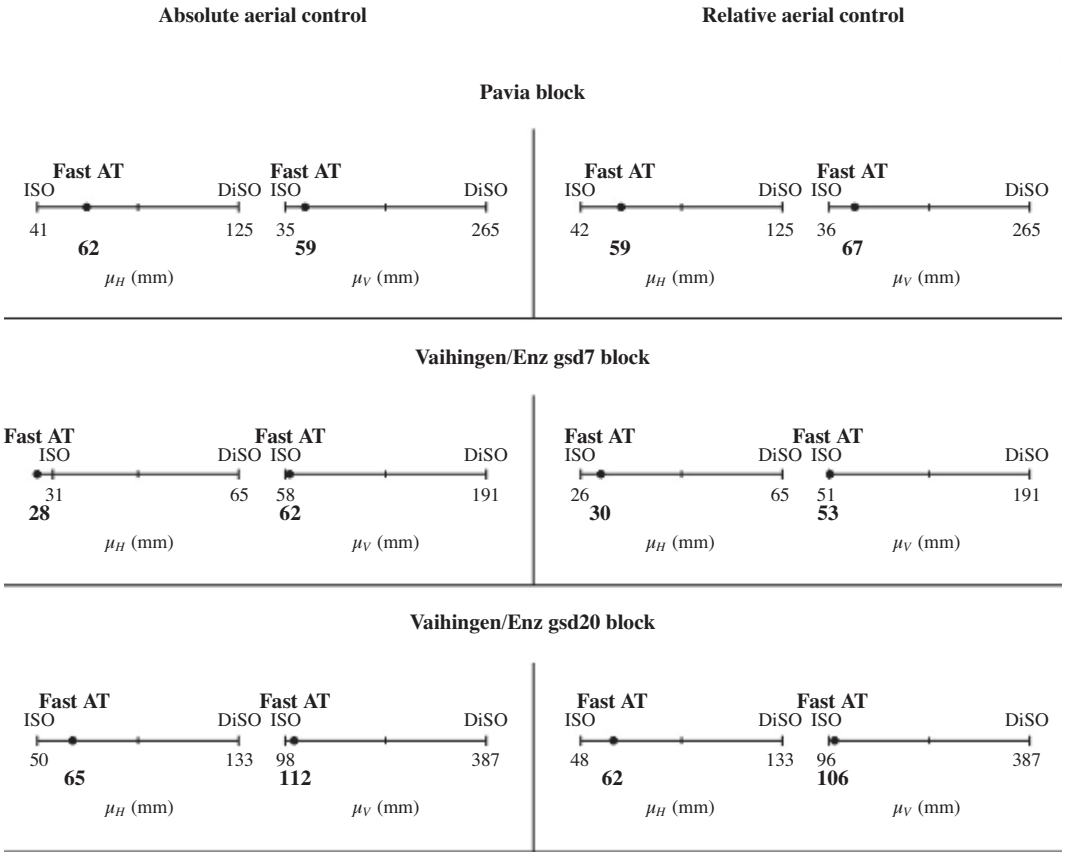


**Table 8**
Fast AT improvement factors $\alpha$ (in %) with respect to DiSO.

| Block | $\alpha(a,H)$ | $\alpha(a,V)$ | $\alpha(r,H)$ | $\alpha(r,V)$ |
|---|---|---|---|---|
| P | 75 | 90 | 80 | 86 |
| V-7 | 109 | 97 | 90 | 99 |
| V-20 | 82 | 95 | 83 | 97 |
| V-20* | 14 | 69 | 48 | 66 |

*a*: absolute aerial control; *r*: relative aerial control; *H*: horizontal; *V*: vertical.

We conclude our analysis of the geometry of Fast AT with a list of "Fast AT facts" that illustrate its behaviour and help mission design.

- Since there are no photogrammetric measurements other than those of the GCPs, the geometry of rectangularly/regularly-shaped blocks is similar to that of irregularly-shaped or corridor blocks.
- A typical Fast AT block consists of several sub-blocks, each sub-block containing various strips, and for small projects, a Fast AT block consists of just one sub-block.
- Each sub-block contains GCPs placed at its ends that are typically shared with other overlapping sub-blocks.
- The number and distribution of GCPs in ISO and Fast AT blocks are the same.
- A sub-block contains a continuous, non-interrupted INS/GNSS observation stream.
- GCPs are measured in as many images as possible (practical experience with test blocks show a significant accuracy improvement along with the number of image measurements per GCP).
- Typically, a Fast AT block will share a single, known or unknown, IMU-to-camera rotation parameter (if relative aerial control is used (Blázquez and Colomina, 2012a) the previous assertion does not apply).
- Fast AT absorbs INS/GNSS errors, reference frame inconsistencies between the local user and the global GNSS frame, camera calibration errors in the camera constant and, depending on the flying direction, principal point errors (in the case of absolute aerial control models, these errors are absorbed by the 3D shift parameters per sub-block. In the case of relative aerial control, the former errors vanish when using relative control observations).
- Fast AT, by itself, does not require physical overlap between images not including GCPs. Thus, for instance, within a strip or sub-block, images in the usual forward constant overlap may be missing with no effects on the block quality (the actual image overlap is, ultimately, set by the requirements of both the image orientation and image exploitation phase).

## 3. Performance analysis

We analyze the performance of Fast AT through its ground accuracy and compare it with those of ISO and DiSO. That is, the Root Mean Square (RMS) of Check Point (ChP) coordinate differences as compared to their pre-surveyed reference values is computed for the same data sets processed with the ISO, Fast AT and DiSO modes. In the rest of the paper, we will refer to this as the RMS Error (RMSE) of the ChPs. In the case of Fast AT, accuracy, both as an absolute quality measure and as a relative one with respect to ISO and DiSO, shall prevail over precision measures because the

**Table 9**
Redundancy numbers (in %) of ground control observations for ISO and Fast AT.

| Test block | Absolute aerial control | | | | | | Relative aerial control | | | | | |
|---|---|---|---|---|---|---|---|---|---|---|---|---|
| | ISO | | | Fast AT | | | ISO | | | Fast AT | | |
| | *E* | *N* | *h* | *E* | *N* | *h* | *E* | *N* | *h* | *E* | *N* | *h* |
| P | 84 | 84 | 80 | 70 | 72 | 56 | 85 | 84 | 82 | 80 | 81 | 78 |
| V-7 | 70 | 67 | 34 | 51 | 53 | 15 | 76 | 72 | 38 | 70 | 67 | 30 |
| V-20 | 33 | 31 | 5 | 19 | 17 | 2 | 36 | 34 | 6 | 28 | 28 | 4 |
| V-20* | 24 | 22 | 4 | 9 | 8 | 1 | 27 | 24 | 4 | 16 | 15 | 2 |

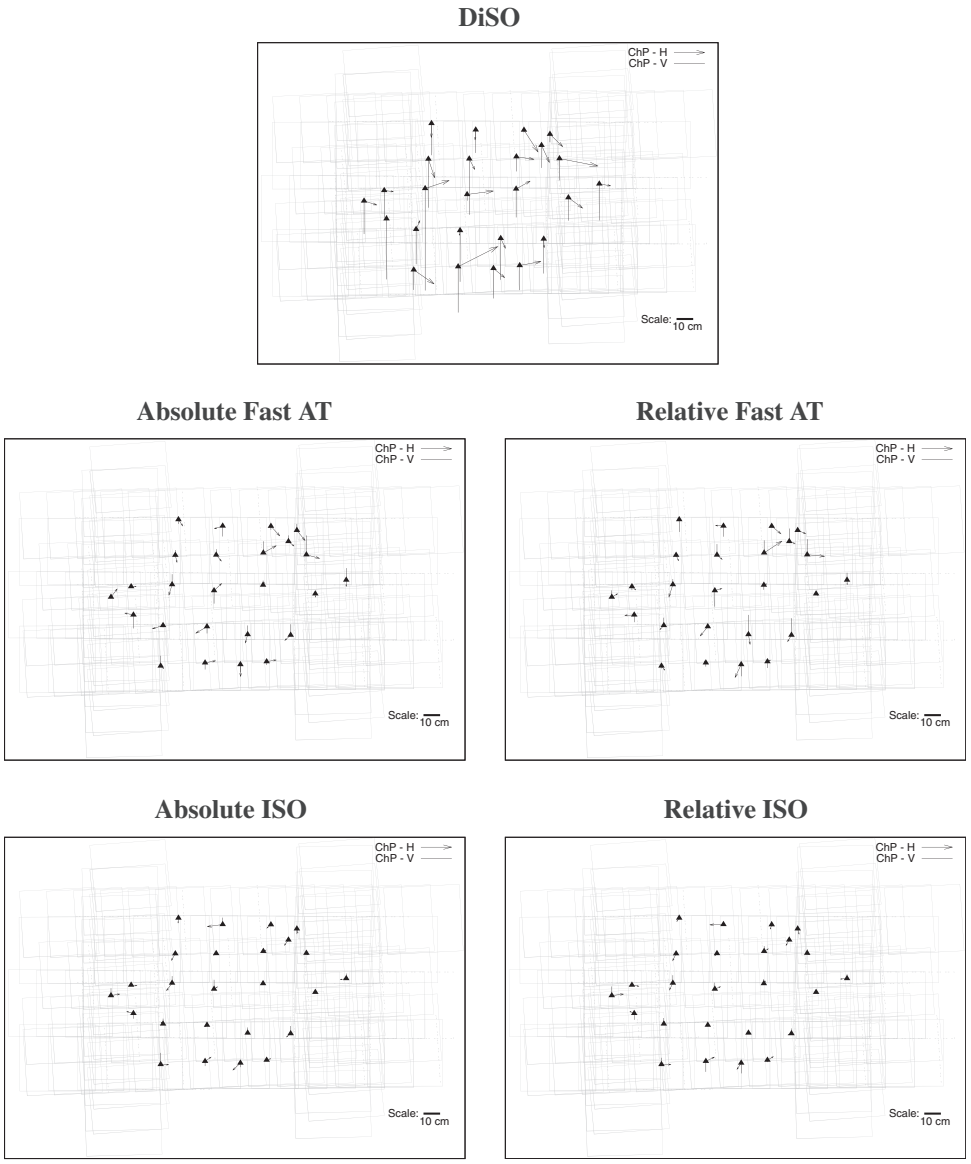


**Fig. 4.** ChPs of P block for DiSO, Fast AT and ISO with absolute and relative aerial control.

Fast AT photogrammetric model does not account for systematic errors and, therefore, a precision estimate does not correctly reflect the actual behaviour of the method. The same argument holds for the DiSO performance analysis. Therefore, as indicated, the main performance measure for Fast AT is ground accuracy.

Halfway between a performance measure and a self-diagnosis tool we also analyze the redundancy numbers of the GCP observations. Since Fast AT heavily relies on GCP observations, this measure is thought to be at least informative and, as we will see, a safeguard mechanism to detect weak geometries that may deteriorate the quality of Fast AT.

### 3.1. Test data

We selected three blocks: Pavia (P), Vaihingen/Enz gsd7 (V-7) and Vaihingen/Enz gsd20 (V-20). The first one was captured with an analogue Leica RC30 camera (Franzini, 2006) and the two Vaihinge/Enz blocks were captured with the dual-head medium

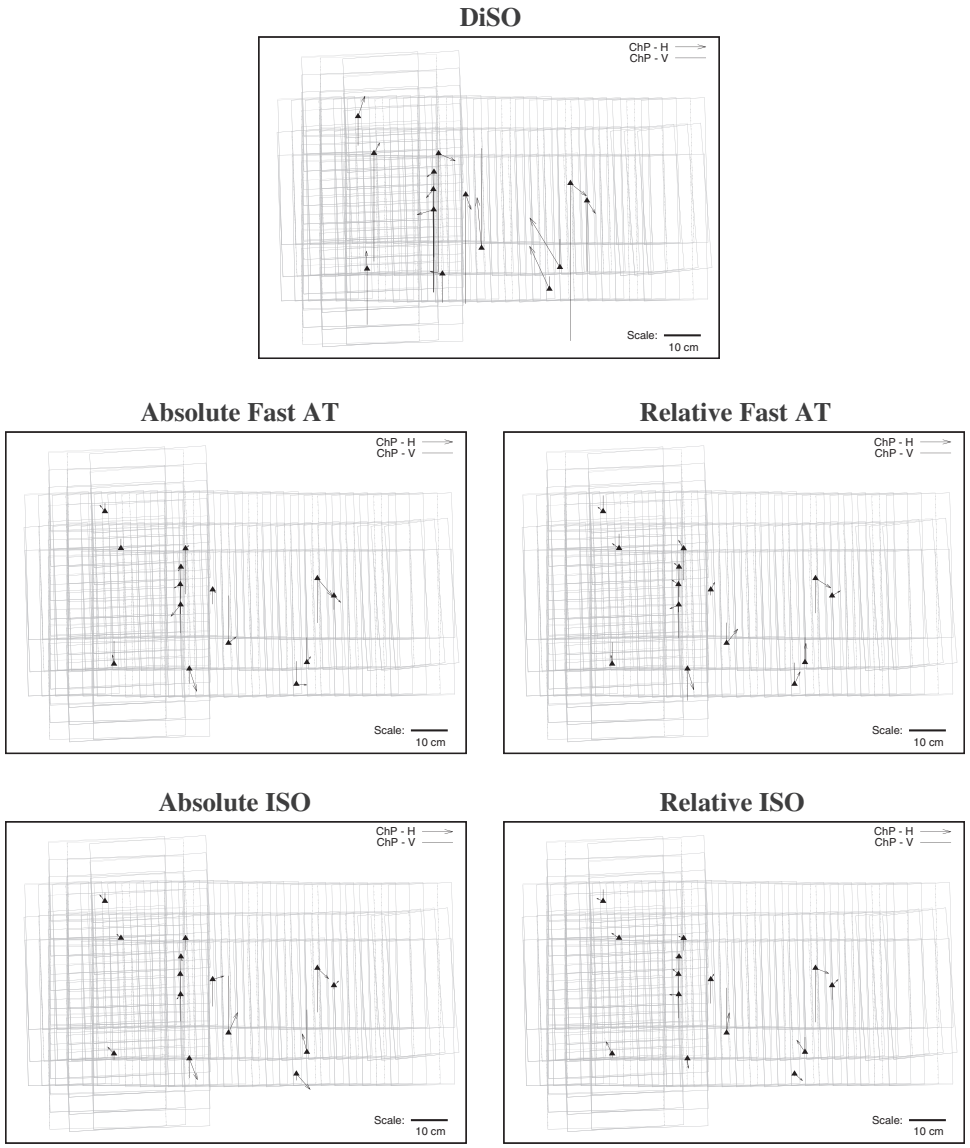


**Fig. 5.** ChPs of V-7 block for DiSO, Fast AT and ISO with absolute and relative aerial control.

format, IGI Dual-DigiCAM-H/39, system camera (Kremer and Cramer, 2008). With this choice we cover single and multiple-head camera designs. Details on the geometric configuration of the blocks, general layouts and the precision of their observations are given in Table 3, Fig. 3 and Table 4, respectively. Table 5 details the number of image coordinate observations and of tie points for ISO and Fast AT.

In addition to the P, V-7 and V-20 blocks, a variant of V-20, the auxiliary V-20* test block will be used. The V-20 and V-20* blocks have the same number of GCPs but those of V-20* have been measured in fewer images (5.5 and 3.5 images per GCP for V-20 and V-20*, respectively). The purpose of the V-20* block is to illustrate the relevance of measuring each GCP in as many images as possible.

### 3.2. Block configurations

For the sake of a fair comparative analysis, we use the same aerial control configurations for ISO, Fast AT and DiSO and the same ground control configuration for ISO and Fast AT. In the case of DiSO, only tPA aerial control observations and a previously-calibrated IMU-to-camera boresight matrix are used. In the case of ISO and Fast AT, we calibrate and orient the images using the tPA aerial control observations in both the absolute and relative modes as proposed in Blázquez and Colomina (2012a). This results in five tests for each data set: DiSO, absolute ISO, relative ISO, absolute Fast AT and relative Fast AT. We recall that the "absolute" mode is the traditional ISO mode where tPA aerial control observations are provided in terms of positions and attitudes and that in the "relative" mode, control observations are provided in terms of relative – differential – positions and attitudes.

According to our previous definition of sub-block, each test block contains just one sub-block. Table 6 summarizes the rest of the relevant block configuration parameters.

### 3.3. Results

Table 7 shows the ground accuracy performance for each orientation and calibration method (ISO, Fast AT and DiSO), for each aerial control mode (absolute and relative) and for each test block (P, V-7 and V-20). In the table, for each combination of method, aerial

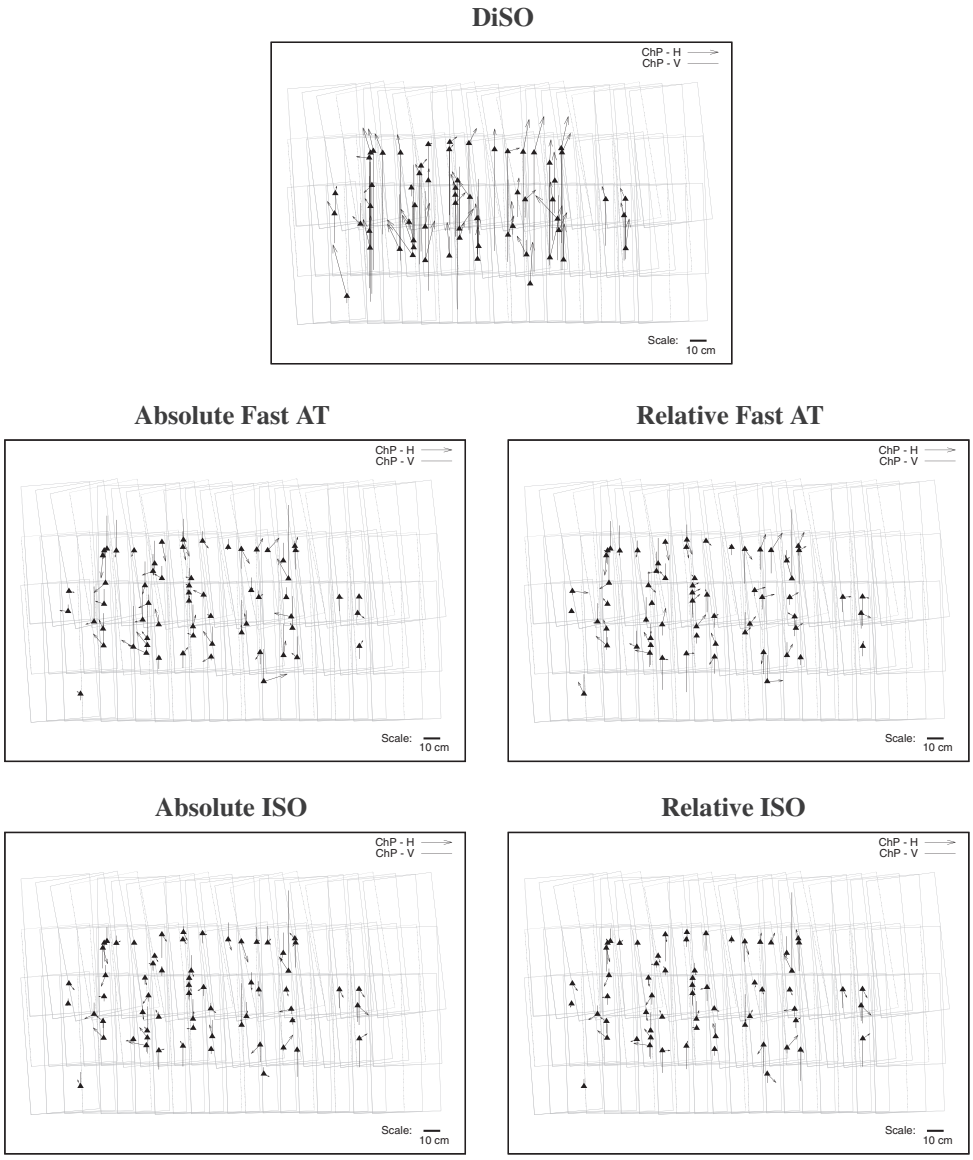


**Fig. 6.** ChPs of V-20 block for DiSO, Fast AT and ISO with absolute and relative aerial control.

**Table 10**
Accuracy ($\mu$) and precision ($\sigma$) of the estimated boresight matrix for absolute Fast AT configuration (units: arc sec).

| | P | | | V-7 | | | V-20 | | |
|---|---|---|---|---|---|---|---|---|---|
| | $v_x$ | $v_y$ | $v_z$ | $v_x$ | $v_y$ | $v_z$ | $v_x$ | $v_y$ | $v_z$ |
| $\mu$ | 22 | 15 | 3 | 18 | 5 | 8 | 5 | 7 | 2 |
| $\sigma$ | 3 | 3 | 6 | 3 | 3 | 7 | 3 | 4 | 11 |

control mode and test block, the horizontal $\mu_H$ and vertical $\mu_V$ ground accuracy measures are computed as

$$\mu_H^2 = R_E^2 + R_N^2, \quad \text{and} \quad \mu_V = R_h$$

where $R_E$, $R_N$ and $R_h$ are the RMSE of ChPs in the east, north and height components, respectively. Each of the six table cells contains two lines, for $\mu_H$ and $\mu_V$, and each line displays the accuracy of Fast AT with respect to ISO and DiSO.

In addition, Table 8 displays the improvement factors. For each given aerial control mode and block, we define the improvement factor for Fast AT with respect to DiSO as

$$\alpha = 1 - \frac{\mu^F - \mu^I}{\mu^D - \mu^I} \quad (\text{for } \mu^D > \mu^I),$$

where $\mu^I$, $\mu^F$ and $\mu^D$ are the ground accuracy measures, horizontal or vertical, for the ISO, Fast AT and DiSO methods respectively. Thus, for example, if Fast AT performed exactly as DiSO did, the improvement factor $\alpha$ would be 0 and if it performed like ISO, then $\alpha$ would be 100%. An improvement factor larger than 100% corresponds to the unlikely event of Fast AT performing better than ISO. Note that Tables 7 and 8 are presenting the same results in different ways.

For the test blocks P, V-7 and V-20, Tables 7 and 8 clearly show that Fast AT accuracy is always closer to that of ISO than that of DiSO, with improvement factors ranging from 75% to 109% resulting in an average factor of 90%. The average horizontal and vertical improvement factors are 87% and 94%, respectively, where the better performance of the vertical component is probably due to the capacity of Fast AT to absorb camera constant errors through the INS/GNSS shift parameters. The average improvement factor for the absolute aerial control mode is 91% and for the relative aerial control mode is 89% although in absolute terms – i.e., if we compare the horizontal $\mu_H$ and vertical $\mu_V$ ground accuracy measures for absolute Fast AT and relative Fast AT – Fast AT with aerial

relative control performs better than Fast AT with absolute control. In other words, for the three test blocks analyzed, the difference between Fast AT and ISO, in terms of accuracy performance is 10%.

We now compare the V-20 and V-20* test blocks. With the exception of the GCP distribution, they are identical. However, while V-20 has an 89% average improvement factor, V-20* benefits just 49% from Fast AT with a modest 14% for the horizontal components in the absolute aerial control mode. This behaviour is related to the GCPs in block V-20* being observed in fewer images (3.5 images per GCP) than in block V-20 (5.5 images per GCP) and is consistent with the results obtained in non-reported P and V-7 Fast AT preliminary computations where the same number of GCPs was used but where the GCPs were measured in fewer images.

We found that a simple measure to characterize the influence of GCPs can be based on the redundancy numbers of the GCP observations as given in Table 9. Although the average number of images in which GCPs are observed is an intuitive, easy-to-understand value, redundancy numbers have the advantage of including the block geometry information. According to Table 9 and our experience after the preliminary Fast AT computations, there is a high correlation between low GCP observation redundancy numbers and the risk of "limited" Fast AT performance, particularly for the horizontal components.

For the reasons given, we can regard V-20* as a "pathological" block and V-20 a "normal" one. However, even more important than speculating with V-20* being a "pathological" block is the fact that the redundancy numbers of the GCP observations seem to provide a self-diagnosis measure for Fast AT which is a valuable tool for daily practical work. At this point in time it is risky to set thresholds for acceptable average GCP redundancy numbers. Moreover, the thresholds have to be set according to the sensor geometry and based on the knowledge of typical redundancy numbers under normal conditions. However, as an example, our results for the IGI Dual-DigiCAM-H/39 camera suggest that, for this particular sensor, they should be around 20% for the horizontal components.

To complete these results and confirm our previous analysis, Figs. 4–6 show all the coordinate differences with respect to the ChPs in DiSO, Fast AT with absolute and relative aerial control and ISO with absolute and relative aerial control for the P, V-7 and V-20 blocks, respectively.

Finally, we note that absolute Fast AT makes it possible to estimate the IMU-to-camera boresight matrix. Table 10 shows the accuracy ($\mu$) and precision ($\sigma$) results of boresight angle estimation for the three test blocks. In the table, $\mu$ is the difference between the boresight angles computed in absolute ISO and absolute Fast AT methods and $\sigma$ is derived from the angles' estimated standard deviations. The quality of the boresight matrix angles estimated with Fast AT, is indirectly and automatically validated by the results in Tables 7 and 8 and, therefore, we regard them as acceptable.

## 4. Conclusions

We have introduced a new orientation method "fast aerial triangulation," Fast AT, and have analyzed its performance with frame camera data sets. On average, Fast AT has improved the ground point determination accuracy of DiSO by 90% as compared to ISO. We have detected that the performance of Fast AT is correlated with the redundancy numbers of GCP observations which suggests that the average of GCP redundancy numbers can be used as a self-diagnosis measure against weak Fast AT geometries.

The method is based on the measurement of just the image coordinates of GCPs and on the use of INS/GNSS position-attitude aerial control. Fast AT is simple and only requires a precise photogrammetric measurement tool for the GCPs and a standard integrated sensor orientation computer programme. As compared to ISO, Fast AT practitioners do not need to modify their orientation and calibration production lines. They simply need to measure less, manually or automatically.

We do not claim that Fast AT has come to replace classical ISO since, in the context of a mapping project, the massive image matching step of ISO introduces neither significant additional costs nor delays. However, because of its performance, which is closer to ISO than to DiSO, for some applications and in some circumstances, it can be an alternative to ISO when being fast matters more than being highly accurate or reliable, or where image matching is difficult. On the other hand, if GCPs are available, Fast AT can considerably improve upon DiSO with a marginal additional effort.

The simplicity of Fast AT and its good performance lead us to believe that practitioners of other orientation and calibration methods can benefit from it and that Fast AT can find its place between DiSO and ISO.

Last, we note that the Fast AT concept is not restricted to frame cameras. Other imaging systems and, in general, remote sensing systems can benefit from the same basic concept.

## Acknowledgements

The data sets were provided by Prof. Vittorio Casella (Università di Pavia, Italy), Dr. Jens Kremer (IGI GmbH, Germany) and Dr. Michael Cramer (Institut für Photogrammetrie, Universität Stuttgart, Germany). Many thanks for these contributions.

The bundle block adjustments to test Fast AT are performed with the Generic Extensible Network Approach (GENA) software platform from GeoNumerics (Barcelona, Spain). This support to our research is greatly appreciated.

The research reported in this paper has been funded by the Spanish project LIRA (Ref. P 44/08, Ministerio de Fomento, Spain).

## References

Ackermann, F., Schade, H., 1993. Application of GPS for aerial triangulation. Photogrammetric Engineering & Remote Sensing 59 (11), 1625–1632.

Alamús, R., Barón, A., Talaya, J., 2002. Integrated Sensor Orientation at ICC, Mathematical Models and Experiences. OEEPE Official Publication No. 43, pp. 153–162.

Barón, A., Kornus, W., Talaya, J., 2003. ICC experiences on inertial/GPS sensor orientation. In: Proceedings of ISPRS WG I/5 "Theory, Technology and Realities of Inertial/GPS/Sensor Orientation", Castelldefels, Spain, 22–23 September, 9p (on CD-ROM).

Blázquez, M., 2008. A new approach to spatio-temporal calibration of multi-sensor systems. International Archives of Photogrammetry, Remote Sensing and Spatial Information Sciences 37 (Part B1), 481–486.

Blázquez, M., Colomina, I., 2012a. Relative INS/GNSS aerial control in integrated sensor orientation: models and performance. ISPRS Journal of Photogrammetry and Remote Sensing 67, 120–133.

Blázquez, M., Colomina, I., 2012b. On INS/GNSS-based time synchronization in photogrammetric and remote sensing multi-sensor systems. PFG Photogrammetrie, Fernerkundung, Geoinformation 2012 (2), 91–104.

Blázquez, M., Colomina, I., 2012c. Performance analysis of Fast AT for corridor aerial mapping. In: Proceedings of the XXII Congress of the International Society for Photogrammetry and Remote Sensing, Melbourne, Australia, 25 August -1 September, 8p (on CD-ROM).

Colomina, I., 1993. A note on the analytics of aerial triangulation with GPS aerial control. Photogrammetric Engineering & Remote Sensing 59 (11), 1619–1624.

Colomina, I., 2007. From off-line to on-line geocoding: the evolution of sensor orientation. In: Proceedings of 51st Photogrammetric Week, Stuttgart, Germany, 3–7 September, pp. 173–183.

Cramer, M., 2009. Digital Camera Calibration. European Spatial Data Research (EuroSDR), Official Publication No. 55, p. 257.

Franzini, M., 2006. Independent and rigorous assessment of standard and refined methodologies for GPS/IMU system calibration in aerial photogrammetry. Ph.D. Thesis, Geodesy and Geomatics XVIII cycle, Politecnico di Milano, 123p.

Friess, P., 2012. Personal communication.

Haala, N., Cramer, M., Jacobsen, K., 2010. The German camera evaluation project – results from the geometry group. International Archives of Photogrammetry, Remote Sensing and Spatial Information Sciences 38 (Part 1), 6p (on CDROM).

Heipke, C., Jacobsen, K., Wegmann, H. (Eds.), 2002. Integrated Sensor Orientation: Test Report and Workshop Proceedings. OEEPE Official Publication No. 43, pp. 31–49.

Ip, A., El-Sheimy, N., Mostafa, M., 2007. Performance analysis of integrated sensor orientation. Photogrammetric Engineering & Remote Sensing 73 (1), 89–97.

Kremer, J., Cramer, M., 2008. Results of a performance test of a dual mid-format digital camera system. International Archives of the Photogrammetry, Remote Sensing and Spatial Information Sciences 37 (Part B1), 1051–1058.

Schwarz, K.P., Chapman, M.A., Cannon, M.E., Gong, P., 1993. An integrated INS/GPS approach to the georeferencing of remotely sensed data. Photogrammetric Engineering & Remote Sensing 59 (11), 1167–1674.

Skaloud, J., Lichti, D., 2006. Rigorous approach to bore-sight self-calibration in airborne laser scanning. ISPRS Journal of Photogrammetry and Remote Sensing 61 (1), 47–59.

# Chapter 6

# Summary and discussion

The paper [Colomina et al., 2012], reprinted in Appendix 1, presents the abstractions and generalizations that form the base of the proposed network approach. The main ideas outlined are: the abstract network concept, the dynamic networks, the new generic network model, the new approach to network adjustments and the features of next-generation estimation systems. The proposed network modeling and estimation fulfill the network software needs of simplicity, genericity, extensibility and protection of intellectual property, avoiding the seven sins of software design: rigidity, fragility, immobility, viscosity, needless complexity, needless repetition and opacity. The validity of the proposed network approach is its materialization in the commercial network software, GENA, and its use cases.

The GENA SW platform is the main tool of this research and some of these use cases are the airborne sensor orientation and calibration models that constitute the proposed method for a systematic approach to airborne sensor orientation and calibration (Figure 1.2). They are presented and validated in the papers reprinted in Chapters 2, 3, 4 and 5.

The papers [Blázquez, 2008] and [Blázquez and Colomina, 2012a], reprinted in Chapters 2 and 3, respectively, present the mathematical functional and stochastic models for using INS/GNSS position and attitude aerial control in relative mode.

The paper [Blázquez, 2008] presents the INS/GNSS relative aerial control observation equations for local cartesian coordinate systems while these observation equations are developed for global compound mapping-geodetic coordinate systems in [Blázquez and Colomina, 2012a]. The stochastic model is also discussed in the latter paper.

The relative aerial control has the advantages of a more accurate stochastic modeling and the elimination of the GNSS linear shift parameter (3D vector that absorbs the INS/GNSS errors) and relative IMU-to-sensor orientation (boresight) matrix.

While the paper [Blázquez, 2008] presents a proof-of-the-concept testing, the paper [Blázquez and Colomina, 2012a] validates the relative aerial control with three actual independent data sets. Analysis of the ground point accuracy of all the performed tests reveals that relative aerial control is slightly better than absolute aerial control, but analyzing the exterior orientation and point estimated precisions, relative aerial control performs slightly worse than absolute

aerial control. From the results and discussion in papers [Blázquez, 2008] and [Blázquez and Colomina, 2012a], under the same conditions, relative aerial control seems to perform comparably to traditional absolute aerial control.

On the other hand, with respect to the mathematical models, the papers of Chapters 2 and 3 also present: the colinearity equations for global compound mapping-geodetic coordinate systems ([Blázquez and Colomina, 2012a]); the absolute aerial control observation equations for local cartesian coordinate systems ([Blázquez, 2008] and [Blázquez and Colomina, 2012a]); and, the absolute aerial control observation equations for global compound mapping-geodetic coordinate systems ([Blázquez and Colomina, 2012a]).

All of these models, like INS/GNSS relative aerial control models, are developed with the aim of avoiding unnecessary re-parameterizations and so-called preadjustment "corrections". In the case of the colinearity equations for global compound mapping-coordinate systems, the previous "height corrections" and "azimuth corrections" are eliminated. In the case of the proposal for traditional INS/GNSS absolute aerial control, the re-parameterizations to go from original Euler angles (heading, pitch, roll), that parameterize the INS/GNSS-derived attitude, to the classical Euler angles (omega, phi, kappa), that parameterize the sensor attitude, are avoided. For all models developed, the principle followed was "do not touch the observations". Then, the original measurements are directly entered into the network software.

Last, the paper [Blázquez and Colomina, 2012a] also presents and validates the position and attitude constraint observation equations for dual-head systems. In light of the presented results, the impact of these restrictions is insignificant in ISO adjustments, but the addition of this model to colinearity equations in InSO adjustments improves the estimation of the exterior orientation parameters. In any case, the use of these observation equations does not add additional measurements or modify the block configurations, so the user can always include these models for all InSO and ISO adjustments of multi-sensor systems.

The papers [Blázquez, 2008] and [Blázquez and Colomina, 2012b], reprinted in Chapter 4, present the time calibration models. To estimate a constant time shift parameter between the INS/GNSS system and the sensor system, the proposal is the use of the available INS/GNSS-derived velocities. In fact, the time dimension of the airborne sensor orientation and calibration problem is traditionally handled at the harward (HW) level by manufacturers. But, these papers detail the observation equations to handle the time dimension of the problem at the SW level. These proposed spatio-temporal aerial control models exploit the full time-position-velocity-attitude solution of the INS/GNSS systems.

The spatio-temporal aerial control is presented in the paper [Blázquez, 2008] in absolute and relative mode. In this case, the models are developed to calibrate a time-constant error through its impact in position and attitude. To do this, the observation equations use the INS/GNSS-derived linear and angular velocites for local cartesian coordinate systems. In [Blázquez and Colomina, 2012b], the detailed spatio-temporal aerial control models calibrate a constant time error through its impact in position. In this case, the detailed observation equations use the INS/GNSS-derived linear velocities in absolute mode for local cartesian and global compound mapping-geodetic coordinate systems. This last paper also discusses the geometry and block configuration for the airborne sensor spatio-temporal orientation and calibration.

The paper [Blázquez, 2008] presents a proof-of-the-concept testing of the spatio-temporal absolute aerial control for local cartesian coordinate systems with a simulated-perturbed data set (actual data set where the INS/GNSS linear velocities were simulated) and [Blázquez and Colomina, 2012b] validates the spatio-temporal absolute aerial control for global compound mapping-geodetic coordinate systems with actual independent data sets (the actual INS/GNSS linear velocities were available). Although [Blázquez, 2008] details the spatio-temporal observation equations with INS/GNSS relative aerial control and the spatio-temporal observation equations with INS/GNSS-derived angular velocities in absolute and relative mode for local cartesian coordinate systems, these models have not yet been implemented and tested in the framework of this thesis. But, the presented results demonstrate that a constant time shift can be estimated with precision at the tenth-of-millisecond level using the available INS/GNSS linear velocities with the appropriate block configuration to decorrelate time errors from space errors.

Last, the paper [Blázquez and Colomina, 2012c], reprinted in Chapter 5, presents the Fast AT procedure. This paper details the concept of Fast AT, proposes some applications and discusses the geometry of this new procedure. Fast AT is a particular case of ISO where the measurements are the ground coordinates of a limited number of ground control points (GCPs), the image coordinates of these GCPs (only) and the INS/GNSS-derived position and attitude of all images.

Fast AT lies between DiSO and ISO and performs better than original hypotheses. The presented results of different actual data sets show that Fast AT improves the ground point determination accuracy of DiSO by 90% as compared to ISO. The tested blocks are regularly-shaped, but similar results (improvements of 74%) are presented in [Blázquez and Colomina, 2012d] for weaker geometries such as the corridor aerial mapping. Moreover, the redundancy numbers of GCP observations seem to be a self-diagnosis measure against weak Fast AT geometries.

# Chapter 7

# General conclusions and outlook

The research of this thesis has been developed within the framework of different public and privately-funded projects:

- ITAVERA, research and development project under contract for GeoNumerics, Spain;
- InTENA, "Innovación Tecnológica y de Negocio en Aerofotogrametría", ref. PTR1995-0841-OP, Ministerio de Ciencia e Innovación, Spain;
- uVISION, "unmanned aerial vehicles & vision for geoinformation and general Earth observation", refs. FIT-350100-2006-383 & TSI-020100-2008-192, Ministerio de Industria, Turismo y Comercio, Spain, ref. RDITS-CON06-1-0037, Generalitat de Catalunya, Spain;
- GLM, "GeoLandModels", ref. PET2008_071, Ministerio de Ciencia e Innovación, Spain;
- LIRA, "Mejora de técnicas LiDAR y Radar multitemporal para el seguimiento de posibles subsidencias asociadas a grandes obras lineales", ref. P44/08, Ministerio de Fomento, Spain.

By conducting applied research and software development in the framework of the mentioned projects and some others, it became clear that a new approach to airborne sensor orientation and calibration was necessary. A more comprehensive approach to general network adjustment and modeling was called for, and the classical concepts mainly established by Carl F. Gauss (1777-1855) needed to be further developed to account for the new challenges of modern geomatics.

All of this has a broad range of consequences, from the new sensor orientation and calibration concepts and procedures that have been presented in the preceding chapters, to the way in which network software is designed and developed.

In fact, the goal and contributions of this research were manifold. One goal of the thesis was to create a method for a systematic approach to airborne sensor orientation and calibration. The method consists of looking at the traditional airborne sensor orientation and calibration from a distance that includes the DiSO and ISO procedures as particular cases. Another goal of the thesis was to validate the models resulting of applying the method; i.e., the new models for

airborne sensor orientation and calibration. All these models are presented and validated in peer-reviewed papers reprinted in the previous chapters.

The main tool of this research is a commercial SW platform "Generic Extensible Network Approach", GENA, that I largely developed for GeoNumerics (Barcelona, Spain). It is based on the proposed network approach detailed in [Colomina et al., 2012], reprinted in Appendix 1.

The presented method and models focus on the exploitation of the available INS/GNSS-derived data for airborne sensor orientation and calibration and make it possible to advance from the traditional panorama depicted in Figure 7.1 to the proposed panorama depicted in Figure 7.2. The transition from Figure 7.1 to Figure 7.2 illustrates the method. The contents of Figure 7.2 illustrates the resulting framework and models.

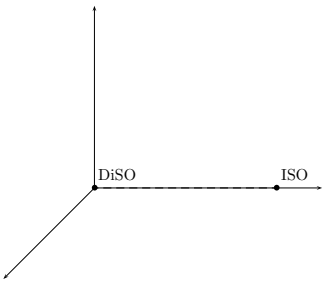


Figure 7.1: Traditional approach.

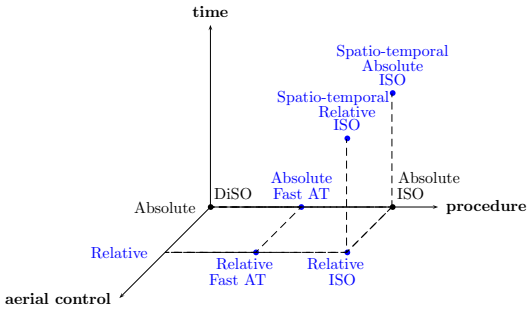


Figure 7.2: Systematic approach: method and models.

The proposed investigation also aims to address a contradictory social and economical situation in which geoinformation has become a critical infrastructure of modern society and, at the same time, geoinformation providers, both public and private, face increasing demands – in terms of resolution, accuracy and currentness – from a society that is not always prepared to pay for what is being demanded. Correct mathematical models and software abstractions add to robustness and automation that ultimately mean lower costs and social

benefits.

The relative aerial control is a real alternative to the absolute aerial control in the sense of: block configurations of relative and absolute aerial control are the same; the relative aerial control accuracy and precision are similar to the traditional absolute aerial control accuracy and precision. Nevertheless, the relative aerial control formulation is simpler and less error-prone. The use of the relative aerial control increases the robustness and reduces the complexity of INS/GNSS-based ISO by concentrating the modeling effort on the models and letting the user concentrate on their use.

Because of their good performance, the use of INS/GNSS-derived velocities to link space and time provides, above all, a SW tool to manufacturers for system verification and calibration purposes.

Fast AT is a new orientation and calibration procedure that does not involve any additional effort of modeling or modifying SW. On the contrary, it implies fewer measurements. Therefore, the simplicity of Fast AT and its good performance lead me to believe that the airborne sensor orientation and calibration community can benefit from it.

The research presented fully develops a systematic approach to airborne sensor orientation and calibration, but it also opens new avenues for research at both the specific and general level. Thus, further specific work can and should be performed with relation to the proposed models, for example:

- testing the relative spatio-temporal aerial control with actual data sets;
- testing the impact of a time-constant error in attitude using INS/GNSSS angular velocities in absolute and relative mode; or,
- testing the Fast AT procedure for weak geometries.

Additionally, further general research can and should be performed on the generic approach to network modeling and adjustment such as:

- modeling and testing the relative spatio-temporal aerial control concept with other sensors;
- generalizing the Fast AT concept to other sensors; and
- reviewing the existing methods for additional parameter selection and outlier detection in general multi-sensor networks.

Moreover, there are other models and applications for a variety of sensors, platforms and systems that the IG team is developing to validate the abstractions and generalizations of the proposed network approach, for example, relevant or upcoming geomatic applications such as:

- the ALS block adjustment or the orientation and calibration problem of combined sensor systems (for example, LiDAR and optical cameras [Angelats et al., 2012]); and
- the radiative transfer modeling and radiometric calibration by means of network adjustments ([Antequera et al., 2012]).

The future of network modeling and adjustment, however, can go far beyond the research lines, ongoing or envisioned, indicated above. This future is related to the research presented in the papers [Colomina and Blázquez, 2004], reprinted in Appendix 2, and [Colomina and Blázquez, 2005] that present the time dependent or dynamic network concept in comparison to the classical geomatic network concept.

In these papers, for the first time, the classical network least-squares technique is extended to parameters that are stochastic processes and to observation equations that, in addition to stochastic equations, can also be stochastic differential equations. In short, the dynamic network concept is introduced to extend the classical network concept of Carl F. Gauss, where the parameters can be not only random variables but also stochastic processes and where the models can be not only stochastic equations but also stochastic differential equations.

This is a major step forward ([Rouzaud and Skaloud, 2011]) and enables a new approach to the solution of many kinematic tasks in modern geomatics, such as kinematic gravimetry, INS/GNSS trajectory determination in aerial, terrestrial and mobile mapping applications or crustal motion modeling and prediction.

The INS/GNSS trajectory determination is the first application that faces up to dynamic networks. In this case, the variables are not random variables; they are position, velocity, attitude and calibration random processes, and the classical observation equations are now the INS stochastic differential mechanization equations. The new technique has many advantages over traditional Kalman filtering and smoothing for non real-time tasks as happens to be the case in most geomatic applications and, in particular, in trajectory determination for kinematic aerial and ground control determination.

Dynamic networks make up one of the largely unexplored fields opened by this thesis and will be my next research goal.

# Acronyms

| | |
|---|---|
| ALS | Airborne Laser Scanning |
| AT | Aeriotriangulation |
| DiSO | Direct Sensor Orientation |
| GCP | Ground Control Point |
| GENA | Generic Extensible Network Approach |
| GMES | Global Monitoring for Environment and Security |
| GNSS | Global Navigation Satellite System |
| GPS | Global Positioning System |
| HW | Hardware |
| IMU | Inertial Measurement Unit |
| INS | Inertial Navigation System |
| InSAR | Interferometric Synthetic Aperture Radar |
| ISO | Integrated Sensor Orientation |
| SCBA | Self-Calibrating Bundle Adjustment |
| SW | Software |

# Definitions

**Coordinate Reference Frame (CRF)** is a pair that consists of a reference frame and a coordinate system.

**Coordinate Reference System (CRS)** is a pair that consists of a reference system and a coordinate system.

**Coordinate System (CS)** is a parameterization of a mathematical space. Or, equivalently, it is a set of mathematical rules to specify the coordinates of an element of a mathematical space. For a 2-dimensional space well-known parameterizations are the cartesian coordinate system and the polar coordinate system. In geomatics, a map projection is a (global or local) coordinate system for the reference geodetic ellipsoid.

**Direct Sensor Orientation (DiSO)** is the determination of the sensor exterior orientation parameters from sensor-unrelated measurements; e.g., satellite ranges (GPS) and inertial measurements (INS).

**Functional Model** is a (mathematical) equation or system of equations.

**Geomatic Model** is an extension of a mathematical model that includes coordinate reference frames, units of measurements, thresholds and any other information required to describe the geomatic properties of the mathematical model entities.

**Geomatics** is the art, the science and the technology of acquiring, storing, processing, delivering and managing spatially referenced information. Geomatics entails sub-disciplines such as geodesy, surveying, positioning and navigation, remote-sensing and photogrammetry, cartography, mapping and geographic information systems.

**Georeferencing** given a ground point $X$ and its projection to a point $x$ in the image, is the determination of (the coordinates of) $X$ from $x$, the Exterior Orientation parameters and the Digital Elevation Model.

**Indirect Sensor Orientation (InSO)** is the determination of the sensor exterior orientation parameters from sensor and ground measurements related through the sensor geometric model.

**Instrument** is a device used to measure. In this thesis, it is one of the four fundamental modeling classes (instrument, observation, parameter and model).

**Integrated Sensor Orientation (ISO)** is the determination of the sensor orientation parameters from all available measurements: image coordinates of

(numerous) points (tie points), ground coordinates of (a few) points (ground control points), satellite ranges and/or positions (GNSS), INS/GNSS derived trajectories.

**Map Projection (MP)** is a 2-dimensional coordinate system for a geodetic reference ellipsoid. The UTM family of 120 local Transverse Mercator maps is an example of a set of local map projections.

**Mathematical Model** is an abstract model that uses mathematical language to describe the behavior of a system. In the context of this thesis, a mathematical model is a functional model plus a stochastic model.

**Model** is an abstract (or actual) representation of an object or system from a particular viewpoint.

**Network Adjustment (NA)** is the estimation process of unknown parameters from (measured) observations and (mathematical) models under a given optimality criteria.

**Object-Oriented Programming (OOP)** is a programming paradigm that uses abstraction to create models based on the real world. Its main techniques and features are encapsulation, inheritance and polymorphism.

**Observable (noun)** is a numerical property of a physical system that can be determined by a sequence of physical or mathematical operations. Technically, it is a random variable.

**Observation** or a **measurement** is one of the values that an observable or random variable may take (for example, the various repeated measurements between A and B of a distance meter instrument – the measured distances – are observations and the abstract concept of distance between A and B is the observable). It is one of the four fundamental modeling classes (instrument, observation, parameter and model).

**Parameter** is a random variable whose expectation and covariance have to be estimated from known observations, instruments and models. It is one of the four fundamental modeling classes (instrument, observation, parameter and model).

**Random Variable** is a measurable function from a sample space to the measurable space of possible values of the variable.

**Reference Frame (RF)** is a realization of a reference system. For geodetic reference systems the most common realization is a list of points, whose coordinates are known and whose physical location is well defined, usually through marks or targets. ITRF96 is, for example, a realization of ITRS. A more recent way to realize a reference system is through the orbits of a GNSS satellite constellation, such as the GPS.

**Reference Model** is an abstract model or template for the consistent development of more specific models.

**Reference System (RS)** is a definition. It is a set of prescriptions and conventions together with the modeling required to define a triad of axes at any time.

**Sensor** is a device, usually electrical, electronic, or electro-mechanical, that converts one type of energy to another for various purposes including meas-

urement or information transfer (for example, pressure sensors). In a broader sense, a transducer is sometimes defined as any device that converts a signal from one form to another.

**Sensor Calibration (SC)** is the determination of the parameters $\bar{x}$ of a sensor model $\bar{f}(l-e, x, \bar{x}) = 0$ that extends the sensor nominal model $f(l-e, x) = 0$.

**Sensor Orientation (SO)** is a functional model $s$ and its parameters $o$ such that

$$\begin{array}{rccl} s_o: & \Re^3 & \longrightarrow & \Re^2 \\ & X & \longmapsto & s_o(X) = x \end{array}$$

where $X$ is an object point and $x$ is a sensor point.

**Sensor Systematic Error** is the difference between a sensors given nominal model f and a new (higher fidelity) model $\bar{f}$. The new model extends $f(l-e, x) = 0$ to $\bar{f}(l-e, x, \bar{x}) = 0$ where $\bar{x}$ are the calibration parameters.

**Software Component (SC)** is an object written to a specification, offering a predefined service and able to communicate with other components. Software components often take the form of objects or collections of objects.

**Software Engineering (SE)** is the design, development, and documentation of software by applying technologies and practices from computer science, project management, engineering, application domains, interface design, digital asset management and other fields.

**Software Framework** is a software support infrastructure i.e., a set of software and data items in which another software project can be organized and developed. A framework may include support programs, code libraries, data, specialized scripting or interface languages, or any other software to help develop and agglutinate the different components of a software project.

**Software Model** is an abstract model that describes a computer program or software system, usually with a special graphical modeling language.

**Software Platform** is a particular type of software framework which allows other software to run.

**Stochastic Model** is a mathematical model that describes the probability distribution of a random variable or stochastic process.

**Stochastic Process** is a set of random variables indexed by time $x := \{x(t)|t \in T, T \subset \Re\}$, where $\Re$ is the set of real numbers.

# Bibliography

[Ackermann et al., 1970] Ackermann, F., Ebner, H., Klein, H., 1970. Ein Programm-Paket für die Aerotriangulation mit unabhängigen Modellen. Bildmessung und Luftbildwesen 38, pp. 218–224.

[Ackermann and Schade, 1993] Ackermann, F., Schade, H., 1993. Application of GPS for aerial triangulation. PE&RS Photogrammetric Engineering and Remote Sensing 59(11), pp. 1625–1632.

[Alamús et al., 2002] Alamús, R., Barón, A., Talaya, J., 2002. Integrated sensor orientation at ICC, mathematical models and experiences. OEEPE Official Publication 43, pp. 153–162.

[Alamús et al., 2007] Alamús, R., Kornus, W., Riesinger, I., 2007. DMC geometric performance analysis. Proc. ISPRS Hannover Workshop 2007 High-Resolution Earth Imaging for Geospatial Information, Hannover, Germany, 29 May - 1 June. 6p. (on CDROM).

[Angelats et al., 2012] Angelats, E., Blázquez, M., Colomina, I., 2012. Simultaneous orientation and calibration of images and laser point clouds with straight segments. Proc. XXII Congress of the International Society for Photogrammetry and Remote Sensing, Melbourne, Australia, 25 August - 1 September. 6p (on CD-ROM).

[Antequera et al., 2012] Antequera, R., Andrinal, P., Colomina, I., Navarro, J., Pros, A., 2012. Corrección radiométrica automática de imágenes generadas por cámaras matriciales ópticas. X Congreso TOPCART 2012: Congreso Iberoamericano de Geomática y Ciencias de la Tierra, Madrid, Spain.

[Barón et al., 2003] Barón, A., Kornus, W., Talaya, J., 2003. ICC experiences on inertial/GPS sensor orientation. Proc. ISPRS WG I/5 "Theory, Technology and Realities of Inertial/GPS/Sensor Orientation", Castelldefels, Spain, 22 - 23 September. 9p. (on CDROM).

[Blázquez, 2008] Blázquez, M., 2008. A new approach to spatio-temporal calibration of multi-sensor systems. International Archives of Photogrammetry, Remote Sensing and Spatial Information Sciences 37(B1), pp. 481–486.

[Blázquez and Colomina, 2008] Blázquez, M., Colomina, I., 2008. On the use of inertial/GPS velocity control in sensor calibration and orientation. Proc. EuroCOW 2008, Castelldefels, Spain, 30 January - 1 February. 8p. (on CDROM).

[Blázquez and Colomina, 2010] Blázquez, M., Colomina, I., 2010. On the role of self-calibration functions in integrated sensor orientation. Proc. EuroCOW 2010, Castelldefels, Spain, 10-12 February. 7p. (on CDROM).

[Blázquez and Colomina, 2012a] Blázquez, M., Colomina, I., 2012. Relative INS/GNSS aerial control in integrated sensor orientation: Models and performance. ISPRS Journal of Photogrammetry and Remote Sensing 67(1), pp. 120–133.

[Blázquez and Colomina, 2012b] Blázquez, M., Colomina, I., 2012. On INS/GNSS-based time synchronization in photogrammetric and remote sensing multi-sensor systems. PFG Photogrammetrie, Fernerkundung und Geoinformation 2012(2), pp. 91–104.

[Blázquez and Colomina, 2012c] Blázquez, M., Colomina, I., 2012. Fast AT: A simple procedure for quasi direct orientation. ISPRS Journal of Photogrammetry and Remote Sensing 71(1), pp. 1–11.

[Blázquez and Colomina, 2012d] Blázquez, M., Colomina, I., 2012. Performance analysis of Fast AT for corridor aerial mapping. Proc. XXII Congress of the International Society for Photogrammetry and Remote Sensing, Melbourne, Australia, 25 August - 1 September. 8p (on CD-ROM).

[Brown, 1956] Brown, D. C., 1956. The simultaneous determination of the orientation and lens distortion of a photogrammetric camera. Air Force Missile Test Center Report 56–20, Patrick AFB, Florida, USA.

[Brown, 1971] Brown, D. C., 1971. Close-range camera calibration. PE&RS Photogrammetric Engineering and Remote Sensing 37(8), pp. 855–866.

[Chandelier and Martinoty, 2009] Chandelier, L., Martinoty, G., 2009. Radiometric aerial triangulation for the equalization of digital aerial images and orthoimages. PE&RS Photogrammetric Engineering and Remote Sensing 75(2), pp. 193–200.

[Colomina, 1993] Colomina, I., 1993. A note on the analytics of aerial triangulation with GPS aerial control. PE&RS Photogrammetric Engineering and Remote Sensing 59(11), pp. 1619–1624.

[Colomina, 1999] Colomina, I., 1999. GPS, INS and Aerial Triangulation: what is the best way for the operational determination of photogrammetric image orientation? International Archives of Photogrammetry, Remote Sensing and Spatial Information Sciences 32, pp. 121–130.

[Colomina, 2007] Colomina, I., 2007. From off-line to on-line geocoding: the evolution of sensor orientation. Proc. 51st Photogrammetric Week, Stuttgart, Germany, 3 - 7 September, pp. 173–183.

[Colomina and Blázquez, 2004] Colomina, I., Blázquez, M., 2004. A unified approach to static and dynamic modeling in photogrammetry and remote sensing. International Archives of Photogrammetry, Remote Sensing and Spatial Information Sciences 35(B1), pp. 178-183.

[Colomina and Blázquez, 2005] Colomina, I., Blázquez, M., 2005. On the stochastic modeling and solution of time dependent networks. Proc. VI International Geomatic Week, Barcelona, Spain, 8 - 11 February. 6p. (on CDROM).

[Colomina et al., 2012] Colomina, I., Blázquez, M., Navarro, J.A., Sastre, J., 2012. The need and keys for a new generation network adjustment software. Proc. XXII Congress of the International Society for Photogrammetry and Remote Sensing, Melbourne, Australia, 25 August - 1 September. 6p (on CD-ROM).

[Colomina et al., 1992] Colomina, I., Navarro, J.A., Térmens, A., 1992. GeoTeX: a general point determination system. International Archives of Photogrammetry, Remote Sensing and Spatial Information Sciences 29(B3), pp. 656–664.

[Cramer, 2007] Cramer, M., 2007. Results from the EuroSDR network on digital camera calibration and validation. Proc. ISPRS Hannover Workshop 2007 High-Resolution Earth Imaging for Geospatial Information, Hannover, Germany, 29 May - 1 June.

[Cramer, 2009] Cramer, M., 2009. Digital Camera Calibration. European Spatial Data Research (EuroSDR), Official Publication 55, pp. 257.

[Cramer, 2010] Cramer, M., 2010. The DGPF-test on digital airborne camera evaluation overview and test design. PFG Photogrammetrie, Fernerkundung, Geoinformation 2010(2), pp. 73–82.

[Dubois, 1997] Dubois, P., 1997. Object technology for scientific computing. The object-oriented series, Prentice Hall, Upper Saddle River, NJ, USA.

[Elassal, 1983] Elassal, A., 1983. Generalized adjustment by least squares (GALS). PE&RS Photogrammetric Engineering and Remote Sensing 49, pp. 201–206.

[Franzini, 2006] Franzini, M., 2006. Independent and rigorous assessment of standard and refined methodologies for GPS/IMU system calibration in aerial photogrammetry. PhD Thesis, Geodesy and Geomatics XVIII cycle, Politecnico di Milano. 123p.

[Frieß, 1990] Frieß, P., 1990. Kinematische Positionsbestimmung für die Aerotriangulation mit dem NAVSTAR Global Positioning System (Ph.D. Thesis). C, Vol. 359, Deutsche Geodätische Kommission, München, DE.

[Frieß, 1991] Frieß, P., 1991. Aerotriangulation with GPS-methods, experience, expectation. Proc. 43rd Photogrammetric Week, Stuttgart, Germany, 9 - 14 September, pp. 43–49.

[Frieß, 2006] Frieß, P., 2006. Toward a rigorous methodology for airborne laser mapping. Proc. EuroCOW 2006, Castelldefels, Spain, 25 - 27 January. 7p. (on CDROM).

[Graham, 2010] Graham, L., 2010. Mobile Mapping Systems overview. PE&RS Photogrammetric Engineering and Remote Sensing 76(3), pp. 222–228.

[Haala et al., 2010] Haala, N., Cramer, M., Jacobsen, K., 2010. The German Camera Evaluation Project - Results from the Geometry Group. International Archives of Photogrammetry, Remote Sensing and Spatial Information Sciences 38(1). 6p. (on CDROM).

[Harrison and Newman, 2011] Harrison, A., Newman, P., 2011. TICSync: knowing when things happened. Proc. IEEE International Conference on Robotics and Automation ICRA2011, Shanghai, China, pp. 356–363.

[Heipke et al., 2000] Heipke, C., Jacobsen, K., Wegmann, H., Andersen, O., Nilsen, B., 2000. Integrated sensor orientation - an OEEPE test. International Archives of the Photogrammetry, Remote Sensing and Spatial Information Sciences 33(B3), pp. 373–380.

[Heipke et al., 2002] Heipke, C., Jacobsen, K., Wegmann, H., eds., 2002. Integrated sensor orientation: test report and workshop proceedings. OEEPE Official Publication 43, pp. 31–49.

[Herring, 2003] Herring, T., 2003. GLOBK: Global Kalman filter VLBI and GPS analysis program, version 10.1. Technical report, MIT, Cambridge, MS, USA.

[Honkavaara, 2008] Honkavaara, E., 2008. Calibrating digital photogrammetric airborne imaging system using a test field. Publications of the Finish Geodetic Institute, No. 140, Masala.

[Honkavaara et al., 2009] Honkavaara, E., Arbiol, R., Markelin, L., Martínez, L., Cramer, M., Bovet, S., Chandelier, L., Ilves, R., Klonus, S., Marshal, P., Schlpfer, D., Tabor, M., Thom, C., Veje, N., 2009. Digital airborne photogrammetry a new tool for quantitative remote sensing? a state-of-the-art review on radiometric aspects of digital photogrammetric images. Remote Sensing 1(3), pp. 577–605.

[Ip et al., 2007] Ip, A., El-Sheimy, N., Mostafa, M., 2007. Performance Analysis of Integrated Sensor Orientation. PE&RS Photogrammetric Engineering and Remote Sensing 73(1), pp. 89–97.

[Jansa et al., 2004] Jansa, J., Studnicka, N., Forkert, G., Haring, A. Kager, H., 2004. Terrestrial laserscanning and photogrammetry acquisition techniques complementing one another. International Archives of Photogrammetry, Remote Sensing and Spatial Information Sciences 35(B7), pp. 948–953.

[Jekeli, 2001] Jekeli, C., 2001. Inertial navigation systems with geodetic applications. Walter de Gruyter, Berlin, New York.

[Kager, 2004] Kager, H., 2004. Discrepancies between overlapping laser scanning strips - simultaneous fitting of aerial laser scanner strips. International Archives of Photogrammetry, Remote Sensing and Spatial Information Sciences 35(B1), pp. 555–560.

[Kalman, 1960] Kalman, R., 1960. A new approach to linear filtering and prediction problems. Transactions of the ASME, Journal of Basic Engineering 82(1), pp. 34–45.

[Klein and Förstner, 1984] Klein, H., Förstner, W., 1984. Realization of automatic error detection in the block adjustment program PAT-M43 using robust estimators. International Archives of Photogrammetry, Remote Sensing and Spatial Information Sciences 25(A3), pp. 234–245.

[Kloeden and Platen, 1999] Kloeden, P., Platen, E., 1999. Numerical solution of Stochastic Differential Equations. Springer Verlag, New York, USA.

[Koch, 1995] Koch, K., 1995. Parameter estimation and hypothesis testing in linear models. Springer Verlag, Berlin, DE.

[Krarup et al., 1980] Krarup, T., Kubik, K., Juhl, J., 1980. Gtterdmmerung over least squares adjustment. International Archives of Photogrammetry, Remote Sensing and Spatial Information Sciences 25(B3), pp. 369–378.

[Kratky, 1989] Kratky, V., 1989. Rigorous photogrammetric processing of SPOT images at CCM Canada. ISPRS Journal of Photogrammetry and Remote Sensing 53(9), pp. 1223–1230.

[Kremer and Cramer, 2008] Kremer, J., Cramer, M., 2008. Results of a performance test of a dual mid-format digital camera system. International Archives of the Photogrammetry, Remote Sensing and Spatial Information Sciences 37(B1), pp. 1051–1058.

[Lawler, 1995] Lawler, G., 1995. Introducttion to Stochastic Processes. Chapman & Hall/CRC, Boca Ratón, FL, USA.

[Leonard and Durrant-Whyte, 1991] Leonard, J., Durrant-Whyte, H., 1991. Simultaneous map building and localization for an autonomous mobile robot. Proc. International Workshop IROS91, 3, IEEE/RSJ, pp. 1442–1447.

[Lucas, 1987] Lucas, J., 1987. Aerotriangulation without ground control. PE&RS Photogrammetric Engineering and Remote Sensing 53(3), pp. 311–314.

[Martin, 2002] Martin, R., 2002. Agile software development: principles, patterns, and practices. Prentice Hall, Hemel Hempstead, UK.

[Martínez and Arbiol, 2008] Martínez, L., Arbiol, R., 2008. ICC experiences on DMC radiometric calibration. Proc. EuroCOW 2008, Castelldefels, Spain, 30 January - 1 February. 7p. (on CDROM).

[Martínez et al., 2007] Martínez, M., Blázquez, M., Gómez, A., Colomina, I., 2007. A new approach to the use of position and attitude control in camera orientation. Proc. 7th International Geomatic Week, Barcelona, Spain, 20 - 23 February. 5 p. (on CDROM).

[Maybeck, 1979a] Maybeck, P., 1979. Stochastic models, estimation and control. Mathematics in science and engineering, 141(1), Academic Press Inc., New York, NY, USA.

[Maybeck, 1979b] Maybeck, P., 1979. Stochastic models, estimation and control. Mathematics in science and engineering, 141(2), Academic Press Inc., New York, NY, USA.

[Mugnier et al., 2004] Mugnier, C.J., Förstner, W., Wrobel, B., Paderes, F., Munjy, R., 2004. The mathematics of photogrammetry. Manual of Photogrammetry, fifth ed. American Society of Photogrammetry and Remote Sensing, McGlone, J.C., Mikhail, E.M., Bethel, J., Mullen, R. (Eds.), Bethesda, MA, pp. 181–316.

[Øksendal, 1993] Øksendal, B., 1993. Stochastic differential equations: an introduction with applications. Universitext, third edn, Springer-Verlag.

[Olson, 2010] Olson, E., 2010. A passive solution to the sensor synchronization problem. Proc. IEEE/RSJ International Conference on Intelligent Robots and Systems (IROS), Taipei, Taiwan, pp. 1059–1064.

[Rouzaud and Skaloud, 2011] Rouzaud, J., Skaloud, J., 2011. Rigorous integration of inertial navigation with optical sensors by dynamic networks. Navigation 58(2), pp. 141–152.

[Scherzinger, 1997] Scherzinger, B., 1997. A position and orientation post-processing software package for inertial/GPS integration (POSProc). Proc. International Symposium on Kinematic Systems in Geodesy, Geomatics, and Navigation (KIS97), Banff, Canada, 3 - 6 June.

[Schmid, 1974] Schmid, H.H., 1974. Worldwide geocentric satellite triangulation. Journal of Geophysical Research 79(35), pp. 5349–5376.

[Schwarz et al., 1993] Schwarz, K., Chapman, M., Cannon, M., Gong, P., 1993. An integrated INS/GPS approach to the georeferencing of remotely sensed data. PE&RS Photogrammetric Engineering and Remote Sensing 59(11), pp. 1667–1674.

[Skaloud and Legat, 2008] Skaloud, J., Legat, K., 2008. Theory and reality of direct georeferencing in national coordinates. ISPRS Journal of Photogrammetry and Remote Sensing 63, pp. 272–282.

[Skaloud and Lichti, 2006] Skaloud, J., Lichti, D., 2006. Rigorous approach to bore-sight self-calibration in airborne laser scanning. ISPRS Journal of Photogrammetry and Remote Sensing 61(1), pp. 47–59.

[Smith et al., 1986] Smith, R., Self, M., Cheeseman, P., 1986. Estimating uncertain spatial relationships in robotics. Proc. Second Annual Conference on Uncertainty in Artificial Intelligence. UAI'86, University of Pennsylvania, Philadelphia, PA, USA, pp. 435–461.

[Stoer and Bulirsh, 1992] Stoer, J., Bulirsh, R., 1992. Introduction to Numerical Analysis. second edn, Springer-Verlag, New York, USA.

[Térmens and Colomina, 2003] Térmens, A., Colomina, I., 2003. Sobre la corrección de errores sistemáticos en gravimetría aerotransportada. Proc. 5th Geomatic Week, Barcelona, Spain.

[Térmens and Colomina, 2004] Térmens, A., Colomina, I., 2004. Network approach versus state-space approach for strapdown inertial kinematic gravimetry. Gravity, Geoid and Space Missions GGSM2004, Porto, Portugal, 30 August - 3 September. 5p.

[Teunissen, 2001] Teunissen, P., 2001. Dynamic data processing. Delft University Press, Delft, NL.

[Tommaselli et al., 2009] Tommaselli, A.M.G., Galo, M., Bazan, W.S., Ruy, R.S., Marcato Junior, J., 2009. Simultaneous calibration of multiple camera heads with fixed base constraint. Proc. 6th International Symposium on Mobile Mapping Technology, Presidente Prudente, SP, Brazil, 21 - 24 July. 6p. (on CDROM).

[Tsingas, 1991] Tsingas, B., 1991. Automatische Aerotriangulation. Proc. 43rd Photogrammetric Week, Stuttgart, pp. 253–258.

[Xu, 2003] Xu, G., 2003. GPS theory, algorithms and applications. Springer-Verlag, Berlin, DE.

# Appendix 1. Next generation network adjustments

This appendix reprints the paper that presents the theoretical basis of the next generation of network adjustment and estimation methods. The detailed theory is materialized in the commercial SW platform "Generic Extensible Network Approach", GENA, developed for GeoNumerics within the framework of the ITAVERA project. This software was the main tool used in the work of this thesis research and is based on:

- the abstract network concept,
- the dynamic networks,
- the new generic network model,
- the new approach to network adjustments, and
- the features of next generation estimation systems.

The abstract network and dynamic network concepts that are developed in sections 1, 2 and 3 of the paper provide the network software with simplicity, genericity and extensibility. While section 4 of the paper is devoted to generic and extensible network software architectures, based on the detailed generic network model, the proposed approach to network adjustments and, in general, the presented features of the estimation systems.

I largely developed the software necessary for this research with Dr. José Antonio Navarro who has also developed parts of the GENA SW platform. I also developed and discussed the ideas with Dr. Ismael Colomina, who had the main ideas and promoted and supervised the research. Dr. Ismael Colomina also wrote the paper with contributions from the rest of the authors.

*Colomina, I., Blázquez, M., Navarro, J.A., Sastre, J., 2012. The need and keys for a new generation network adjustment software. Proc. XXII Congress of the International Society for Photogrammetry and Remote Sensing, Melbourne, Australia, 25 August - 1 September. 6p (on CD-ROM).*

# THE NEED AND KEYS FOR A NEW GENERATION NETWORK ADJUSTMENT SOFTWARE

I.Colomina[1], M.Blázquez[1], J.A.Navarro[1], J.Sastre[2]

[1]Institute of Geomatics, Generalitat de Catalunya & Universitat Politècnica de Catalunya
Av. Carl Friedrich Gauss 11, Parc Mediterrani de la Tecnologia, Castelldefels, Spain, ismael.colomina@ideg.es
[2]GeoNumerics, Josep Pla 82, Barcelona, Spain, jaume.sastre@geonumerics.com

**KEY WORDS:** network adjustment, orientation, calibration, modeling.

**ABSTRACT:**

Orientation and calibration of photogrammetric and remote sensing instruments is a fundamental capacity of current mapping systems and a fundamental research topic. Neither digital remote sensing acquisition systems nor direct orientation gear, like INS and GNSS technologies, made block adjustment obsolete. On the contrary, the continuous flow of new primary data acquisition systems has challenged the capacity of the legacy block adjustment systems —in general network adjustment systems— in many aspects: extensibility, genericity, portability, large data sets capacity, metadata support and many others. In this article, we concentrate on the extensibility and genericity challenges that current and future network systems shall face. For this purpose we propose a number of software design strategies with emphasis on rigorous abstract modeling that help in achieving simplicity, genericity and extensibility together with the protection of intellectual proper rights in a flexible manner. We illustrate our suggestions with the general design approach of GENA, the generic extensible network adjustment system of GeoNumerics.

## 1 INTRODUCTION

Orientation and calibration of photogrammetric and remote sensing instruments in their various modes, from direct to integrated, from geometric to radiometric, is a critical capacity of modern mapping systems and continues to be an active field of academic research. One of the key components of this capacity is the more than 200 year old method of network adjustment based in turn on the even older least-squares estimation method. Contrary to what the introduction of electronic light sensors made us fear or hope, digital cameras did not kill block adjustment for sensor calibration. Contrary to what the introduction of navigation technologies, mainly GPS and INS, made us fear or hope, INS/GPS did not kill block adjustment for sensor orientation. Furthermore, even in the strict navigation domain, there are environments and circumstances, where navigation cannot be performed only with "navigation instruments" and where the "imaging instruments" —in principle not designed for navigation purposes— have to come to the rescue. Thus, concepts like vision-aided navigation and Simultaneous Localization and Mapping (SLAM) have become fundamental in the field of robotics navigation (Leonard and Durrant-Whyte, 1991, Smith et al., 1986).

In the geomatic field, it is well known that the network adjustment method started with geodetic surveying for horizontal terrestrial networks at the beginning of the 19th century. In the second half of the 20th century it was applied to geodetic photogrammetry for global 3D networks (Schmid, 1974), to close-range photogrammetry (Brown, 1956, Brown, 1971), to aerial photogrammetry (strip, independent model and bundle adjustment), and reached remote sensing with the SPOT satellites (Kratky, 1989). Airborne laser scanning (Kager, 2004, Frieß, 2006, Skaloud and Lichti, 2006), terrestrial mobile mapping (Jansa et al., 2004), radiative transfer modeling and radiometric calibration (Chandelier and Martinoty, 2009, Honkavaara et al., 2009), and spatio-temporal orientation and calibration (Blázquez, 2008, Blázquez and Colomina, 2012b) are recent new beneficiaries from the method.

The network adjustment method has also stepped into the realm of INS/GPS post-processing. Indeed, until recently, the method was used for static problems; i.e., to estimate unknown parameters that are not time dependent (random variables) and that are related to observations by observation equations (stochastic equations). However, in 2004-2005 (Colomina and Blázquez, 2004, Colomina and Blázquez, 2005) we introduced the "dynamic network" concept where unknown parameters can be both time independent (random variables) and time dependent (stochastic processes), and where observations can be related to parameters by both static observation equations (stochastic equations) and by dynamic observation equations (stochastic differential equations). Classical [static] networks are a particular case of dynamic networks. The dynamic network (DN) method is an alternative to Kalman filtering and smoothing (KFS) for non real-time estimation tasks. DN is more flexible than KFS and supports models involving unknowns at different time epochs. The DN method has been proposed for airborne gravimetry (Térmens and Colomina, 2004) and for trajectory determination in terrestrial mobile mapping (Rouzaud and Skaloud, 2011).

That DN and KFS are two different ways to solve the same problem indicates that the network adjustment method is also a modeling technique, where problems are formulated in terms of four fundamental entities: instruments, observations, parameters (random variables and stochastic processes) and models (stochastic equations). Consequently, we will talk about "network modeling and adjustment" rather than network adjustment and will shortly refer to it as the "network approach" or "network method." Analogously we will talk of "network software" when referring to network modeling and adjustment software.

From a software point of view, the long and successful history of the network approach is that of one of changing requirements. In geomatics and everywhere else, changing requirements, beyond certain point and in the absence of software development methods, can make clean software designs become a tangle. It is understandable then, that the big success of the network method has translated into the big challenge of the network software. Unfortunately, though understandably and not always (Colomina et al., 1992, Elassal, 1983), most network software packages are designed, developed and commercialized for niche geomatic markets (geodetic surveying, surveying, aerial photogrammetry, close-

range photogrammetry, satellite-based remote sensing, aerial laser scanning, terrestrial laser scanning, terrestrial mobile mapping systems, etc.). This fragmentation makes software development and evolution unnecessarily expensive, error-prone and does not let different geomatic measurement techniques be easily integrated. Moreover, with today's wave of new sensing techniques and observation platforms, refactoring[1] and/or patching the software is too long and expensive an option every time that a new instrument or configuration appear.

In general, changing of requirements together with old, legacy, or poorly designed code make the software to rot. Because of this (Martin, 2002), some software designs are said to suffer from the seven deadly smells, namely: rigidity, fragility, immobility, viscosity, needless complexity, needless repetition and opacity. *Rigidity* means that changing one part of the system forces changes in other parts; *fragility* that changes in one part cause bugs in unrelated parts; *immobility* that system components cannot easily be isolated for reuse; *viscosity* that doing things right is harder than doing things wrong; *needless complexity* that there is infrastructure or abstraction without immediate, direct benefit; *needless repetition* that there is repeated code that could be unified under a single abstraction; and *opacity* that the code is hard to read or understand.

These problems affect most software systems and that network software aged in the past is understandable. Today, however, software engineering is a mature discipline and the drifting of the requirements cannot longer be blamed for the degradation of the design. The capability to cope with changing user requirements is a system design requirement of modern software systems which translates into one of the fundamental challenges of software design: achieving simplicity and extensibility.

The above considerations make us believe that modern network software shall be generic and extensible. In software engineering, the algorithms of *generic* software are written in terms of abstract types that are instantiated as required for specific types provided as parameters. *Extensible* software is software prepared for future growth.

Last not least, there is the design challenge of promoting the use and growth of software while protecting the intellectual property. It is frequently the case that new instrument models cannot be included into the established network software: the one who knows the instrument and its model does not have access to either source code or extensible software and may not be interested in providing the models for integration into existing network software. The one who owns the software may not be interested in extending it if sales are not guaranteed, particularly if it is not extensible. Beyond generic and extensible, network software shall be designed in a way that balances fast circulation and growth, fair compensation of everyone's effort and protection of knowledge and intellectual property.

This paper discusses how the previously identified needs of network software

- simplicity,
- genericity,
- extensibility, and
- protection of intellectual property

[1]Refactoring is the disciplined practice of changing the structure of code without changing what it does.

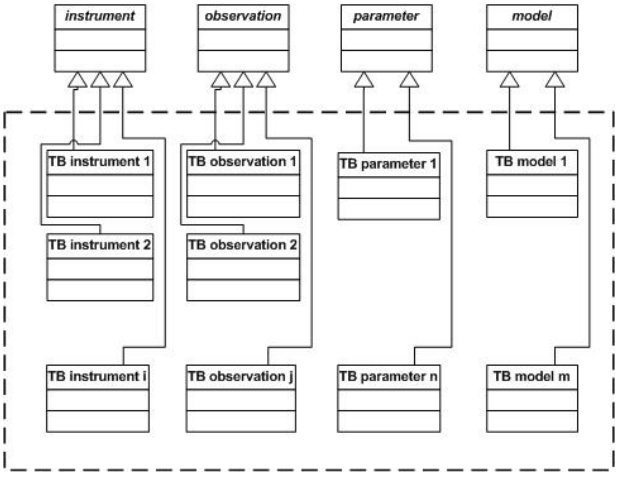


Figure 1: The GENA reference model and inheritance scheme.

can be achieved and illustrates the process by referring to GeoNumeric's network software GENA. GENA stands for Generic Extensible Network Approach, is a product of GeoNumerics and the Institute of Geomatics has developed a significant part of it under contract.

This paper is organized as follows. Sections 2 and 3 discuss software simplicity, genericity and extensibility, section 4 is devoted to generic and extensible network software architectures, section 5 provides references to use cases where the same software system (GENA) was used for different network types and section 6 summarizes the article ideas.

## 2 BALANCING SIMPLICITY AND EXTENSIBILITY

Software simplicity and extensibility have to be balanced. For a correct, consistent and complete software system, simplicity is obviously harder to achieve than complexity. Simple and extensible design requires correct domain models and well tuned abstraction levels. Correct domain modeling requires technical specialization as well as context awareness. Abstraction requires an additional effort to find common traits and behaviors of domain entities. Insufficient or needless abstraction leads to complex systems. Wrong abstraction leads to non extensible systems. Correct abstract models are, therefore, the key to simple and extensible systems.

In GENA, the main abstract model is the fundamental reference model based on four abstract classes: instruments, observations, parameters and mathematical models (figure 1). In other words, the fundamental data types of GENA are grouped in four categories: instruments, observations, parameters and mathematical model types. A concrete type, like for instance "GNSS receiver" will inherit from the abstract data type "instrument." A new instrument would probably generate measurements (observations) different from others. These measurements would be probably related to some unknown parameters of interest like points or orientation parameters and to some other unknown parameters like the self-calibration ones. The relation between the observations and the parameters, possibly with the participation of the instrument constants, is materialized by the mathematical models (stochastic equations).

"All" what has to be done to deal with a new instrument or system of instruments is to identify the instrument and its characteristic values, to characterize the type of its related measurements, to

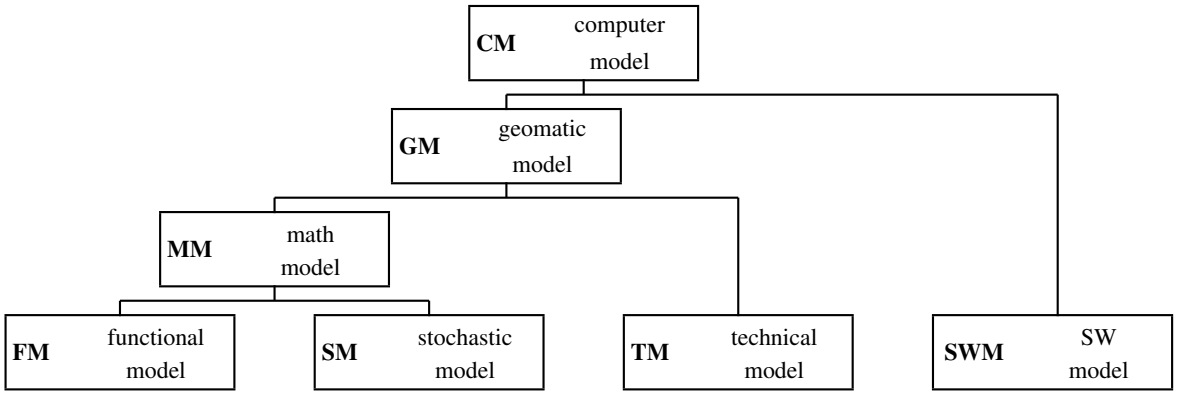


Figure 2: A modeling hierarchy in a network software system.

identify the parameters and the mathematical models that relate them. Once this is done, specific classes that inherit from the fundamental reference model can be reused or newly developed (figure 1). In other words, extending GENA to cope with new types of instruments, measures or mathematical models reduces to creating new data types. This is "all."

In practice, however, there are other aspects that count beyond the mathematical models and the other fundamental modeling entities (instruments, observations and parameters). In GENA, these "other aspects" correspond to other abstraction levels and models as depicted in figure 2. Thus, easy extensibility of input and output components, extensibility of metadata specification, support for physical units in the input and output (IO) tasks and internal computations and standardization of analysis tools, from outlier detection to numerical convergence criteria have to be tackled. In this case, it is "simplicity" for the developer of extensions that prevails. The approach taken by GENA is that, once the modeling entities are built, its software framework shall provide resources so that the above and other possible tasks are solved in a transparent (automatically, not known to the developer and user) or generic (activated by the data types or data type codes) way.

## 3 BALANCING GENERICITY AND EXTENSIBILITY

Balancing genericity and extensibility is deciding and designing what shall be newly coded —an extension action— and what shall work automatically upon reception of a data type argument —a generic behavior.

Extensibility and genericity are mutually dependent. In object-oriented design, for instance, the effective construction of a new data type requires the implementation of its interface. Thus, if the system design is based on correct abstract models, the standardized interface of the abstract data types guarantees that specific data types provide the necessary and sufficient information for other software components to behave generically.

In GENA, the four fundamental abstract data types provide the interface that allows the IO, least-squares estimation, numerical control, quality control, etc. components to behave generically. The specific, instantiated data types are grouped in "model toolboxes." The set of all generic components are grouped in the GENA software platform that does not change when new instruments/measurements have to be modeled and the models have to be coded. Thus, in GENA, the balance between extensibility and genericity is achieved by the "GENA model toolboxes" and by the "GENA platform." The model toolboxes, or more to the point the four abstract data types, their interface and the inheritance mechanisms, contribute the extensibility capacity. The platform provides the genericity capacity.

## 4 ON THE SOFTWARE FRAMEWORK AND ARCHITECTURE FOR GENERICITY AND EXTENSIBILITY

A software framework is a set of software libraries that expose a well defined application programming interface (API). The goal of a software framework is to facilitate the development of applications, products and solutions by isolating the domain developers from low-level programming details. In other words, a software framework is an abstraction in which software providing *specific* —and in the application domain context *generic*— functionality can be used for the medium- and high-level development of domain-specific applications.

The software architecture of a system is an abstraction that describes the software components, the relations among them and the properties of both components and relations.

In order to describe our vision of a modern network software, we further describe the modeling concepts of figure 2 through the following definitions.

*Mathematical Model* (MM): is an abstract model that uses mathematical language to describe the behaviour of a system. In the context of this article, a mathematical model is a functional model plus and stochastic model.

*Geomatic Model* (GM): is an extension of a mathematical model that includes coordinate reference frames, units of measurements, thresholds and any other information required to describe the geomatic properties of the mathematical model entities.

*Technical Model* (TM): In our context, a technical model is the difference between a geomatic model and a mathematical model.

*Software Model* (SWM): is an abstract model that describes a computer programme or software system, usually with a special graphical modeling language.

*Computer Model* (CM): is a computer program that simulates an abstract model of a particular system. (In a network adjustment system, for instance, the network computer model simulates the [abstract] network geomatic model.)

With the above definitions, we can now define the *Network Model* as a computer model of a physical reality; i.e., a computer model

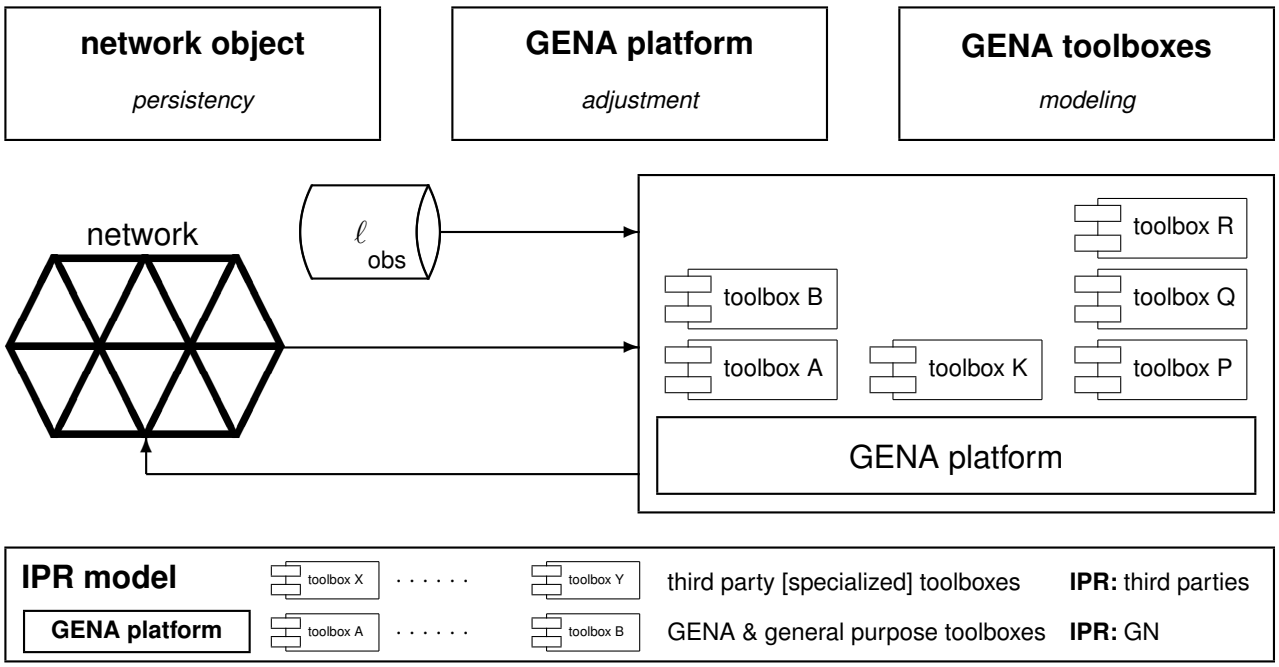


Figure 3: Network-centric architecture and IPR model.

of a of a set of measurements, the involved instruments and unknown parameters, and the mathematical models that relate them. (Note that the network model is a function of each particular network.)

Thus, in GENA, the mathematical models are materialized in the *GENA model toolboxes*, the *generic GENA software platform* is built with libraries of the *GENA software framework* that materialize the technical model and the software model corresponds to the software structure which includes the "network" data type.

The network data type models a network object that is both transient —exists as an entity during a network adjustment— and persistent —remains as a file after a network adjustment. The concept of persistent network objects or network files is instrumental in designing network-centric architectures as opposed to traditional process based ones (figure 3). In a network-centric architecture, input data are set into the network, the network is adjusted and, later on, the adjusted data can be extracted and adjustment reports can be generated.

### 4.1 Generic and dialectal man-machine interfaces

Most software systems communicate to other software systems and to human beings. To cover these two interface actors, the following types of interfaces are usually employed:

- Application Programming Interface (API);
- File Interface (FI);
- Command Line Interface (CLI); and
- Graphical User Interface (GUI).

In general, the API is used to communicate to other software systems, the GUI to humans, and the FI and CLI to both.

We will not devote a special attention to the API, as it can be seen as one more component of the generic software framework. We will also not discuss the CLI. A CLI uses to accept a number of arguments and behave generically with respect to them. The GUI and FI are of interest because

(a) the GUI interacts with a human operator who cannot be asked to behave generically, and

(b) ideally, the extension of the network software through the creation of new data types should

  (b.1) not require the coding of new IO software and
  (b.2) allow for the use of existing standards or de facto standards with a reasonable coding effort.

In the GUI case, if we assume that the FI can be generic, particularly for production environments where productivity and specialization are high, a reasonable approach is that

(a.1) the GUI is built around the generic FI (the GUI speaks the language of the generic platform when communicating "inwards" to the platform), and

(a.2) the GUI adapts to the particular domain environment (the GUI speaks the language of the domain —surveying, photogrammetry, remote sensing, etc.— when communicating "outwards" to the user),

which translates into building specific GUIs if the size of the targeted user segment and market permits.

In the case of the FI, for the input of measurements and the output of adjusted measurements, residuals and parameters, it is possible to specify formats parameterized by the network data types —therefore generic formats— that can be used in the IO operations. These formats can be generic or *open* because of their ability to represent any kind of network data type, which paves the way to automated, uniform IO.

The generic format specification can always be the same no matter the network data to read or write. However, the specific format to read or write depends on the particular data type. In the case of GENA, its generic software platform —also taking care of IO operations— may retrieve the particular characteristics of each network data type interrogating these in execution time. This makes the formats *closed* and fully operational in spite of their openness (genericity and extensibility). Moreover, in GENA,

the format specification for instruments, observations, parameters and [formal input of] model data are the same. In this way, for instance, the adjusted calibration parameters output of one adjustment can be read as input instrument calibration constants in the next one.

The addition of new network data types implies no change in generic network platforms. The characterization of new network model data types as described in section 2 is enough to integrate these in the FI. This contributes to simplicity and mitigates the burden of the unavoidable development of software bridges to legacy and/or external formats.

### 4.2 Generic metadata

Bridging the gap between genericity and a truly operational FI goes beyond giving the generic platform the ability to delegate to the network data types the responsibility of providing with the specific details related to IO. Lack of data metadata is behind many delays and data processing accidents.

The FI must also make room for metadata describing key aspects of the data included. Some of these aspects will be structural ones while other will describe variable traits of the information.

Structural metadata must describe aspects so important as the identification of the network data types included in the files —so the built-in, automated IO mechanisms may be triggered correctly and automatically. Variable metadata takes care of no less relevant aspects that, however, may not be considered as structural traits of data, as, for instance, the physical units used in a particular measurements data set, or the coordinate reference frames in use, or the role played by a parameter —constant or variable— in a particular adjustment.

### 4.3 Generic numerical kernel

Scientific computing can also benefit from modern computer science and software engineering (Dubois, 1997). And, although modern programming languages generate executable code that is no faster than that generated by old FORTRAN and C, the use of their programming mechanisms and available libraries often result in higher performance. That said, the numerical kernel of a network software platform has to implement the functions of a robust non-linear least-squares (RNLLS) estimator for large data sets of observations and parameters —i.e., threshold-monitored iteration of the cycle linearization, solution (for parameters and residuals), detection and removal of outliers, covariance estimation, variance component estimation, etc.— in one of its many possible forms.

Once the numerical- and statistical-control threshold abstractions are defined to let the generic convergence- and statistical-monitoring algorithms work, the construction of a generic RNLLS estimator is a common practice in numerical analysis and programming. There are many examples thereof like the generic subroutines, functions or methods to find polynomial roots, solve differential equations or optimize functions. In the case of GENA, we follow the standard generic numerical approach where the mathematical functional model $g$, where $g(\ell + v, x_1, \ldots, x_n) = 0$, is passed as a function argument with standardized interfaces to retrieve, given observations $\ell$ and parameters $x_1, \ldots, x_n$, the value of $g$ and its jacobian matrix with respect to $\ell, x_1, \ldots, x_n$. Also, in the case of GENA, for the sake of modeling simplicity and flexibility, the Gauß-Helmert formulation ($g(\ell + v, x_1, \ldots, x_n) = 0$) is preferred over the more restrictive Gauß-Markov one ($\ell + v = f(x_1, \ldots, x_n)$) and a mechanism to numerically compute jacobian matrices is provided.

In general, there is the open issue of parameter initial approximations' generation for the initialization of the iterative RNLLS solver. Most non-trivial mathematical models in geomatics are non-linear. Generally speaking, there is no universal method to compute initial approximations for non-linear problems, even not to network adjustment problems restricted to geomatics. Thus, in the best of cases, a generic RNLLS initializer may be provided as part of the generic network platform with applicability limited to a subset of models and circumstances.

### 4.4 Generic numerical and statistical control

Numerical and statistical control for various purposes is an essential feature of a RNLLS solver. Making numerical and statistical decisions, like declaring numerical convergence or divergence, or accepting or rejecting a measurement, is not a minor issue for disparate data sets and network geometries. Therefore, the abstract data types shall be able to provide this information to the generic algorithms. In most cases this design aspect corresponds to the technical model (TM, see figure 2) as answering questions like "how small is small?" depends on technical domain aspects; for instance, a correction to an Earth reference frame transformation parameter can be considered small below few millimeters whereas a correction to a camera principal point may only be acceptable below few micrometers. These, and other similar abstractions for the TM are often neglected in spite of their practical relevance.

## 5 USE CASES

The generic and extensible approach discussed throughout the paper has been demonstrated in practice by using GENA for various orientation and calibration tasks: simultaneous orientation and calibration of frame camera and laser scanners (Angelats et al., 2012), radiative transfer modeling and camera radiometric calibration (Antequera et al., 2012), new camera orientation methods like the use of relative aerial control (Blázquez and Colomina, 2012c), spatio-temporal calibration of frame cameras (Blázquez and Colomina, 2012b), or quasi-direct orientation (Fast AT) (Blázquez and Colomina, 2012a). Also, the similar and early approach reported in (Colomina et al., 1992) has been successfully applied to geodetic surveying, airborne photogrammetry, satellite remote sensing and to airborne gravimetry simulations with the dynamic network method (Térmens and Colomina, 2004).

## 6 SUMMARY AND CONCLUSIONS

The construction of modern network adjustment software able to cope with today's continuous flow of new geomatic instruments is a typical software engineering task of dealing with changing requirements where simplicity, genericity, extensibility and performance have to be balanced. In the article, we have tried to demonstrate that this software engineering task is, above all, a modeling exercise where the identification of a network's abstract data types is the main part. We have illustrated the preceding statement with the GENA fundamental reference model that is based on four abstract data types: instruments, observations, parameters and models. If a complete and correct collection of abstract data types is provided, it is possible to construct software that is both generic and extensible. We have illustrated this with a software architecture concept that separates the common network adjustment functions from the particularities of each instrument and its associated measurements and models. The concept concentrates the common functions in a *generic network adjustment platform* and the instruments' particularities in *model toolboxes*

that, in the GENA case, include the specific instrument, observation, parameter and model data types.

The proposed concept, as indicated, has been implemented in GeoNumeric's GENA software platform and used, with the corresponding specific model toolboxes, for different network adjustment use cases including radiative transfer modeling and radiometric calibration, spatio-temporal orientation and calibration of cameras, orientation and calibration of airborne laser scanners, and combined orientation and calibration of airborne laser scanners and cameras.

## REFERENCES


Angelats, E., Blázquez, M. and Colomina, I., 2012. Simultaneous orientation and calibration of images and laser point clouds with straight segments. In: International Archives of Photogrammetry, Remote Sensing and Spatial Information Sciences, Melbourne, Australia.

Antequera, R., Andrinal, P., Colomina, I., Navarro, J. and Pros, A., 2012. Corrección radiométrica automática de imágenes generadas por cámaras matriciales ópticas. In: X Congreso TOPCART 2012: Congreso Iberoamericano de Geomática y Ciencias de la Tierra, Madrid, Spain.

Blázquez, M., 2008. A new approach to spatio-temporal calibration of multi-sensor systems. In: International Archives of Photogrammetry, Remote Sensing and Spatial Information Sciences, Vol. 37-B1, Beijing, China.

Blázquez, M. and Colomina, I., 2012a. Fast AT: a simple procedure for quasi direct orientation. ISPRS Journal of Photogrammetry and Remote Sensing.

Blázquez, M. and Colomina, I., 2012b. On INS/GNSS-based time synchronization in photogrammetric and remote sensing multi-sensor systems. PFG Photogrammetrie, Fernerkundung und Geoinformation 2012(2), pp. 91–104.

Blázquez, M. and Colomina, I., 2012c. Relative INS/GNSS aerial control in integrated sensor orientation: models and performance. ISPRS Journal of Photogrammetry and Remote Sensing 67(1), pp. 120–133.

Brown, D., 1956. The simultaneous determination of the orientation and lens distortion of a photogrammetric camera. Air Force Missile Test Center Report 56-20, Patrick AFB, Florida, USA.

Brown, D., 1971. Close range camera calibration. Photogrammetric Engineering 37(8), pp. 855–866.

Chandelier, L. and Martinoty, G., 2009. Radiometric aerial triangulation for the equalization of digital aerial images and orthoimages. Photogrammetric Engineering and Remote Sensing 75(2), pp. 193–200.

Colomina, I. and Blázquez, M., 2004. On the stochastic modeling and solution of time dependent networks. In: Proceedings of the VI International Geomatic Week, Barcelona, Spain.

Colomina, I. and Blázquez, M., 2005. On the stochastic modeling and solution of time dependent networks. In: Proceedings of the VI International Geomatic Week, Barcelona, Spain.

Colomina, I., Navarro, J. and Térmens, A., 1992. GeoTeX: a general point determination system. In: International Archives of Photogrammetry and Remote Sensing, Vol. 29-B3, International Society for Photogrammetry and Remote Sensing, pp. 656–664.

Dubois, P., 1997. Object technology for scientific computing. The object-oriented series, Prentice Hall, Upper Saddle River, NJ, USA.

Elassal, A., 1983. Generalized adjustment by least squares (GALS). Photogrammetric Engineering and Remote Sensing 49, pp. 201–206.

Frieß, P., 2006. Toward a rigorous methodology for airborne laser mapping. In: Proceedings of the EuroCOW 2006, European Spatial Data Research - EuroSDR, Castelldefels, Spain.

Honkavaara, E., Arbiol, R., Markelin, L., Martínez, L., Cramer, M., Bovet, S., Chandelier, L., Ilves, R., Klonus, S., Marshal, P., Schlpfer, D., Tabor, M., Thom, C. and Veje, N., 2009. Digital airborne photogrammetry –a new tool for quantitative remote sensing?– a state-of-the-art review on radiometric aspects of digital photogrammetric images. Remote Sensing 1, pp. 577–605.

Jansa, J., Studnicka, N., Forkert, G. and Haring, A. Kager, H., 2004. Terrestrial laserscanning and photogrammetry — acquisition techniques complementing one another. In: International Archives of Photogrammetry and Remote Sensing, Vol. 35-B7, International Society for Photogrammetry and Remote Sensing, pp. 948–953.

Kager, H., 2004. Discrepancies between overlapping laser scanning strips - simultaneous fitting of aerial laser scanner strips. In: International Archives of Photogrammetry and Remote Sensing, Vol. 35-B1, International Society for Photogrammetry and Remote Sensing, pp. 555–560.

Kratky, V., 1989. Rigorous photogrammetric processing of SPOT images at CCM Canada. ISPRS Journal of Photogrammetry and Remote Sensing 53(9), pp. 1223–1230.

Leonard, J. and Durrant-Whyte, H., 1991. Simultaneous map building and localization for an autonomous mobile robot. In: Proceedings of the International Workshop IROS'91, Vol. 3, IEEE/RSJ, pp. 1442–1447.

Martin, R., 2002. Agile software development: principles, patterns, and practices. Prentice Hall, Hemel Hempstead, UK.

Rouzaud, J. and Skaloud, J., 2011. Rigorous integration of inertial navigation with optical sensors by dynamic networks. Navigation 58(2), pp. 141–152.

Schmid, H., 1974. Worldwide geocentric satellite triangulation. Journal of Geophysical Research 79(35), pp. 5349–5376.

Skaloud, J. and Lichti, D., 2006. Rigorous approach to boresight self-calibration in airborne laser scanning. ISPRS Journal of Photogrammetry and Remote Sensing 61, pp. 47–59.

Smith, R., Self, M. and Cheeseman, P., 1986. Estimating uncertain spatial relationships in robotics. In: Proceedings of the Second Annual Conference on Uncertainty in Artificial Intelligence. UAI '86, University of Pennsylvania, Philadelphia, PA, USA, pp. 435–461.

Térmens, A. and Colomina, I., 2004. Network approach versus state-space approach for strapdown inertial kinematic gravimetry. In: Gravity, Geoid and Space Missions - GGSM2004, Porto, Portugal.



Colomina,I.,Blázquez,M.,Navarro,J.A.,Sastre,J.,2012.
The need and keys for a new generation network adjustment software. *International Archives of Photogrammetry, Remote Sensing and Spatial Information Sciences*, 2012-08-25–09-01, Melbourne, Australia.

# Appendix 2. Dynamic Networks

It is (wrongly) believed that the derivation of GNSS position and INS/GNSS position-velocity-attitude trajectories requires the use of the "predictor-Kalman filter" approach. This is only true for real-time applications, whereas network adjustment-based solutions can be used to take advantage of additional tie information like cross-over points, for better exploitation of velocity and coordinate update points and can deliver information – like actual residuals of INS measurements – for quality control.

This appendix reprints the paper in which this dynamic network concept is presented. The proposed concept extends the classical geomatic concept of network. A dynamic or time dependent network is a classical network that incorporates stochastic processes and stochastic differential equations. The dynamic networks are the real challenge of the proposed network approach (Appendix 1).

For this research, I discussed the ideas and developed the theory with Dr. Ismael Colomina, who also outlined his ideas and wrote the paper with my contributions.

*Colomina, I., Blázquez, M., 2004. A unified approach to static and dynamic modelling in photogrammetry and remote sensing. International Archives of the Photogrammetry, Remote Sensing and Spatial Information Sciences 35(B1), pp. 178–183.*

# A UNIFIED APPROACH TO STATIC AND DYNAMIC MODELLING IN PHOTOGRAMMETRY AND REMOTE SENSING

I. Colomina, M. Blázquez

Institute of Geomatics
Generalitat de Catalunya & Universitat Politècnica de Catalunya
Castelldefels, Spain

**KEY WORDS:** calibration, orientation, static, dynamic, modelling, estimation, GPS/INS, networks.

**ABSTRACT:**

Modern photogrammetry and, more generally, the current technology for Earth observation are dependent on various forms of data processing. After the sensing or acquisition step, the data are available in digital format and all what has to be done is to calibrate, to orient and to extract georeferenced information. In this context, data processing for trajectory determination, sensor calibration and sensor orientation follows various patterns, all of them particular cases of the general time dependent parameter estimation problem defined by the equation $f(t, \ell(t) + v(t), x(t), \dot{x}(t)) = 0$, where $f$ is the mathematical functional model, $t$ is the time, $\ell(t)$ is the time dependent observation vector, $v(t)$ is a white-noise generalized process vector, $x(t)$ is the parameter vector and $\dot{x}(t)$ the time derivative of $x(t)$. A number of different approaches to estimate parameters $x(t)$ from data $\ell(t)$ has been developed according to the particular form of the above model equation. $\ell + v = f(x)$, $f(\ell + v, x) = 0$, $f(t, \ell(t) + v(t), x(t)) = 0$ and $\dot{x}(t) = f(t, \ell(t) + v(t), x(t))$ are examples of model equations leading to network and Kalman filter/smoother solution strategies. Although these two procedures have proven to be well suited to their respective model equation structure, the paper discusses some of their limitations and alternatives, particularly for time dependent problems. The proposed family of methods uses numerical techniques that integrate the rigorous least-squares method and the finite difference methods for the solution of the Boundary-Value problem of Ordinary Differential Equations. Although we do not claim that this has to substitute existing, proven techniques, the paper indicates how hybrid static and dynamic data processing can be easily integrated with this new approach.

## 1 INTRODUCTION

Nowadays, trajectory determination [1] for navigation, geodetic positioning and remote sensing orientation is mainly based on two parameter estimation methodologies: least-squares network adjustment —the network approach (NA)— and Kalman filtering and smoothing —the state-space approach (SSA). It is known that Kalman filtering is a general form of sequential least-squares. However, in practice, there is no much connection between the two approaches other than some output estimated parameters following the network approach being used as input observations for a second estimation step following the state-space approach. And vice versa. It must be mentioned that the GPS research related community has since long been faced to the problem of making a decision between classical least-squares, Kalman filtering and smoothing and some intermediate approaches (Xu, 2003). The dilemma holds for both the processing of moving object trajectories and for the processing of stationary or quasi-stationary objects. For the family of problems just mentioned (static, quasi-static and kinematic) there are examples of successful application of both the state space approach and of the network approach. To illustrate the statement, we cite two "classics" that have had and still have a significant impact in geomatics in the past decade. The GLOBK system (Herring, 2003) uses Kalman filtering and has been successfully applied to time-dependent precise networks for deformation monitoring originating from VLBI and GPS. At the opposite end, the GPS aircraft trajectories for Earth observation applications like aerial triangulation or LIDAR aerial surveys were determined under the network approach (Frieß, 1990).

The goal of the ongoing research behind this paper is not to devise a "unified" algorithm that package both classical least-squares and state-space estimation in "one." The approach is rather pragmatic —numerical, algorithmic and software oriented— as the theories of least-squares estimation (Koch, 1995) and state-space estimation (Maybeck, 1979a, Maybeck, 1979b) are well established. The actual goal is to interpret stochastic dynamic models —i.e., differential or difference equations— and their time dependent unknown parameters —i.e., stochastic processes— in a way that, for the time dependent parameter estimation problem, both the network approach and the state-space approach are applicable. We do not claim that both approaches be fully interchangeable. We do claim that in some circumstances, it might be advantageous to apply the network approach to the estimation of time dependent parameters. As well, we claim that time dependent problems in geomatics do not necessarily require a SSA treatment.

In addition to the numerical, algorithmic, software data modelling and software use potential advantages of a unified approach, there are a number of estimation problems that might benefit from it. They include the modelling

[1] In this paper trajectory determination is understood as the determination of a time series of positions, velocities and attitudes.

of trajectories for airborne and spaceborne imaging linear arrays, the calibration of inertial instruments (angular rate sensors and accelerometers) with "cross-over" type of observation equations and the modelling/estimation of geodetic networks for monitoring and prediction purposes. It has to be mentioned that a parallel research effort is being conducted by A. Térmens for inertial strapdown kinematic airborne gravimetry (Térmens and Colomina, 2003, Térmens and Colomina, 2004) for an optimal calibration of accelerometers.

The key idea behind this investigation is that a stochastic dynamic model (a stochastic differential equation) and its stochastic processes can be transformed through discretization into a family of stochastic difference equations and discrete time processes. Those, in turn, can be seen as a family of observation equations and parameters that can be processed under the network approach.

The paper begins by reviewing some definitions and concepts from the theory of stochastic processes and stochastic differential equations. We take this approach because of the available sound theory that includes continuity theorems and numerical solution methods consistent with the stochastic nature of the problem. Then, the state-space and the network approaches are defined and compared. Once this is done, in section 6 we define time dependent networks in a way that generalize the traditional least-squares based networks. Here, the scope of the concept of a dynamic or time dependent network is precisely defined. The algorithmic and software implementation implications of section 6, should be clear at that point. However, we underline them in section 7 for readers not familiar with the development of network adjustment systems.

## 2 STOCHASTIC PROCESSES

A stochastic process is a parametrized collection of random variables defined on a probability space $(\Omega, \mathcal{F}, P)$ (Law ler, 1995). The parameter space $T$ is usually the time or a time interval. In other words, a stochastic process $x$ is a set of random variables indexed by time

$$x := \{x(t) \,|\, t \in T, T \subset R\}$$

where $R$ is the set of real numbers. In this paper, and in most applications, the parametrizing, indexing or tagging subset $T$ is either $N$, the set of natural numbers, or $R$. If $T = N$, $x$ is called a discrete time process and in the other case, $T = R$ or $T = [a, b] \subset R$, it is called a continuous time process. The set where the random variables take values, typically $R^n$, is called the state space.

From the definition, it is clear that for each $t \in T$, we have a random variable $\omega \longrightarrow x(t)(\omega) := x(t, \omega)$ for $\omega \in \Omega$. But the function $x(t, \omega)$, for a given fixed $\omega$, can be seen as a function of $t$, $t \longrightarrow x(t, \omega)$ for $t \in T$. This function is a *path*. We introduce the concept of a path because it is close to our intuition in INS and GPS trajectories, satellite orbits, etc. When we look at a trajectory, $\omega$ can be seen as a point or one of our repetitive experiments and thus $x(t, \omega)$ would represent the position of the point at time $t$ or the result of the particular experiment.

A fundamental stochastic process is the *Brownian motion* (or *Wiener process* or *continuous random walk*) named after a 19th century botanist who observed that pollen grains on a liquid described an irregular trajectory. Its formal derivative is called white noise. White noise is formally considered a stochastic process to facilitate the visualization and interpretation of the continuous idealization of discrete time processes whose random variables are independent, normally distributed ones. (Sometimes, in the engineering literature, it is said that the white noise process is a helpful concept that does not exist in the world of mathematics. In fact, this statement is wrong. White noise exists as a generalized stochastic process (Øksendal, 1993), a slightly more complex concept than a stochastic process.)

The stochastic analogs of *ordinary differential equations* (ODE) are the *stochastic differential equations* (SDE). The theory for SDE can be found in (Øksendal, 1993). SDE arise naturally from real-life ODE whose coefficients are only approximately known because they are measured by instruments or deduced from other data subject to random errors. The initial or boundary conditions may be also known just randomly. In these situations, we would expect that the solution $p$ of the problem be a stochastic process. We will call $p = p(t, \omega)$ a *prediction*. Under certain [non-restrictive] hypotheses $p$ has a number of properties including that it is t-continuous (Øksendal, 1993, pp. 48-49).

Assume now that we have managed to predict the stochastic process $p$ —the *system*— over a time interval $[t_0, t_f]$. In our application, determining $p$ reduces to determine an estimate of the path $E(p(t))$ and estimates of the process auto-covariance functions

$$C(t_1, t_2) := E\left((p(t_1) - E(p(t_1)))(p(t_2) - E(p(t_2)))^T\right).$$

Assume further that we are able to relate $p$ through some linear model —the observation equations— to another process $z$ —the *observations*— so we have additional information of $p$. A natural question arises: can we improve our estimates of $p$ with the additional information $z$?. The answer, in general, is yes, and the tool is the well known filtering and smoothing. Filtering at time $s$ refers to finding a best estimate for the system $\hat{p}(s)$, $t_0 < s < t_f$ given the observations $z$ in the interval $[t_0, s]$. Smoothing, refers to finding the best estimate for $\hat{p}(s)$ at any time by using the information of $z$ all over $[t_0, t_f]$. Saying that $\hat{p}(s)$ is best means that $E\left(\|p - \hat{p}\|^2\right)$ is minimal over all solutions of the system SDE that verify the observation equations (see (Øksendal, 1993, pp. 58-59) for a detailed description of the probability function associated to the SDE and to the observations white noise processes).

## 3 THE STATE-SPACE APPROACH

We will call *state-space approach* (SSA), the methodology and principles of solving the above problem of prediction,

filtering and smoothing for time discrete processes (section 2).

The SSA is the well known Kalman filtering and smoothing published by R.E.Kalman in 1960 (Kalman, 1960) and discussed in numerous textbooks from different points of view (Maybeck, 1979a, Øksendal, 1993). Equivalent later formulations in terms of sequential least-squares can be found in (Teunissen, 2001). The SSA has been successfully applied to precise navigation for surveying applications (Scherzinger, 1997).

We borrow the state-space name from the state-space representation of a dynamical system. A state vector is a minimal set of variables whose values are able to describe a system. The optimal solution to the prediction-filtering-smoothing (section 2) is obtained through one of the recursive algorithms of the Kalman filter type.

In the prediction-filter cycle, the most important entity is the state vector. All the rest are subordinated parameters. In a way, the state vector dominates the scene which, in some situations, may represent a problem. One example is the difficulty in the feedback of the results of adaptive Kalman filter steps to a correct scaling of the inertial observations (angular rates and linear accelerations) in the inertial navigation equations. (In the *network approach* (NA), this reduces to a classical estimation of variance components). Another example of the weaknesses of the SSA is the estimation of gravity error states in the inertial navigation equations. We may estimate the gravity error of our gravity model in better or worse ways, depending on a number of instrumental, modelling and mission related factors. But we cannot impose that the gravity error estimated at time $t_1$ at point $x_1$ is the same as the gravity error estimated at a later time $t_2$ at point $x_2$ if $x_2 = x_1$ —the so-called cross-over points— as discussed in (Térmens and Colomina, 2003, Térmens and Colomina, 2004).

## 4 THE NETWORK APPROACH

In geomatics, a network is a set of instruments, observations and parameters that are inter-related through mathematical models. The mathematical models are the observation equations. To *solve the network* is to perform an optimal estimation of its parameters in the sense of least-squares; i.e., the expectation of the parameters and their covariance is known. Moreover, their covariance is minimal (Koch, 1995). The network approach exhibits superior performance when the connectivity that observations create between the unknown parameters is high.

In the network approach, our network will be solved in a grand, single adjustment step where all parameters, time dependent and independent, will be simultaneously estimated. This is giving us some hint on how to implement the network approach for time dependent networks in a computer programme. We discuss this in sections 6 and 7.

An [unknown] random variable —a time independent parameter— is to the classical network approach what an [unknown] stochastic process —a time dependent parameter— is to the state-space approach. In the following, the names "time dependent parameter" and "stochastic process" will be used indistinctly.

Note that the state-space approach can be used, as well, for the estimation of time independent parameters as they can be modeled as stochastic constant processes. A stochastic constant takes the same value $c$ over time. $c$ may or may not be known before the estimation process; but once it is estimated it will not change over the time period where the stochastic process is defined. An example of a random constant is a GPS ambiguity —integer or real— in a phase observation equation.

Note, as well, that a stochastic dynamic model (stochastic differential equation) can be transformed into a set of stochastic difference equations. Then, the family of stochastic difference equations can be seen as a set of observation equations and the network approach can be used. To discretize a stochastic dynamic model, we propose the difference methods (it is the "natural" way to do it). We are aware of limitations and/or inferior performances of the numerical difference methods for the solution of ODEs. However, the comparative analysis between difference methods and other more sophisticated numerical methods (variational methods, multiple shooting, ...) is usually done in the context of deterministic ODE (Stoer and Bulirsh, 1992). But, while the extension or generalization of the difference methods for deterministic ODE to the SDE is straightforward, the extension of the other mentioned methods is less obvious. In future investigations we will explore these numerical issues. Further, we refer the reader to the specific literature on the numerical solution of SDE (Kloeden and Platen, 1999).

## 5 COMPARATIVE ANALYSIS

In the previous sections we have looked at the SSA and the NA as different approaches to, essentially, solve the same problem. Before we introduce and discuss time dependent networks we summarize their main advantages and disadvantages from a geomatic perspective.

NETWORK APPROACH

- Advantages:
    1. Support for connectivity of parameters regardless of time.
    2. Support for both traditional networks and for SDE.
    3. Possibility to compute the covariance of a limited number of selected parameters.
    4. Variance component estimation.
- Disadvantages:
    1. Large system of linear equations.[2]

[2]The matrices are essentially of the band-bordered type and we can apply sparse matrix techniques, fill-in reduction techniques and memory paging to solve the system of linear equations.

2. Real-Time parameter estimation not feasible in general.

STATE-SPACE APPROACH

- Advantages:
  1. Real-Time parameter estimation capability.
  2. The state vector dominates the scene.[3] That is, there is a clear definition of what the system is.
- Disadvantages:
  1. Connectivity of parameters through static observation equations is not supported.
  2. Filter divergence.
  3. Computation of covariance matrices for all the state vectors cannot be avoided.

The above list is by no means comprehensive but, in our opinion, the only situation where the SSA is clearly superior is real-time parameter estimation. This statement should not be taken as a recommendation. In real life problems, other factors may be taken into account. For instance, in INS/GPS trajectory determination, a SSA based software engine can be applied to both real-time and post-processing computation modes. This aspect may be fundamental before making implementation decisions.

## 6 TIME DEPENDENT NETWORKS

A *time dependent network* is a network such that some of its parameters are time dependent; i.e., that some of its parameters are stochastic processes. Analogously, we define that to *solve a time dependent network* is to perform an optimal estimation of its parameters which include some stochastic processes. (However, this is easier said than understood and done. In this section we clarify the meaning of the above statement and in section 7 we suggest some implementation mechanisms.) We recall that optimality in estimating a stochastic process means to estimate the best expectation function path $\hat{x}(t)$ in the sense of having minimal $E\left(\|x-\hat{x}\|^2\right)$ as mentioned in section 2.

Note that we are asked to solve for more information in time dependent networks that in time independent ones. Accordingly, as it was to be expected, we will be given more information before the estimation process. This new information is the dynamic observation model for the random process. If we now rename our traditional observation equations as the static observation model(s), then the global picture of time dependent networks becomes clear and clean.

An static observation model is an equation of the type

$$f(t, \ell + v, x(t)) = 0 \tag{1}$$

where $v$ is a normally distributed variable of null expectation. A dynamic observation model —or a stochastic dynamic model— is an equation of the type

$$f(t, \ell(t) + v(t), x(t), \dot{x}(t)) = 0 \tag{2}$$

where $v(t)$ is a white noise process. In more global terms, we will refer to the family of static observation equations as the network static model. And to the family of dynamic observation equations[4] as the network dynamic model. Typically, a particular dynamic model (2) will be given for $t \in S'$ where $S' \subset S$. Note that a dynamic observation equation may include time independent parameters and that a static observation equation may include time dependent parameters but not its derivatives. Note, as well, that the static model may be of the form (1). This is not only consistent with the concept of an static observation equation but necessary when it contains a time dependent parameter.

The dynamic model is a key component of a time dependent network. Indeed, all what we know about $x(t)$ before solving the network is that $x(t)$ is a stochastic process. Indeed, the static model contributes to the determination of $x(t)$. However, without the dynamic model there is no "dynamics" in the process; i.e., we cannot guarantee that the set $\{\hat{x}(t)|t \in S'\}$ is a continuous path. In principle, strictly speaking, mathematical continuity does not tell us much about the roughness or smoothness of the solution path but practical experience proves its effectiveness. (The lack of dynamic modelling results, in practice, in somewhat rough solutions for $\hat{x}(t)$. A typical example of this is found in the determination of GPS trajectories under the network approach when compared with the same trajectory determined under the state-space approach which are, usually, smoother.)

Note, last, that in practice, we do not have to compute the auto-covariance function; we just have to provide a mechanism to compute it if requested.

We illustrate the above simple definition with two examples: a geodetic monitoring network and an airborne imaging network (block) with INS/GPS aerial control. These two examples are time dependent networks as they include dynamic observation models and time dependent parameters. Note, for instance, that the orientation parameters of a block can be seen as a set of time independent, unrelated parameters $\{p_i|i = 1, \ldots, n\}$ or as a time dependent parameter $\{p(t)|t \in [a, b], a, b \in R\}$.

The airborne network (block) with INS/GPS aerial control is a time dependent network because its unknown orientation parameters position, velocity and attitude depend on the time. The "flight" is a stochastic process. This one is a stochastic process over $[t_0, t_f]$, where $t_0$ and $t_f$ are the initial and the final time of the flight respectively. The stochastic process is just defined over a finite time period and we cannot predict the system beyond $t_f$ because

[3] For some models this advantage could be a disadvantage. See section 3 for a related discussion.

[4] In this paper no distinction is made between "equations" and "models" (both terms including the stochastic and functional components). We will use both terms as appropriate to highlight the parallelism between the dynamic and static aspects of the problem.

INS/GPS observations are required for the dynamic observation equations. The general network model is made up of the dynamic observation model —INS observation equations— and the static observation model —GPS observation equations, ground control points and the photogrammetric collinearity equations.

The geodetic monitoring network is a time dependent network in that it is a network of observed and measured points at given epochs and we want to know the situation of the network points within the time observation epochs and in future time epochs. We have the measured points at epochs $[t_0,\, t_1,\, \cdots,\, t_f]$ and we want to determine the position of the network points at epoch $t_f + \Delta t$. This is, in principle, a stochastic process over $[t_0,\, +\infty)$. This model is made up of the static observation model —GPS static observation equations, known control point equations, known constant 3D coordinate differences for points in a same tectonic plates, etc.— and the dynamic observation model — known variable coordinate differences according to some geophysical deformation model.

## 7 A UNIFIED APPROACH

The implications of the definition of time dependent networks of the preceding section are obvious. However, for the sake of clarity we underline them under the theoretical, algorithmic, software and production viewpoints.

### 7.1 A unified theoretical approach

The classical network is a set of instruments, observations and parameters. They are related through static observation models. The network approach is a procedure to estimate the parameters. The inputs are the values of observations and, if needed, the initial approximations of the parameters. The outputs are the estimated values of the parameters. On demand, the network approach can generate the covariance of the parameters and/or the auto-covariance function.

The time dependent network concept that we propose in this paper is a set of instruments, observations and time dependent and independent parameters. They are related through static and dynamic observation models. A time dependent parameter generates a set of equations, one equation for every time epoch. Now, the network approach is a procedure to estimate both time dependent and time independent parameters. The inputs are the values of the observations and, if needed, initial approximations of the parameters (note that, in this case, initial approximations are for time dependent and independent parameters). The outputs are the estimated values of the parameters including the stochastic processes. On demand, the network approach can generate the covariance of the parameters and/or the auto-covariance function. We insist on the parallelism of the time dependent and time independent network concepts.

We claim that the time dependent network concept proposed provides a unified theoretical framework that covers the estimation of time dependent and time independent parameters. The time dependent network is based on static and dynamic observation models. The time independent network is (solely) based on static observation models. Thus, the classical network can be seen as a particular case of the new time dependent networks.

This unified approach is the basis for the reasonable development of time dependent network determination software, which is at the same time rigorous and simple. We discuss this aspect in the next section.

### 7.2 A unified algorithmic and software approach

A modern well designed software system of the class we are discussing here is based in the object-oriented paradigm. Combining object-oriented design and the previous theory, a simple and powerful time dependent network determination software can be generated. This software system shall include these fundamental entity classes: observation, instrument, parameter and model. See (Colomina et al., 1992) for a related discussion and modelling in time independent networks.

The observations may have an associated time (time epoch of the observation). We call them time-tagged observations. However, we emphasize that our observations, although time dependent, are stochastically independent as they are only subject to a white noise process. In principle, it should not come as a surprise that for a time dependent networks, all what we have to do is to generalize time dependent parameters and dynamic observation models from time independent parameters and static observation models, respectively.

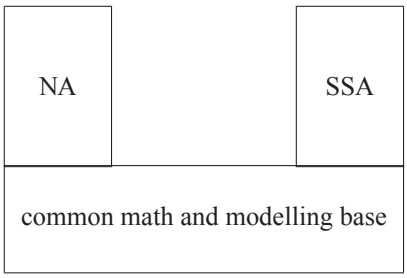


Figure 1: Unified SW approach

Interestingly enough, in our unified software approach, the mathematical foundation libraries are not much different from the classical approach. This applies both to internal software aspects and to interface aspects. Moreover, with minor changes, most of the organizational parts and discrete mathematical components of existing [well designed] network adjustment packages can be kept. Even more interesting is the fact that the NA and SSA computational engines can share the same model libraries, as the estimation engines work with the same models, their software implementation and their external interfaces. In other words, the parallel development and maintenance of an NA and an SSA engine within the frame of a general system is possible.

### 7.3 A unified exploitation approach

Unified theoretic frameworks lead to simple and efficient algorithms and software. Unified software approaches lead to simple and efficient exploitation procedures. In particular, an eventual software implementation of the concepts presented, would lead to common shareable input/output formats for a number of estimation engines.

A benefit of a unified approach is that we can follow different strategies and that we can combine them. In some situations, one approach should be preferred. In other situations we can combine them. For a family of problems, one approach may be preferred for calibration tasks whereas the other may be preferred for orientation tasks.

Note, as mentioned in section 1, that the output estimated parameters of a static network may be used as input observations for a time dependent network. Similarly, an SSA engine can be used to generate initial approximations for a NA engine. In all the cases, it is clear that interoperability is easier to achieve with a unified approach.

## 8 CONCLUSION, ONGOING WORK AND FURTHER RESEARCH

In this paper we have defined in a precise way the concept of time dependent networks. The proposed concept extends the classical unified (from geodesy, photogrammetry and remote sensing) geomatic concept of network. In short, a time dependent network is a classical network that incorporates stochastic processes —that we call time dependent parameters— and dynamic models —that we call dynamic observation models. We have related time dependent networks and their solution approaches to the existing Kalman filtering/smoothing and network methodologies —what we call the SSA and the NA solution approaches— and have discussed their advantages and disadvantages. Last, we have given some hints on how this unified approach can be exploited at the software development and data processing levels.

We are currently developing an experimental software prototype that implements the concepts presented in this paper. Further research will be related to the numerical solution of SDEs for geomatic applications and to their optimization in terms of speed and memory/disk storage requirements.

## REFERENCES


Colomina, I., Navarro, J. and Térmens, A., 1992. GeoTeX: a general point determination system. In: International Archives of Photogrammetry and Remote Sensing, Vol. 29-B3, International Society of Photogrammetry and Remote Sensing, pp. 656–664.

Frieß, P., 1990. Kinematische Positionsbestimmung für die Aerotriangulation mit dem NAVSTAR Global Positioning System (Ph.D. Thesis). C, Vol. 359, Deutsche Geodätische Kommission, München, DE.

Herring, T., 2003. GLOBK: Global Kalman filter VLBI and GPS analysis program, version 10.1. Technical report, MIT, Cambridge, MS, US.

Kalman, R., 1960. A new approach to linear filtering and prediction problems. Transactions of the ASME, Journal of Basic Engineering 82(1), pp. 34–45.

Kloeden, P. and Platen, E., 1999. Numerical solution of Stochastic Differential Equations. Springer Verlag, New York, US.

Koch, K., 1995. Parameter estimation and hypothesis testing in linear models. Springer Verlag, Berlin, DE.

Law ler, G., 1995. Introducttion to Stochastic Processes. Chapman & Hall/CRC, Boca Ratón, FL, US.

Maybeck, P., 1979a. Stochastic models, estimation and control. Mathematics in science and engineering, Vol. 141-1, Academic Press Inc., New York, NY, US.

Maybeck, P., 1979b. Stochastic models, estimation and control. Mathematics in science and engineering, Vol. 141-2, Academic Press Inc., New York, NY, US.

Øksendal, B., 1993. Stochastic differential equations: an introduction with applications. Universitext, third edn, Springer-Verlag.

Scherzinger, B., 1997. A position and orientation post-processing software package for inertial/GPS integration (POSPROC). In: Proceedings of the KISS'97 Symposium, Calgary, AB, CA, pp. 197–204.

Stoer, J. and Bulirsh, R., 1992. Introduction to Numerical Analysis. second edn, Springer-Verlag, New York, US.

Térmens, A. and Colomina, I., 2003. Sobre la corrección de errores sistemáticos en gravimetría aerotransportada, (in Spanish). In: Proceedings of the 5. Geomatic Week, Barcelona, ES.

Térmens, A. and Colomina, I., 2004. The Network Approach versus the State-Space Approach for strapdown inertial kinematic gravimetry. Abstract submitted to the IAG International Symposium Gravity, Geoid and Space Missions - GGSM2004, Porto, PT.

Teunissen, P., 2001. Dynamic data processing. Delft University Press, Delft, NL.

Xu, G., 2003. GPS theory, algorithms and applications. Springer-Verlag, Berlin, DE.


## ACKNOWLEDGEMENTS


The research reported in this paper has been performed within the frame of the ITAVERA project that the Institute of Geomatics is conducting for GeoNumerics and with partial support of the Spanish Ministry of Science and Technology, through the OTEA-**g** project of the Spanish National Space Research Programme (reference: ESP2002-03687).